

SEASONAL AND MESOSCALE VARIABILITY IN THE
DISTRIBUTION OF ANTARCTIC KRILL, *EUPHAUSIA SUPERBA*,
WEST OF THE ANTARCTIC PENINSULA

by

Cathy Meyer Lascara
B.S. June 1978, Florida Institute of Technology
M.S. May 1982, College of William and Mary

A Dissertation submitted to the Faculty of
Old Dominion University in Partial Fulfillment of the
Requirement for the Degree of

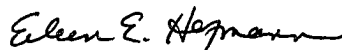
DOCTOR OF PHILOSOPHY

OCEANOGRAPHY

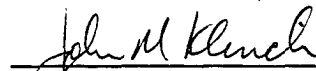
OLD DOMINION UNIVERSITY

May 1996

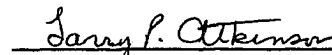
Approved by:



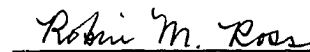
Eileen E. Hofmann (Director)



John M. Klinck (Member)



Larry P. Atkinson (Member)



Robin M. Ross (Member)
University of California

UMI Number: 9624123

**UMI Microform 9624123
Copyright 1996, by UMI Company. All rights reserved.**

**This microform edition is protected against unauthorized
copying under Title 17, United States Code.**

UMI
300 North Zeeb Road
Ann Arbor, MI 48103

ABSTRACT

SEASONAL AND MESOSCALE VARIABILITY IN THE DISTRIBUTION OF ANTARCTIC KRILL, *EUPHAUSIA SUPERBA*, WEST OF THE ANTARCTIC PENINSULA.

Cathy Meyer Lascara
Old Dominion University, 1996
Director: Dr. Eileen E. Hofmann

Observations collected between November 1991 and September 1993 during four multidisciplinary cruises were analyzed to provide a description of seasonal and mesoscale variability in the distribution and abundance of Antarctic krill, *Euphausia superba*, within continental shelf waters west of the Antarctic Peninsula and to investigate possible relationships between variability in krill distributions and variability in selected environmental parameters. Acoustic measurements of krill were made each season at designated locations to estimate the abundance of krill, in terms of vertically-integrated krill biomass and the number of aggregations, characterize the depth distribution of krill, and provide a quantitative description of the size, shape, and biomass of individual krill aggregations. The acoustic observations were coupled in time and space to environmental conditions defined by measurements of weather and sea ice parameters, hydrographic structure, concentrations of algal pigments, and net-based density estimates of krill and other zooplankton.

Spatially-averaged estimates of krill biomass increased three-fold from spring to summer (34 to 110 g m⁻²) and then decreased by an order of magnitude to the low values (<10 g m⁻²) observed in fall and winter. The number of aggregations detected per unit sampling effort followed a similar seasonal pattern with maximum and minimum values observed in summer (12.1 aggregations km⁻¹) and winter (0.4 aggregations km⁻¹), respectively. The depth distribution of krill varied between seasons, with most of the krill biomass positioned within the upper 50 m during the summer in contrast to winter when krill were primarily distributed deeper than 100 m. A seasonal shift in the character

of aggregations was apparent with small ($<500 \text{ m}^2$), dense ($>150 \text{ g m}^{-3}$) aggregations dominant during summer and large ($>10^4 \text{ m}^2$), less dense ($<10 \text{ g m}^{-3}$) aggregations prominent during the winter.

Krill were most abundant ($>50 \text{ g m}^{-2}$), in all seasons, at locations on the inner shelf within 100 km of the Antarctic Peninsula. Across-shelf gradients were also observed in the environmental conditions measured during this study and these gradients were strongest during the summer and fall. A spatial separation in krill size classes was observed in all seasons except winter, with small adults ($<40 \text{ mm}$) generally located in inshore regions characterized by relatively lower surface salinities (<33.8). The distribution of large ($>45 \text{ mm}$), reproducing adults during the summer was spatially correlated with surface salinities exceeding 33.8 and the presence of Circumpolar Deep Water at depth. The seasonal and mesoscale variability in the distribution of krill along the west coast of the Antarctic Peninsula observed in this study was consistent with descriptions of krill distributional patterns provided for other regions of the Southern Ocean. Moreover, the temporal change in the mesoscale distribution of krill over an annual cycle is consistent with a shift in the primary habitat of krill between seasons.

ACKNOWLEDGEMENTS

First and foremost, I thank my advisor, Dr. Eileen Hofmann, for giving me the opportunity to work in the Antarctic, an environment which has always fascinated me. Eileen provided guidance throughout this study and fostered my development, in many ways, as a member of the scientific community. I also thank Dr. John Klinck, who single-handedly indoctrinated me into the mysterious world of geophysical fluid dynamics. I appreciate the advice and continual encouragement of Dr. Larry Atkinson, both as a committee member and as the director of the Center for Coastal Physical Oceanography. I am grateful to Drs. Robin Ross and Langdon Quetin for contributing their time and effort to the betterment of this study and for many discussions concerning the complexities of krill ecology.

To the Palmer LTER principal investigators: Drs. Hofmann, Klinck, Fraser, Trivelpiece, Ross, Quetin, Prézelin, Karl, and Smith, I appreciate the scientific interaction which fostered the multidisciplinary nature of this program. I also recognize that several of the data sets analyzed in this study were generously provided by LTER scientists.

I am fortunate to have had the opportunity to become friends and colleagues with many individuals who have at some point called CCPO their professional residence: Glen Wheless, Liz Smith, Arnolde Valle-Levinson, John Moisan, Yvette Spitz, Caitlen Mullen, Marge Deksheniaks, and Dave Smith. To my running partners, Caitlen, Marge, and John, thanks for ensuring that at least during some time each week the wind was at my back.

To my parents, Bill and Carol, I am extremely thankful for their encouragement and enthusiasm towards all my goals, past, present, and future. Finally, to my husband, Joe, and two sons, Brock and Brett, I can not begin to express my love and gratitude that we are a family.

TABLE OF CONTENTS

	Page
LIST OF TABLES	vi
LIST OF FIGURES	vii
1 INTRODUCTION	1
2 BACKGROUND	9
2.1 Palmer LTER Program	9
2.2 Acoustics Technology	10
2.3 Krill distributional patterns	13
3 METHODS	25
3.1 Cruise Descriptions	25
3.2 Acoustic sampling	30
3.3 Post-processing of acoustic measurements	31
4 RESULTS	38
4.1 Sea ice	38
4.2 Hydrography	40
4.3 Phytoplankton	50
4.4 Krill	50
4.5 Mesoscale relationships	69
5 DISCUSSION	118
5.1 Characterization of physical environment	118
5.2 Distribution and abundance of krill	120
5.3 Factors affecting seasonal variations in krill distributions	132
5.4 Variability in krill abundance on smaller space and time scales	144
6 CONCLUSIONS	149
REFERENCES	154
VITA	167

LIST OF TABLES

	Page
1 Summary of research cruises conducted within the region west of the Antarctic Peninsula, which provide acoustic- and net-derived estimates of krill biomass (g m^{-2})	14
2 Summary of acoustic processing parameters	31
3 Summary of krill length-weight relationships by season	34
4 Definitions of dimensional parameters computed for each aggregation	35
5 Summary of the magnitude and timing of peak sea ice coverage observed in winter and summer 1991-1993, relative to mean values derived over the time period, January 1973 through August 1994	39
6 Summary of the abundance of krill aggregations, as defined by transect parameters, observed for all and high-biomass ($HB, >10 \text{ kg m}^{-1}$) aggregations	59
7 Summary of statistics used to describe the mean, median, 90 th percentile, and maximum values observed for the dimensional parameters measured for each krill aggregation	62
8 Acoustically-derived values of krill abundance observed in spring 1991	77
9 Acoustically-derived values of krill abundance observed in summer 1993	91
10 Acoustically-derived values of krill abundance observed for each habitat group and hydrographic regime in summer 1993	94
11 Acoustically-derived values of krill abundance observed in fall 1993	105
12 Acoustically-derived values of krill abundance observed in winter 1993	115

LIST OF FIGURES

	Page
1 A simplified representation of the Antarctic marine food web illustrating the key position occupied by krill, <i>Euphausia superba</i>	2
2 The Southern Ocean with regions of highest krill concentration indicated by stippling	4
3 Basemap of the Palmer LTER study region along the west coast of the Antarctic Peninsula	6
4 Distribution of acoustically-detected krill concentrations (stippled regions, $>100 \text{ g m}^{-2}$) during February 1977 along the Antarctic Peninsula	15
5 A classification scheme for krill aggregations	16
6 Hypothesized migration (solid arrows) by adult krill A) into oceanic waters during spawning season and B) into neritic waters after spawning	18
7 Mean krill abundance, based on net collections, obtained for several years in Bransfield Strait and adjacent areas	20
8 Locations sampled during A) spring, 7 - 21 November 1991 and B) summer, 8 January - 7 February 1993	26
9 Locations sampled during A) fall, 3 March - 5 May 1993 and B) winter, 23 August - 30 September 1993	27
10 Schematic of acoustic post-processing steps	32
11 Schematic of krill aggregation size definitions	35
12 Temperature-salinity diagrams constructed for the upper 500 m: A) winter, B) spring, C) summer, and D) fall	41
13 Vertical distribution of hydrographic variables observed in winter 1993: A) 400 Line (temperature), B) 200 Line (temperature), C) 500 Line (salinity), and D) 300 Line (salinity)	43
14 Frequency distribution of the depth of the 34 salinity isoline which was used as an index of the vertical location of the permanent pycnocline	44
15 Vertical distribution of hydrographic variables observed in summer 1993: A) 400 Line (temperature), B) 500 Line (temperature), C) 200 Line (salinity), and D) 300 Line (salinity)	46
16 Example vertical profiles of bouyancy frequency: A) simple form observed in winter and B) complex form observed in summer	47

	Page
17	Frequency distribution of the mixed layer depth for stations sampled during A) winter, B) spring, C) summer, and D) fall 47
18	Composite distribution of CDW and MCDW along the west coast of the Antarctic Peninsula based on the maximum temperature observed below the permanent pycnocline 49
19	Spatially-averaged estimates of pigment concentrations integrated over the upper 80 m (mg m^{-2}): A) chlorophyll-a, B) fucoxanthin, and C) hex-fucoxanthin 51
20	Example acoustic echograms observed in this study 53
21	Coefficient of variability ($\frac{\text{StdDev}}{\text{Mean}} \times 100\%$) in krill biomass estimates as a function of the elementary distance sampling unit (EDSU) 55
22	Estimates of krill biomass computed from acoustic observations averaged over one elementary distance sampling unit (EDSU, 750 m): A) spring, B) winter, C) summer, and D) fall 56
23	Seasonal changes in spatially-averaged, vertically-integrated krill biomass (g m^{-2}) for: A) all locations, and B) nine locations that were sampled during all four seasons 58
24	The frequency distribution of aggregation dimensional parameters, in terms of number (solid line) and total biomass (dotted line), obtained using the composite data set of aggregations ($n=950$) from all seasons: A) length, B) height, C) cross-sectional area, and D) mean biomass 61
25	Aggregation length versus height by season: A) spring, B) summer, C) fall, and D) winter 64
26	Aggregation area versus mean biomass by season: A) spring, B) summer, C) fall, and D) winter 65
27	A) Cumulative frequency of krill biomass as a function of depth by season: spring (solid), summer (dotted), fall (dashed), and winter (dash-dotted). B) The approximate depth distribution of Antarctic Surface Water (AASW), Circumpolar Deep Water (CDW), and the mixed layer (heavy solid lines) for each season 67
28	Krill depth distribution as a function of time of day by season: A) spring, B) summer, and C) fall 68
29	Same as Figure 28 for subset of acoustic transects collected: A) over a 24-hour period at station 400.060 during the summer, and B) from several locations on the inner shelf of the 300 line during the summer 70

	Page
30 Example acoustic echograms illustrating surface aggregations observed during night: A) station 400.100 in summer and B) station 400.120 in fall.	70
31 Distribution of A) salinity, B) temperature ($^{\circ}\text{C}$), C) chlorophyll-a concentration (mg m^{-2}), and D) habitat groups (A-G, see text for definitions) observed in spring 1991	72
32 Correlations between selected environmental variables used to partition the locations occupied during spring 1991 into habitat groups: A) salinity and total chlorophyll, and B) fucoxanthin and hex-fucoxanthin	73
33 Length frequency distribution (LFD) of krill individuals (1 mm resolution) collected in net samples during spring 1991: A) group 1, B) group 2, C) group 3, and D) mesoscale distribution of LFD groups	75
34 Distribution of vertically-integrated krill biomass (g m^{-2}) observed at locations sampled during spring 1991	78
35 Relationship between cross-sectional area (m^2) and mean biomass (g m^{-3}) for aggregations observed during spring 1991 at locations associated with each habitat group	80
36 Echograms illustrating different aggregation patterns observed during spring 1991: A) typical pattern of solitary or small groups of aggregations irregularly spaced along the acoustic transect (500.160); B) vertically restricted layer observed in Dallman Bay (700.020); C) vertical alignment observed near ice edge (600.080); and D) deeper distribution observed at upwelling station (600.100)	82
37 Vertical distribution of normalized krill biomass (\diamond), buoyancy frequency ($10^{-4} \text{ rad}^2 \text{ s}^{-2}$, solid black line), chlorophyll (mg m^{-2} , dashed line with + symbols), and fucoxanthin (mg m^{-2} , solid line with + symbols) observed during spring 1991 at stations: A) 500.160, B) 600.100, C) 600.080, and D) 700.020	83
38 Distribution of A) salinity, B) temperature ($^{\circ}\text{C}$), C) chlorophyll-a concentration (mg m^{-2}), and D) habitat groups (A-C, X-Z, see text for definitions) observed in summer 1993	86
39 Correlations between selected environmental variables used to partition the locations occupied during summer 1993 into habitat groups: A) salinity and total chlorophyll, and B) fucoxanthin and hex-fucoxanthin	88
40 Length frequency distribution (LFD) of krill individuals (1 mm resolution) collected in net samples during summer 1993: A) LFD group 1, B) LFD group 2, C) LFD group 3, D) LFD group 4, and E) mesoscale distribution of LFD groups	90

	Page	
41	Distribution of vertically-integrated krill biomass (g m^{-2}) observed at locations sampled during summer 1993	92
42	Relationship between cross-sectional area (m^2) and mean biomass (g m^{-3}) for aggregations observed during summer 1993 at locations associated with each habitat group	95
43	Echograms illustrating different aggregation patterns observed during summer 1993: A) typical pattern observed for stations with krill biomass $<100 \text{ g m}^{-2}$ (600.080); B) closely packed dense aggregations observed at station on the inner shelf (400.060); C) same as B) at station 300.100 on the middle shelf; D) very large ($>5000 \text{ m}^2$) aggregations observed at station 400.080	97
44	Vertical distribution of normalized krill biomass (\diamond), temperature ($^{\circ}\text{C}$, solid black line), chlorophyll (mg m^{-2} , dashed line with + symbols), and fucoxanthin (mg m^{-2} , solid line with + symbols) observed during summer 1993 at stations: A) 300.060, B) 400.140, C) 600.040, and D) 300.100	99
45	Distribution of A) salinity, B) temperature ($^{\circ}\text{C}$), C) chlorophyll-a concentration (mg m^{-2}), and D) habitat groups (A-C, X-Z, see text for definitions) observed in fall 1993	101
46	Correlations between selected environmental variables used to partition the locations occupied during fall 1993 into habitat groups: A) salinity and total chlorophyll, and B) fucoxanthin and hex-fucoxanthin	103
47	Length frequency distribution (LFD) of krill individuals (1 mm resolution) collected in net samples during fall 1993: A) LFD group 1, B) LFD group 2, C) LFD group 3, D) LFD group 4, and E) mesoscale distribution of LFD groups	104
48	Distribution of vertically-integrated krill biomass (g m^{-2}) observed at locations sampled during fall 1993	106
49	Relationship between cross-sectional area (m^2) and mean biomass (g m^{-3}) for aggregations observed during fall 1993 at locations: A) on the inner shelf, B) near the shelfbreak, and C) all other regions	108
50	Echograms illustrating different aggregation patterns observed during fall 1993: A) typical pattern of solitary or small groups of aggregations (station 300.140); B) example of large aggregations found on the inner shelf (station 200.000); C) unique, horizontally extensive, layer-like aggregation observed at station 500.020; D) deep, large aggregations observed at shelfbreak station 250.160	109
51	Distribution of A) salinity, B) temperature ($^{\circ}\text{C}$), and C) chlorophyll-a concentration (mg m^{-2}) observed in winter 1993	111

	Page	
52	Correlations between selected environmental variables observed at locations sampled during winter 1993: A) salinity and total chlorophyll, and B) fucoxanthin and hex-fucoxanthin	112
53	Length frequency distribution (LFD) of krill individuals (1 mm resolution) collected in net samples during winter 1993: A) station 500.060 (6 September), B) station 500.060 (8 September), and C) five stations on outer and middle shelf	113
54	Distribution of vertically-integrated krill biomass (g m^{-2}) observed at locations sampled during winter 1993	114
55	Echograms illustrating different aggregation patterns observed during winter 1993: A) large aggregations observed at station 500.060 on 6 September; B) same as A) for different acoustic transect sampled 30 minutes later; C) same as A) on 8 September; D) typical pattern observed for other stations (400.140)	116
56	Idealized schematic of the distribution of water masses observed within the region west of the Antarctic Peninsula: Antarctic Surface Water (AASW), Circumpolar Deep Water (CDW), and Modified-CDW (MCDW)	119
57	Comparison of acoustically-derived, spatially-averaged estimates of krill biomass (g m^{-2}) by month	122
58	Conceptual model of krill interactions within the Antarctic ecosystem . . .	133
59	Schematic of the upper ocean circulation west of the Antarctic Peninsula, including Bransfield Strait, constructed from historical data sources	135

INTRODUCTION

The Antarctic krill, *Euphausia superba*, has been recognized as an important species in the Southern Ocean since the early 1800s. Anecdotal reports, primarily from whalers and sealers, of dense concentrations of krill, which “turned the sea red”, were frequently noted, not as a target for fishing efforts, but as the source of food for whales. The British *Discovery Committee* sponsored a series of scientific expeditions to the Southern Ocean between 1926-1939 with the purpose of investigating relationships between the pelagic ecosystem and the physical environment (Hardy and Gunther, 1935). The extensive collections made during these circumpolar surveys represent the foundation of much of today’s knowledge concerning the distributional patterns and life history of the Antarctic krill (Fraser, 1936; Bargmann, 1945; Marr, 1962; Mackintosh, 1972; 1973). These results clearly established krill as a major link between primary producers and many populations of Antarctic carnivores (Figure 1), including whales, seals, seabirds, penguins, squids and fishes (Marr, 1962; Gulland, 1970; Knox, 1970).

Krill became a commercially harvested species during the late 1960s and today is the subject of an active fishery by several nations. Concern over the conservation of the Antarctic marine ecosystem prompted the international scientific community to establish the Biological Investigations of Marine Antarctic Systems and Stocks (BIOMASS) program, which had the objective of developing a sound ecological strategy for the exploitation of Antarctic marine living resources (El-Sayed, 1977). Several large field studies were conducted in selected areas of the Southern Ocean as part of this ten-year program and efforts were focused on quantifying the standing stock and productivity of the krill population (El-Sayed, 1994).

Influenced largely by the BIOMASS program, the Antarctic Treaty nations formed

This dissertation conforms to the journal model *Deep-Sea Research*.

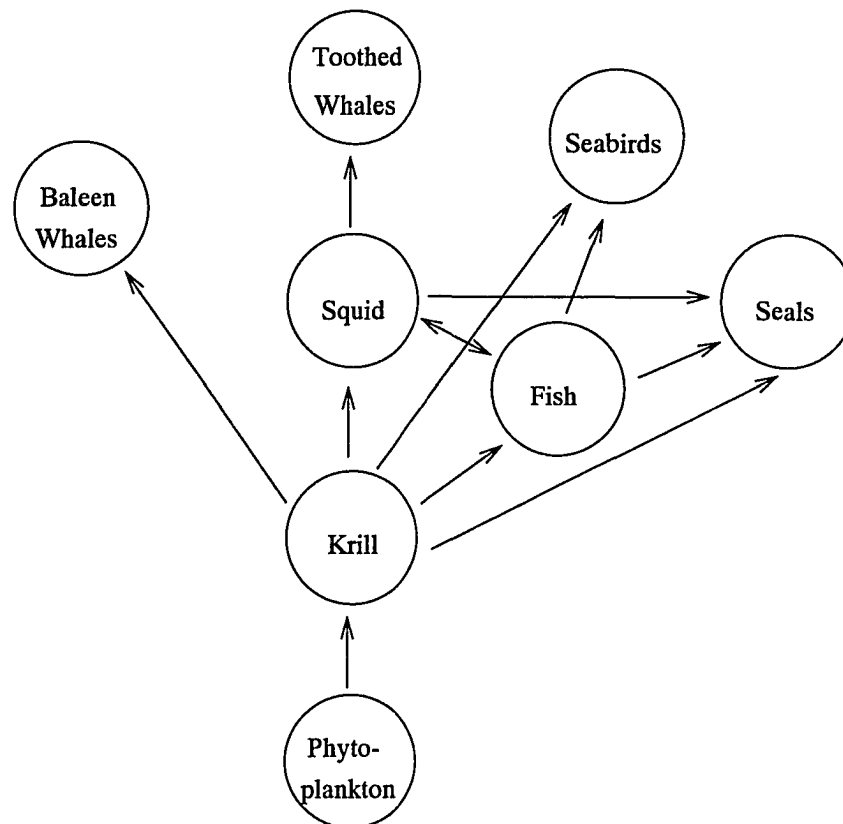


Figure 1: A simplified representation of the Antarctic marine food web illustrating the key position occupied by krill, *Euphausia superba*. Figure adapted from Murphy *et al.* (1988).

the Committee for the Conservation of Antarctic Marine Living Resources (CCAMLR), to manage Southern Ocean marine resources including krill (Anon, 1981). An ecosystem approach to resource management was adopted by CCAMLR and krill catch quotas have been established in an effort to maintain the size of the krill population at a level which supports stable recruitment and furthermore at a level which does not disrupt the ecological relationships between krill and dependent predator species. Many nations involved in BIOMASS have continued scientific research of the Antarctic marine ecosystem in support of the goals of CCAMLR.

Krill inhabit the broad, circumpolar region between the Antarctic Polar Front and the Antarctic continent (Figure 2); however, the highest concentrations are confined to the area affected by the seasonal advance and retreat of annual pack ice (Marr, 1962; Mackintosh, 1972; 1973). Standing stock estimates of krill from net and acoustic surveys conducted in several regions of the Southern Ocean have shown several orders of magnitude variation between regions, within regions, and between years (Everson, 1983; Hampton, 1985; Priddle *et al.*, 1988; Miller and Hampton, 1989a; Everson and Miller, 1994).

Krill distributions on all spatial scales are characteristically very heterogeneous and this patchiness is generally attributed to the combination of three main factors: environmental variability (Amos, 1984; Witek *et al.*, 1988; Nast *et al.*, 1988; Sahrhage, 1988; Daly and Macaulay, 1991), swarming behavior (Marr, 1962; Miller and Hampton, 1989a) and the strong swimming capabilities of krill (Kils, 1981; Hamner *et al.*, 1983; Hamner, 1984). In particular, the tendency to form discrete cohesive aggregations (10-10000 individuals m^{-3}) is a fundamental characteristic of the Antarctic krill which differentiates this species from other zooplankters (Marr, 1962). Moreover, krill aggregations span a broad range of time and space scales (Kalinowski and Witek, 1985) and thus provide multiple levels of organization through which the krill population may interact with environmental variability (Murphy *et al.*, 1988).

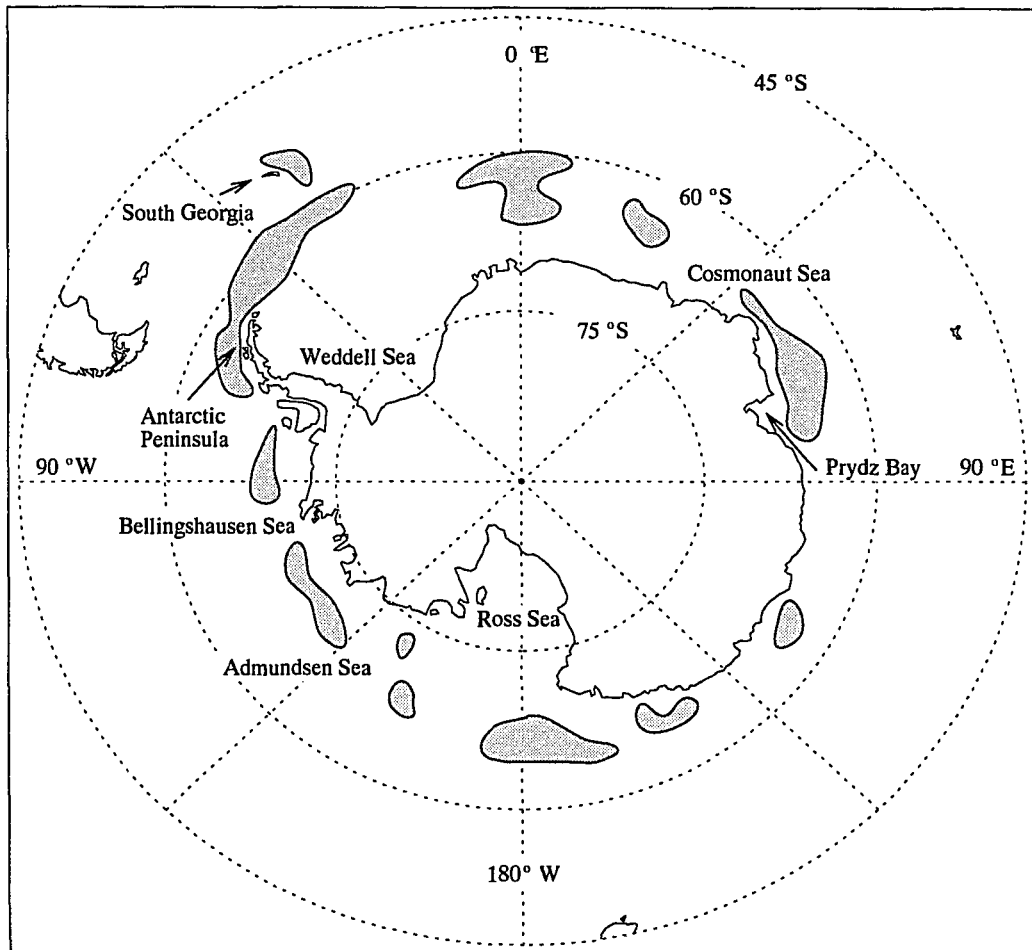


Figure 2: The Southern Ocean with regions of highest krill concentration indicated by stippling. Figure adapted from Everson and Miller (1995).

There is still a large degree of uncertainty regarding the assessment of krill biomass and production at the global, regional and even local scales (Everson, 1988; Ross and Quetin, 1988; Miller and Hampton, 1989a), yet this information is integral to an improved understanding of the Antarctic ecosystem and to the successful management of the krill fishery. Some of this uncertainty stems from the bias of historical observations of krill distributions towards collections made during a single season, the summer, and towards selected regions, most notably those targeted by the BIOMASS program.

The establishment of an Antarctic Long-Term Ecological Research (LTER) program, by the National Science Foundation at Palmer Station on Anvers Island (Figure 3), provided an unique opportunity for collection of long-term data sets that can be used to study the pelagic ecosystem of the Southern Ocean. The central tenet of the Palmer LTER program is that the annual advance and retreat of sea ice is a major physical determinant of spatial and temporal changes in the structure and function of the marine ecosystem west of the Antarctic Peninsula (Smith *et al.*, 1995). This region exhibits high interannual and annual variability in ice coverage (Parkinson, 1992) which is expected to greatly influence the distribution and production of all levels of the marine ecosystem on the same time scales (Smith *et al.*, 1995). The Palmer LTER field studies began in 1991 and are still continuing. A diverse set of multidisciplinary measurements are made within a defined region west of the Antarctic Peninsula during annual summer cruises and occasional process cruises.

The objective of the research described in this study is to characterize the distribution of krill and selected environmental parameters, in terms of space and time variability, within the coastal region west of the Antarctic Peninsula. This study is based on analysis and interpretation of multidisciplinary data sets collected as part of the Palmer LTER program and focuses specifically on variability observed at the temporal scale of seasons and spatial scales of 10 to 100 km (mesoscale). The basic data set, around which this analysis is formed, consists of acoustic measurements of the distribution and abundance

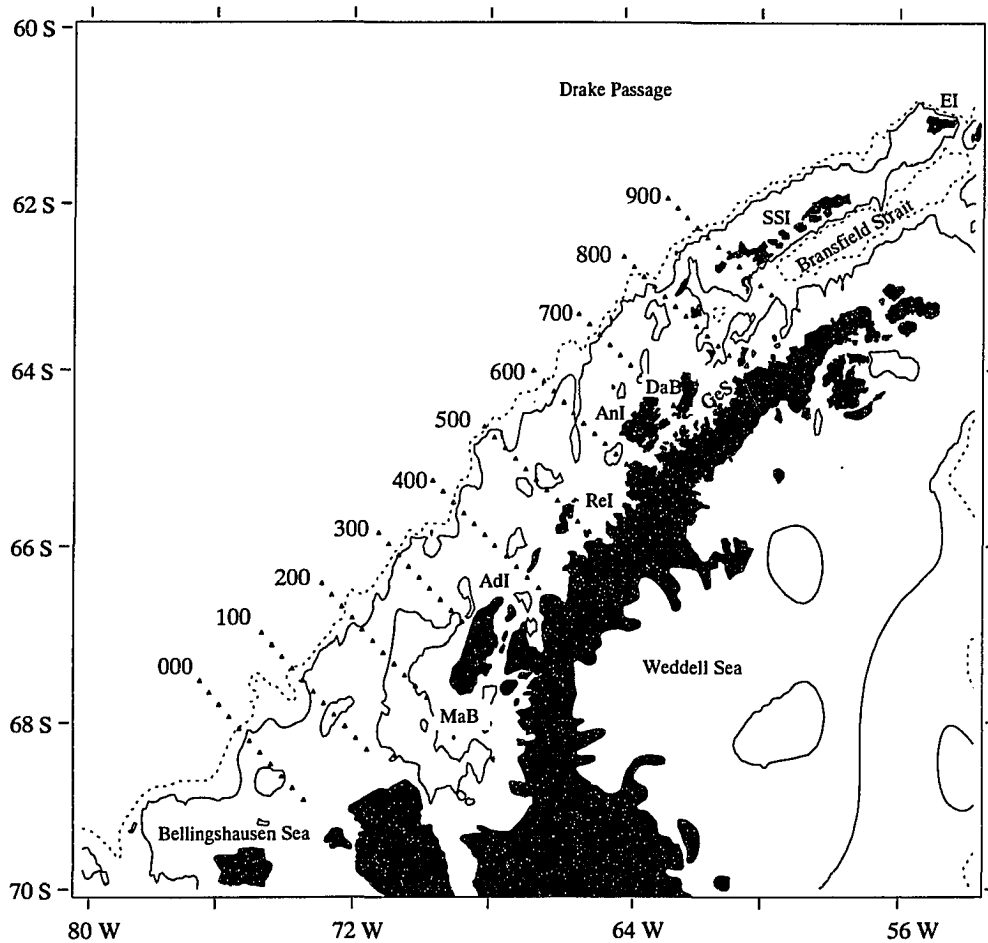


Figure 3: Basemap of the Palmer LTER study region along the west coast of the Antarctic Peninsula. Stations (Δ) are located at 20 km intervals along ten transect lines which are spaced 100 km apart. The solid and dashed lines represent the 500- and 1000-m isobaths, respectively. The coastline and bathymetry were derived from the JEBCO and ETOPO5 datasets, respectively. Geographic locations are abbreviated as: AdI-Adelaide Island, AnI-Anvers Island, DaB-Dallman Bay, EI-Elephant Island, GeS-Gerlache Strait, MaB-Marguerite Bay, ReI-Renaud Island, and SSI-South Shetland Islands.

of Antarctic krill. Multidisciplinary data from the first four Palmer LTER cruises are used and these provide full seasonal coverage, with three of the seasons sampled consecutively in a single year.

The acoustic observations of krill are analyzed to generate distributional maps of vertically-integrated krill biomass and to characterize the depth distribution of krill. Given the significant impact of swarming behavior on krill distributions, the acoustic measurements are also used to provide a quantitative description of krill aggregation characteristics. The krill observations are coupled in time and space to environmental conditions defined by measurements of weather and ice parameters, hydrographic structure, total chlorophyll and concentrations of chemotaxonomic pigments, and net estimates of zooplankton and micronekton. The following specific research questions are addressed:

- What is the horizontal and vertical distribution of krill, in terms of total biomass and aggregation characteristics, in the region west of the Antarctic Peninsula?
- How do these spatial distributions of krill change between seasons?
- To what extent are the seasonal and mesoscale krill distributional patterns coupled to environmental variability, in particular the hydrographic character of the upper ocean, local ice conditions, and the concentration and composition of food resources?

This research is expected to increase the general understanding of the ecological consequences of physical and biological interactions within the Southern Ocean. This baseline understanding is required to facilitate future predictions of how the Antarctic marine ecosystem will respond to perturbations, e.g., climate change, habitat modification, and fishery exploitation.

Since Antarctic krill is widely recognized as an important species in the Antarctic marine food web, an improved understanding of variations in the distribution of krill should

provide insight to the understanding of variations in the distribution of phytoplankton (primary food item of krill) as well as variations in the distribution of predators which are dependent on krill as food. For this reason, it is anticipated that the results of this study will be of particular interest to CCAMLR and also to two new international programs currently under development. The Joint Global Ocean Flux Study (JGOFS) has identified the Southern Ocean as a key geographic region in which to study processes that control primary production and fluxes of biogenic materials (Anderson, 1993). Likewise, the Global Ocean Ecosystem Dynamics (GLOBEC) program has established an initiative to examine processes controlling secondary production (GLOBEC, 1993) in the Southern Ocean.

A distinguishing feature of the Palmer LTER study region is that it is a coastal shelf system and thus this program provides data sets for comparison with those collected by other Southern Ocean programs in predominantly oceanic regions. Historical observations of the region west of the Peninsula are limited, especially for the southern portions, however, this area is considered a source of krill for downstream regions including Bransfield Strait and South Georgia, which have been intensively sampled over the last two decades (Siegel, 1988; Priddle *et al.*, 1988; Everson and Miller, 1994).

The next chapter presents background information on the Palmer LTER program, acoustic techniques, and historical descriptions of krill distributions. The methods used to collect and analyze the krill and environmental data sets are described in Chapter 3. Chapter 4 provides a description of the results obtained from analysis of the multidisciplinary data sets. Seasonal and mesoscale variations observed in the environmental and krill distributions are discussed in Chapter 5 and placed within the context of observations from other programs. The final chapter provides a summary.

BACKGROUND

This chapter provides a review of several topics considered important to the design and implementation of this study. The first section describes the LTER program in terms of objectives and the physical setting of the study region. A brief review of the application of acoustics techniques to estimate krill biomass is presented in the second section. An overview of observations describing historical krill distributional patterns is given in the final section.

2.1 Palmer LTER Program

The central hypothesis of the Palmer LTER program is that physical processes, particularly the extent of winter sea ice, impact all trophic levels of the Antarctic pelagic marine ecosystem, from total annual primary production to breeding success in apex predators (Smith *et al.*, 1995). To address this hypothesis, long term multidisciplinary data sets are being collected to document interannual and annual variations in selected environmental and ecosystem parameters; establish linkages between ecological processes and physical environmental variables; and, construct numerical models to simulate ice-ecosystem dynamics. The study area of the Palmer LTER program covers a large geographic region extending from the southern end of Bransfield Strait to the northern end of Alexander Island (Figure 3). The continental shelf in this region is roughly 150 km wide and 200 to 500 m deep. Variability in the 500 m isobath illustrates the presence of several topographic cuts and channels along the shelfbreak which may influence exchange processes between shelf and oceanic waters.

The sampling grid established by the Palmer LTER program (Figure 3) is oriented with the alongshore axis running approximately parallel to the Peninsula over a 900 km distance and the across-shelf axis running 200 km offshore from the Antarctic Peninsula (Waters and Smith, 1992). Ten standard transects have been defined which are spaced

100 km apart with primary sampling stations located every 20 km along each transect (Figure 3). Each transect is designated by a three digit number (ranging from 000 to 900) which identifies the distance (km), of a transect, from the southern-most transect. Sampling locations are identified by coordinates of the form xxx.yyy, where xxx is the transect number and yyy is the distance (km), of a location, from the inner-most primary station. For example, station 300.100 refers to the location positioned 300 km from the southern-most transect line and 100 km from the inner-most primary station. The 000.000 location is positioned at latitude 68.983°S and longitude 73.579°W. Five cardinal transect lines (200, 300, 400, 500, and 600) have been established between Anvers and Adelaide Islands (Figure 3) and the annual cruises focus on this region.

The general character of the marine habitat and pelagic ecosystem for the general area west of the Antarctic Peninsula has recently been summarized based on a compilation and synthesis of historical data sets from this region. This monograph was undertaken by the principle investigators of the Palmer LTER program to provide a foundation for ongoing and future LTER research efforts. Rather than provide an extensive review here, the following chapters in the monograph which describe environmental and ecological observations are referenced: weather (Smith *et al.*, in press b), sea ice (Stammerjohn and Smith, in press a), hydrography and circulation (Hofmann *et al.*, in press), phytoplankton (Bidigare *et al.*, in press; Smith *et al.*, in press a), zooplankton (Ross *et al.*, in press; Quetin *et al.*, in press), and upper level predators (Costa and Crocker, in press; Kellerman, in press; Fraser and Trivelpiece, in press a; Trivelpiece and Fraser, in press).

2.2 Acoustics Technology

The results derived from the *H.M.S. Discovery* expeditions indicated that nets were an inappropriate sampling method to quantify the abundance of krill. As a result, the BIOMASS program examined several different sampling methods and ultimately demonstrated that acoustic techniques provide a powerful tool for the estimation of krill abun-

dance and for investigating krill aggregations (Anon, 1986). Comprehensive reviews of the fundamental principles of underwater acoustics and its application to abundance estimation of biological organisms are available in Clay and Medwin (1977) and MacLennan and Simmonds (1992).

Acoustic techniques provide a continuous measurement of echo returns along a survey track over a defined vertical range. The depth of the transducer establishes the minimum sampling depth and the acoustic frequency determines the effective sampling range. Typically, acoustic surveys for krill use a hull-mounted or surface towed transducer with an operating frequency of 120 kHz and so in practice, no information is provided concerning the distribution of krill within the near-surface layer (0-10 m), deeper than 200 m, or dispersed below the noise detection limit.

2.2.1 Target strength

Conversion of acoustic echoes into measurements of krill biomass employs the technique of echo integration, in which the returned echo energy is assumed to represent the linear sum of echoes from individual animals randomly distributed within the sample volume (MacLennan and Simmonds, 1992). The quantity of returned echo energy is related to two factors: the quantity of incident energy and the reflectivity of the insonified organisms. The magnitude of incident energy depends upon the characteristics of the transmitting sounder which are defined by the equipment calibration factors.

The reflectivity of an organism is defined in terms of its backscattering cross-section (σ_{bs}), which has units of area (m^2), but is generally expressed as target strength (TS), where $TS = 10 \log(\sigma_{bs})$ (Greenlaw, 1979). The factors affecting target strength values are poorly understood for most zooplankton taxa including krill. Target strength varies between species, between different sized individuals of the same species, and between acoustic frequencies (Stanton *et al.*, 1994). Typically relationships are established which express TS as a function of an easily measured index of the organism's acoustic size,

such as length or weight (Weibe *et al.*, 1990). Thus there are three prerequisites to the application of bioacoustics: 1) identification of the taxonomic groups responsible for the scattering; 2) determination of their size distribution; and, 3) identification of TS-size relationships. Net samples are generally used to satisfy the first two requirements.

Identification of TS relationships has been investigated using two methods: theoretical modeling and direct measurements. In theoretical models, the species of interest is represented as an object of uniform composition, that has a defined shape, and scattering is predicted based on the contrast in specific density and the speed of sound between the organism and seawater. Scattering models have been derived for a wide variety of shapes ranging from fluid spheres (Greenlaw, 1979; Holliday and Pieper, 1980) to regular and irregular cylinders (Stanton, 1989; Stanton *et al.*, 1993). The target strength versus krill length relationship used during the BIOMASS program (Anon, 1986) was based on predictions from a fluid sphere model.

An extensive set of direct measurements, made on encaged krill near South Georgia, indicated that the TS value for krill is much lower than previously thought (Foote *et al.*, 1990; Everson *et al.*, 1990). In response, Greene *et al.* (1991) provided new TS-length relationships over the full size range of krill at the acoustical frequencies commonly used in field studies. This relationship was computed from an empirically derived linear regression equation established based on direct measurements on a variety of zooplankton taxa (Wiebe *et al.*, 1990). Using an acoustic dual-beam system, Hewitt and Demer (1991) made *in-situ* measurements of krill target strength and these observations were consistent with predictions provided by the Greene *et al.* (1991) relationship. These measurements also indicate that krill target strength is best represented by theoretical models based on bent or deformed cylinders (Chu *et al.*, 1993; Demer and Hewitt, in press).

2.2.2 Line intercept measurements

Towed downward-looking acoustic systems provide instantaneous two-dimensional

representations of dynamic three-dimensional entities. An acoustically-detected krill aggregation is represented by only that portion of the aggregation which is intercepted by the acoustic survey track (i.e., line intercept measurement). Assuming that aggregations are irregular in shape and that the orientation of any particular aggregation is random with respect to the survey track, each alongtrack measurement of aggregation length is considered a stochastic sample of the true length and therefore may range from 0 to the maximum horizontal dimension of the aggregation (MacLennan and Simmonds, 1992). As such, histograms of aggregation intercept measurements must be considered crude representations of the true size distribution.

The large degree of uncertainty associated with each individual measurement of aggregation length, however, does not preclude comparisons between the frequency distributions of these measurements made on a large number of aggregations. Furthermore, the reliability of these comparisons should improve as a function of the number of observations. Characterizing the size of aggregations is sensitive to the stochastic nature of the line intercept measurement and comparisons made with small sample sizes should be treated with caution.

2.3 Krill distributional patterns

Since the region west of the Antarctic Peninsula, south of Anvers Islands (Figure 3), has not been well studied, the approach taken in this section is to combine observations from within this region with those collected during the BIOMASS program which focused on the large area extending from Anvers Island northeast to South Georgia and encompassing Bransfield Strait, the South Shetland Islands, Elephant Island and the Weddell/Scotia confluence. Studies from outside the Atlantic sector will be described only in support of observations relevant to the study region. A summary of cruises which provided estimates of krill abundance along the Peninsula is given in Table 1.

Table 1: Summary of research cruises conducted within the region west of the Antarctic Peninsula, which provide acoustic- and net-derived estimates of krill biomass (g m^{-2}).

Sampling Method	Sampling Period		Krill Biomass	Reference
	Months	Year		
Acoustics	Feb-Mar	1977	Range: 0-100*	Witek <i>et al.</i> (1981)
	Feb	1979	Range: 0-100*	Witek <i>et al.</i> (1988)
	Feb-Apr	1978	not available	Cram <i>et al.</i> (1979)
Nets	Dec-Jan	1990	Mean: 4.50**	Siegel (1992)
	Feb	1982	Mean: 4.90**	Siegel (1985)
	Mar	1985	Mean: 4.23**	Siegel (1986)
	May-Jun	1986	Mean: 0.55**	Siegel (1989)
	Nov-Dec	1987	Mean: 6.13**	Siegel (1989)
	Nov-Dec	1984	Mean: 17.0**	Endo <i>et al.</i> (1985)

* Adjusted by factor of 4.76 (Trathan *et al.*, 1993a) to correct for improper target strength.

** Estimate also includes data from Bransfield Strait.

2.3.1 Observations from west of the Antarctic Peninsula

2.3.1.1 Acoustic surveys

The earliest acoustic surveys conducted in the Southern Ocean, to explore the possibility of using this technique to map the distribution of krill, took place during the late 1970s. Three of these (Cram *et al.*, 1979; Witek *et al.*, 1981; Witek *et al.*, 1988) included sampling along the west coast of the Peninsula and these pioneer surveys represent the only published descriptions of quantitative krill biomass estimates using acoustic measurements for the study region.

During the summer of 1977 and 1979, krill aggregations were acoustically-detected throughout a large survey region which extended from Adelaide Island to Elephant Island (Witek *et al.*, 1981; Witek *et al.*, 1988). The highest concentrations of vertically-integrated krill biomass, 100 g m^{-2} , were observed over the shelf with notably lower biomass values located on the outer-shelf and beyond the shelfbreak (Figure 4). No correlation was found between krill abundance and hydrographic variables (temperature, salinity, oxygen, nutrients) or phytoplankton concentrations (Witek *et al.*, 1981). However, Witek *et*

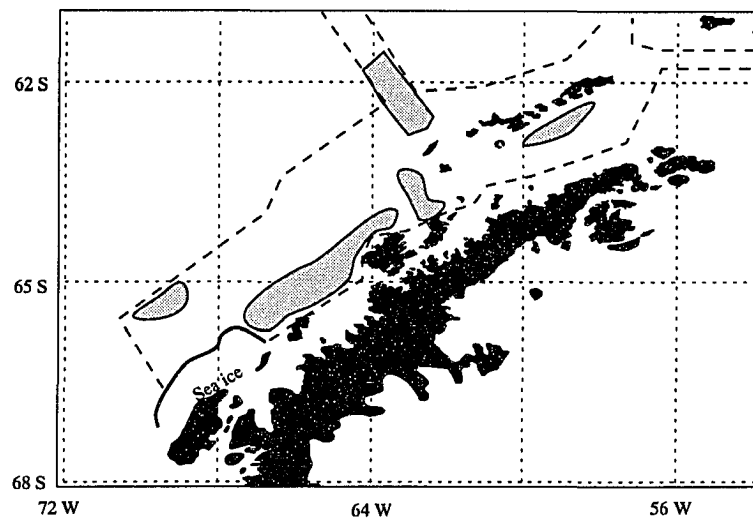


Figure 4: Distribution of acoustically-detected krill concentrations (stippled regions, 100 g m^{-2}) during February 1977 along the Antarctic Peninsula. The dashed lines frame the region of acoustic observations. Figure adapted from Witek *et al.* (1988).

al. (1988) suggested that the distribution of krill was related to water circulation and that the highest krill biomass generally occurred in areas characterized by high gradients in current velocity, e.g., fronts, meanders, and eddies. This distributional feature was consistent with earlier net-based observations from other regions which suggested that the formation of krill concentrations was linked with variations in large-scale and mesoscale circulation patterns (Marr, 1962; Mackintosh, 1973; Maslennikov and Solyanin, 1980; Stein and Rakusa-Suszczewski, 1984)

The vertical distribution of krill was also described by Witek *et al.* (1981) based on acoustic measurements collected over the depth range 10-200 m during the summer of 1977. Over 90% of the krill biomass was observed in the upper 90 m of the water column and there was a distinct diel change with krill swarms deeper and more cohesive during the day compared to a more dispersed, shallower night distribution.

The acoustic observations described by Witek *et al.* (1981; 1988) also represent the first efforts to quantify the physical size and internal density structure of individual krill

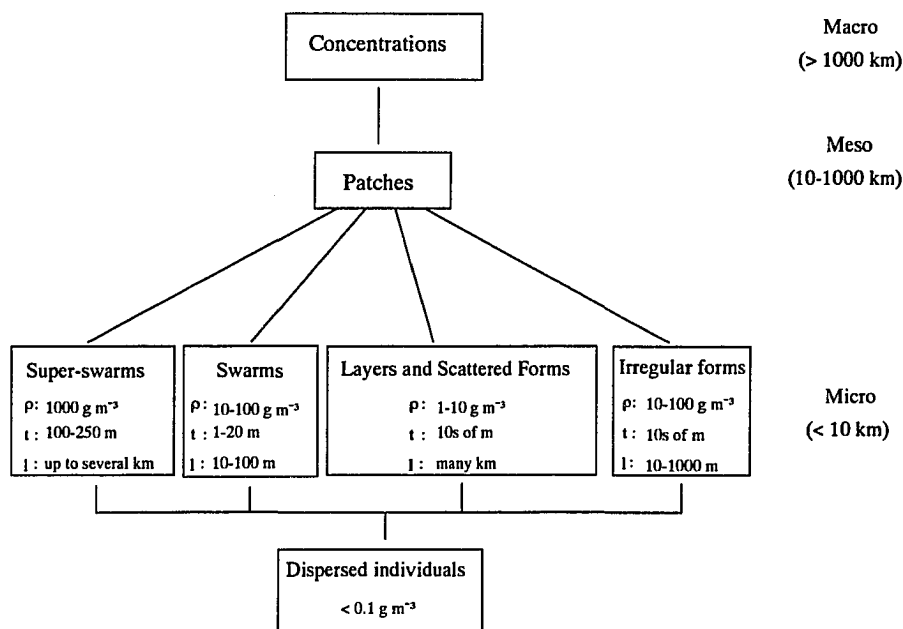


Figure 5: A classification scheme for krill aggregations. Figure adapted from Miller and Hampton (1989a) as modified from Kalinowski and Witek (1985). Aggregation parameters are abbreviated as ρ -density, t -thickness, l -length.

aggregations. Measurements from over 1200 aggregations, detected between Adelaide and Anvers Islands, showed that on average swarms were small, between 50-90 m in length, and exhibited volumetric biomass values between 50-200 g m⁻³ (Witek *et al.*, 1988). Larger aggregations, which were layer-like in appearance and extended up to one kilometer in length, were observed within a concentration of krill located near Adelaide Island (Witek *et al.*, 1981).

During the late summer of 1978, an acoustic survey was conducted in the vicinity of Gerlache Strait by a South African expedition (Cram *et al.*, 1979). Three major types of aggregations were described: layers, swarms, and super-swarms, and these observations combined with those of Witek *et al.* (1981) provided the basis for the classification scheme presented by Kalinowski and Witek (1985) as illustrated in (Figure 5). Small (<100 m) cohesive swarms by far represent the numerically dominant aggregation type (Witek *et al.*, 1988). The terms, layer and irregular form, are used to describe aggregations which extend

continuously over large distances (100s - 1000s m) and vary in thickness and continuity (Figure 5). These forms occur less frequently than swarms, and may represent the merging of cohesive aggregations or multi-species aggregations (Kalinowski and Witek, 1985). Super-swarms are exceptionally large, both horizontally (1-10 km) and vertically (100-200 m), and exhibit very high volumetric densities (100-1000 g m⁻³). This form occurs infrequently and has been observed in Gerlache Strait (Cram *et al.*, 1979), near Elephant Island (Macaulay *et al.*, 1984), and in the Prydz Bay region (Higgenbottom and Hosie, 1989).

2.3.1.2 Net surveys

In support of BIOMASS and CCAMLR, a series of German expeditions were made along the Antarctic Peninsula, which included net collections of krill over a period of several years (Table 1) (Siegel, 1985; 1986; 1988; 1989; 1992). All net tows were collected on the same predefined survey grid and processed in a standardized manner which facilitated direct comparisons between cruises (Siegel, 1992). Two main features concerning the distribution of krill were derived from these data sets. First, the spatially-averaged estimate of krill biomass was similar between years for spring and summer cruises (4.2 - 6.1 g m⁻², Table 1), but was an order of magnitude lower during the single winter cruise (0.55 g m⁻²).

The second feature was the observation of a distinct spatial separation in the maturity stage and size class of krill during summer cruises which represent the time period of spawning activity (Siegel, 1988). Gravid and spawning adults occurred along the continental slope and in oceanic waters; whereas, subadult krill dominated nearer the coast, and juveniles were confined to inner shelf waters. Siegel (1988) hypothesized that active migration movements by adult krill (Figure 6) at the onset and completion of spawning activity were responsible for the across-shelf pattern in krill size structure observed during the summer. Trathan *et al.* (1993a) provided additional support for Siegel's (1988)

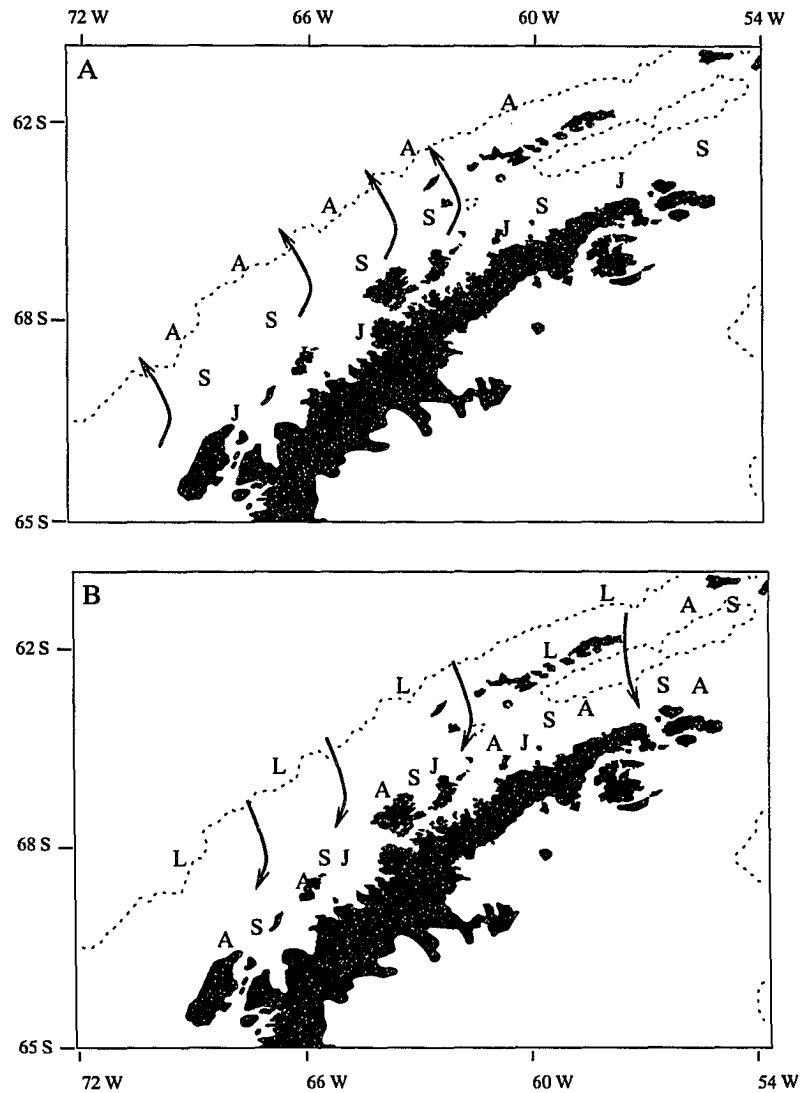


Figure 6: Hypothesized migration (solid arrows) by adult krill A) into oceanic waters during spawning season and B) into neritic waters after spawning. The distribution of larvae (L), juvenile (J), subadult (S), and adult (A) krill developmental stages is also shown. Figure adapted from Siegel (1988).

hypothesis using FIBEX data and furthermore showed a summer correlation between krill size classes and oceanographic variables.

Krill collections were made as part of a Japanese cruise to the Antarctic Peninsula during SIBEX in the early summer of 1984 (Endo *et al.*, 1985). The average biomass observed during this study was four-fold higher than that observed by Siegel (1992)(Table 1). However the stations occupied in the Japanese study were restricted to the shelf region, where elevated concentrations of krill of the same relative magnitude were noted by Siegel (1992).

2.3.2 Studies within the BIOMASS Atlantic sector

2.3.2.1 Temporal variability

There were several other German expeditions which included net sampling surveys outside of the Palmer LTER study region which were focused within Bransfield Strait and around the South Shetland Islands. The mean monthly abundance of krill from eleven data sets compiled by Siegel (1988) shows a general trend of low krill abundance during the winter, increasing krill density from October to February and then a decrease during the fall (Figure 7). This seasonal progression in krill abundance was consistent with year-round observations made by Stepnik (1982) within Admiralty Bay, on King George Island. Using multi-national data from 32 cruises over the time period 1976-1987, Godlewska and Rakusa-Suszczewski (1988) also described a similar seasonal pattern for the broad region encompassing FIBEX sampling efforts. However, variability was highest (2-3 orders of magnitude) at the interannual time scale which was probably due to compilation of data sets regardless of sampling effort, subarea coverage, or differences in collection and processing methods (Godlewska and Rakusa-Suszczewski, 1988).

Acoustically-derived krill biomass estimates have been made since 1987 in support of a United States sponsored CCAMLR program to monitor populations of seabirds and seals off Elephant Island (Holt *et al.*, 1991). This program conducts several acoustic

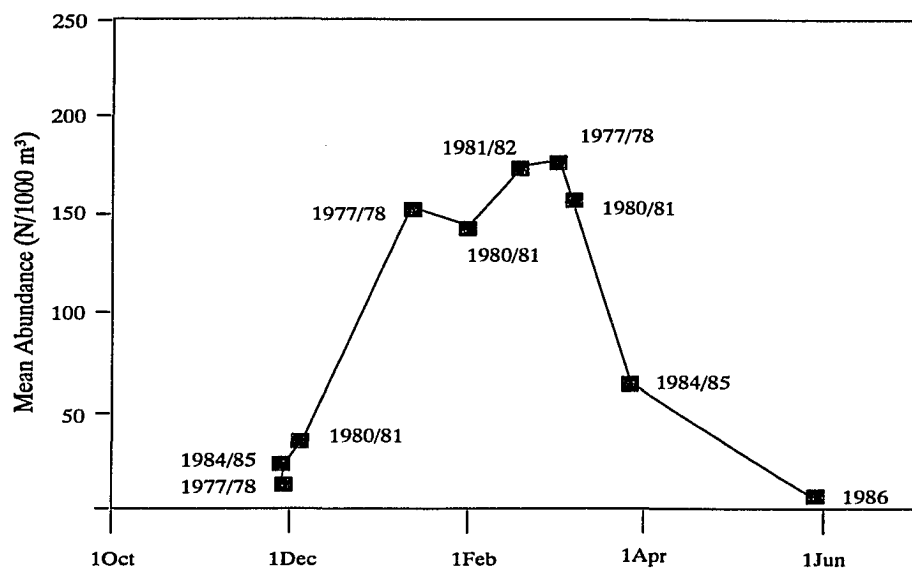


Figure 7: Mean krill abundance, based on net collections, obtained for several years in Bransfield Strait and adjacent areas. Figure adapted from Siegel (1988).

surveys within each year over the time period December through March (Rosenberg, 1991). Spatially-averaged estimates of krill biomass have varied by a factor of eight ($17\text{--}135\text{ g m}^{-2}$) for surveys conducted within the AMLR study region between 1987 and 1993 (Hewitt and Demer, 1993a;b). Interannual comparisons indicate that in some years, krill biomass increased from January to March (e.g., 17 to 90 g m^{-2} in 1990); whereas, in other years a decrease was observed (e.g., 60 to 30 g m^{-2} in 1992) (Hewitt and Demer, 1993a).

2.3.2.2 Spatial variability

A distinct offshore-inshore variation in krill biomass levels and maturity stages of krill, was observed during a combined acoustic/net survey conducted north of the South Shetland Islands during the summer of 1991 (Ichii *et al.*, 1993). Vertically-integrated krill abundance was low ($<10\text{ g m}^{-2}$) in the oceanic zone, slightly higher (37 g m^{-2}) in the slope frontal zone and very high (135 g m^{-2}) along the shelfbreak in the inshore region. Large, reproductive krill dominated in the oceanic and frontal zones, whereas small adults

and sub-adults prevailed inshore. Ichii *et al.* (1993) hypothesized that variations in the distribution of krill observed during summer 1991 were related to mesoscale variations in circulation patterns, with the inshore regions characterized by complicated flow patterns and convergent eddies.

2.3.2.3 Winter observations

The first winter cruise, since the *H.M.S. Discovery* expeditions, was conducted around South Georgia in 1983 (Heywood *et al.*, 1985). The abundance of krill determined by net samples was lower by a factor of 30 compared to observations from the previous summer and acoustic measurements indicated the absence of krill aggregations in the upper water column. Echogram traces revealed the presence of scattering layers up to 20 m thick near the bottom over selected regions of the shelf and net samples showed that krill were found in these layers. However, their localized nature led Heywood *et al.* (1985) to conclude that krill within these layers could not account for the observed reduction in krill biomass from summer to winter.

During another winter cruise, June-July in 1987, interactions were observed between fur seals and krill aggregations near Smith Island adjacent to a well-defined ice edge (Fraser *et al.*, 1989). Qualitative acoustic observations documented a typical diel migration pattern for two large aggregations. As krill rose towards the surface, the dive duration of a group of fur seals decreased and the incidence of chewing and swallowing increased. Additionally, seabirds were observed circling and foraging while krill were acoustically detected near the surface (Fraser *et al.*, 1989).

As part of the Research on Antarctic Coastal Ecosystem Rates (RACER) program (Huntley *et al.*, 1991), net samples were collected during the winter of 1992 within Gerlache Strait and on the inner shelf along a transect from Anvers Island to Crystal Sound (Nordhausen, 1994). Net estimates of krill density were high (>100 ind. per 1000 m^3) at several locations and similar in magnitude to summer observations from other RACER

cruises (Brinton, 1991). Acoustic measurements were also collected during the RACER cruise using acoustic doppler current profiling (ADCP) techniques and large dense aggregations, typically hundreds of meters in extent, were observed in the upper 100 m of the water column in Gerlache Strait (Zhou *et al.*, 1994).

2.3.3 Other relevant studies

2.3.3.1 Influence of sea ice on krill distributions

Several studies have documented the importance of sea ice as an overwintering habitat for adult and juvenile krill. Sea ice is a prominent physical feature that modifies the structure and function of the marine ecosystem of the Antarctic. The seasonal change in the areal extent of sea ice affects more than 20 million km² of the sea surface (Zwally *et al.*, 1983). The presence of ice widens the spectrum of ecological niches (Eicken, 1992) available in the Antarctic marine system. In terms of its importance to krill, sea ice is thought to modify food availability and predation pressure (Quetin *et al.*, 1994). A diverse algal and micro-heterotroph assemblage (Garrison and Buck, 1989; Garrison *et al.*, 1993), which is trapped within sea ice, is productive during the winter. All life history stages have been observed feeding on sea ice biota (Daly and Macaulay, 1988; Marschall, 1988; O'Brien, 1987; Kottmeier and Sullivan, 1987; Stretch *et al.*, 1988; Hamner *et al.*, 1989; Daly, 1990). A few studies suggest that krill show a preference in relation to structure and thickness of sea ice and the distribution and abundance of ice algae (Bergstrom *et al.*, 1990; Marshall, 1988; Daly and Macaulay, 1991). The impact of increased food availability provided by ice biota may be greatly enhanced by a behavioral response on the part of krill to selectively remain in ice-covered regions.

The increased structural complexity provided by the ice surface itself may provide a refugium from certain predators (Hamner *et al.*, 1989; Kottmeier and Sullivan, 1987). On the other hand, the ice edge and adjacent ice-covered areas may attract predators and thus increase potential mortality upon krill due to higher abundances of predators (Ainley

and Jacobs, 1981; Daly and Macaulay, 1991). The degree to which rates of growth, development, and removal by predators vary as a function of ice coverage has yet to be determined (Quetin *et al.*, 1994). Nevertheless, interpretation of biological distributional patterns should include an understanding of the recent cryographic history of the region (Ainley *et al.*, 1988).

2.3.3.2 Benthopelagic habitat

During a summer cruise, in the southwest Weddell Sea, the existence of benthopelagic aggregations of krill were documented (Gutt and Siegel, 1994). Using a video camera attached to a benthic remotely-operated vehicle, scattered krill and krill aggregations were observed positioned within 200 cm of the bottom, near the shelfbreak in water depths of 400-500 m. Positive observations were infrequent with krill present in only 2 of 16 video transects and most of the krill were adults at least 45 mm total length. A shift from a pelagic to a benthopelagic habitat was also observed by Kawaguchi *et al.* (1985) for krill (20 - 45 mm) overwintering under fast ice in a shallow coastal region. Reports of krill in the stomachs of starfish (Fratt and Dearborn, 1984) further support the hypothesis that some portion of the krill population may inhabit the benthopelagic habitat.

2.3.3.3 Diel vertical migration

Although vertical migration is generally considered a behavioral component of krill ecology (Marr, 1962; Mauchline and Fisher, 1969; Everson, 1983), a consistent pattern describing the relationship between the depth distribution of krill and the time of day or diel light cycle is lacking. The tendency for krill to rise to the surface and to disperse at night has been frequently observed (Witek *et al.*, 1981; Marr, 1962; Nast, 1979; Godlewska and Klusek, 1987; Godlewska, 1993; Everson and Murphy, 1987), however, the difference in day-night depth ranges observed in these studies is variable. Several studies found no evidence of diel periodicity in the vertical distribution of krill (Shulenberger *et al.*, 1984; Daly and Macaulay, 1991; Higgenbottom and Hosie, 1989; Hampton, 1985).

Attempts to reconcile these different observations, have led to the development of conceptual models which describe variations in the vertical distribution of krill as a complicated function of several interacting factors. For example, Everson and Ward (1980) linked vertical movements of krill to light, food availability, and animal size. Similarly, Godlewska and Klusek (1987) suggested that krill diel migration patterns vary with light conditions, size of the animal, and region of occurrence. Based on a synthesis of field observations off South Georgia (Morris and Ricketts, 1984), Morris (1985) proposed a model describing krill movements which integrated feeding, moulting, and swarming activities with vertical migration. However, Morris (1985) stressed that this conceptualization may be appropriate only for the environmental conditions observed at the time of the field collections.

METHODS

3.1 Cruise Descriptions

Portions of the Palmer LTER study region were surveyed during research cruises conducted in all seasons: spring (7–21 November 1991), summer (8 January – 7 February 1993), fall (25 March – 15 May 1993), and winter (23 August – 30 September 1993). A survey-mode sampling design was employed with multidisciplinary data collected at a designated set of locations, which were occupied sequentially along the transects sampled (Figure 8-9). Typically, sampling at each station required between 3-4 hours with 1-2 hours transit time between stations.

The locations at which acoustic and environmental observations were made are shown for each cruise in Figures 8-9. The sampling intensity and region occupied differed between cruises. However, sampling for each of the three 1993 surveys, included the five transect lines (200-600 in Figures 8 - 9) positioned between Anvers and Adelaide Island. All cruises were conducted aboard the RV *Polar Duke* except the fall cruise which used the RVIB *Nathaniel B. Palmer*.

3.1.1 Measurements of physical parameters

Throughout each cruise, alongtrack measurements were made at one minute intervals of: latitude, longitude, bottom depth, ship speed and heading, and total surface irradiance (R. Smith, unpublished data). During all cruises, except spring 1991, alongtrack measurements were made at one minute intervals of surface temperature, salinity and fluorescence (R. Smith, unpublished data). Weather observations and sea ice conditions were recorded at four hour intervals and at each station.

Vertical profiles, from the surface to the bottom (or 500 m depth), were collected of: pressure (db), temperature (°C), and salinity (practical salinity scale, dimensionless). The data were averaged into 1-meter depth bins and a 5-m running average was applied

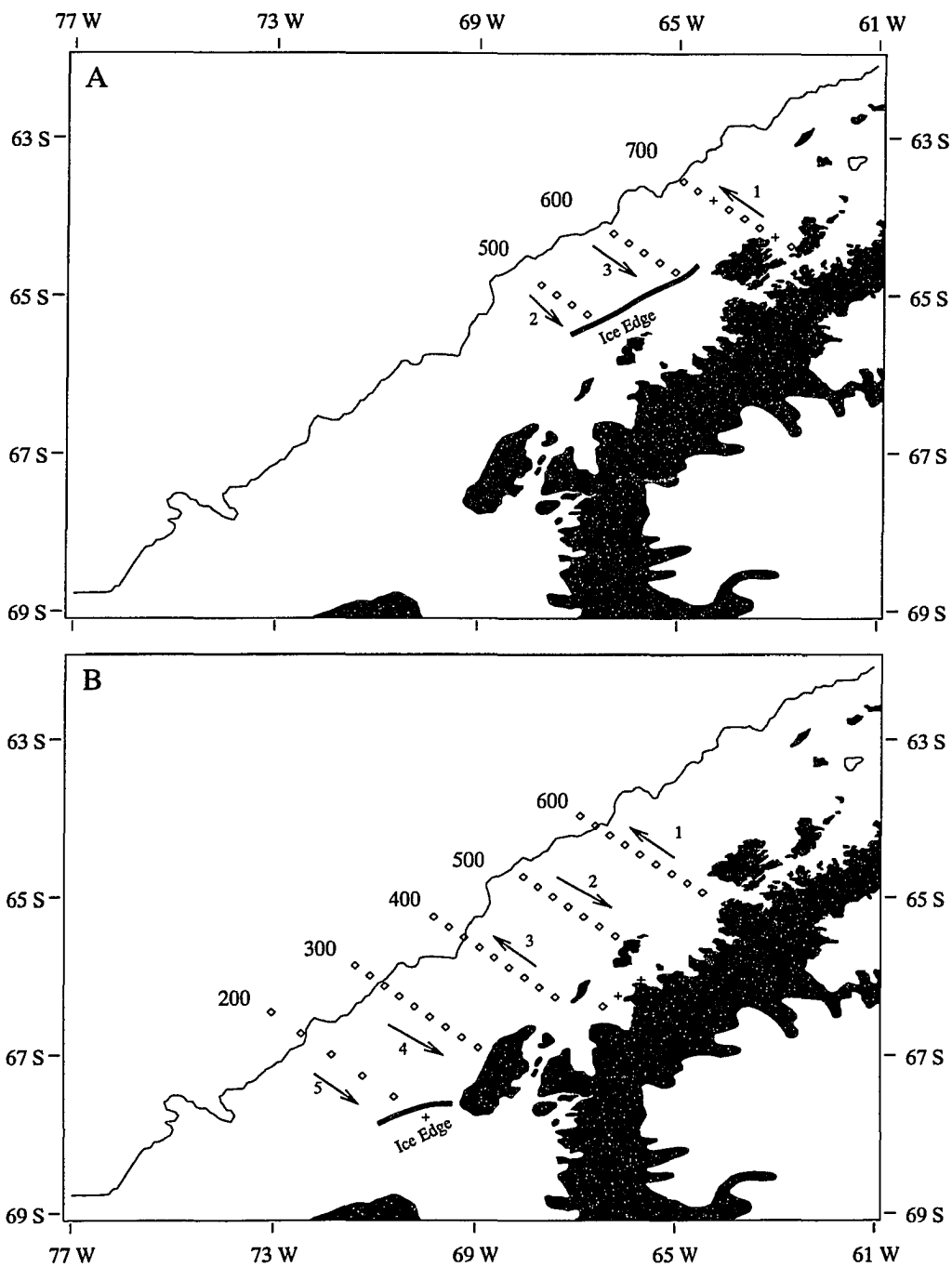


Figure 8: Locations sampled during A) spring, 7 - 21 November 1991 and B) summer, 8 January - 7 February 1993. The \diamond indicates stations where environmental and acoustic measurements were collected; the X indicates environmental measurements only. The 1000-m isobath is denoted by the solid line and the ice edge by the heavy line. Numbered arrows show the direction and the order in which cross-shelf transects were occupied.

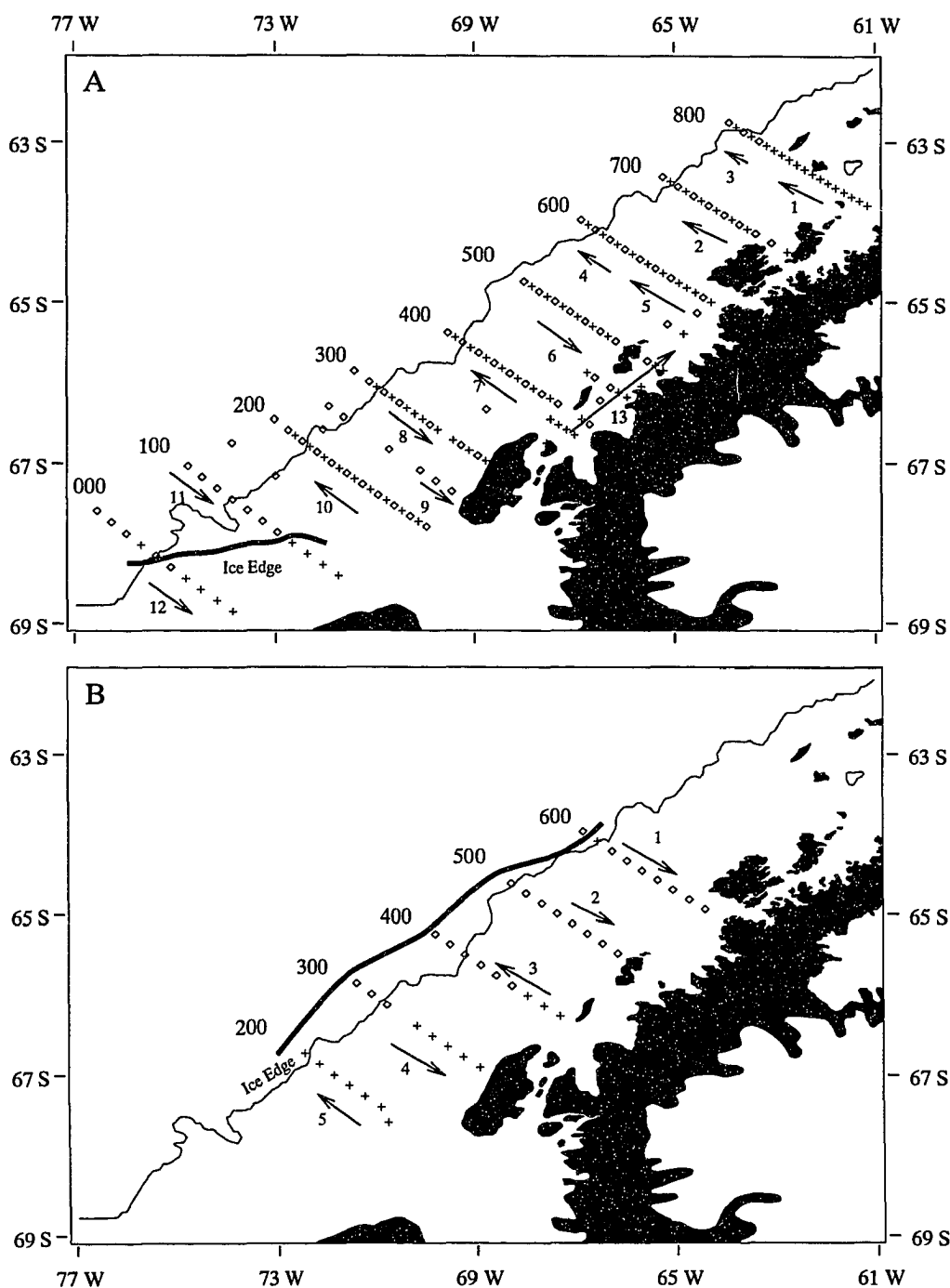


Figure 9: Locations sampled during A) fall, 3 March - 5 May 1993 and B) winter, 23 August - 30 September 1993. The \diamond indicates stations where environmental and acoustic measurements were collected; the X indicates environmental measurements only. The 1000-m isobath is denoted by the solid line and the ice edge by the heavy line. Numbered arrows show the direction and the order in which across-shelf transects were occupied.

to the temperature and salinity data to generate smoothed profiles. Density (σ_t , kg m^{-3}) was computed from temperature and salinity using the International Equation of State of Seawater (UNESCO, 1983). The buoyancy or Brunt-Väisälä frequency (N^2 , $\text{rad}^2 \text{s}^{-2}$), was calculated from density profiles according to Fofonoff and Bray (1981) using an 11-m averaging window. This parameter was used as an index of water column stability, e.g., low values are characteristic of well mixed regions. A full description of the hydrographic observations obtained at each location are available for spring 1991 (Lascara *et al.*, 1993a), summer 1993 (Lascara *et al.*, 1993b), fall 1993 (Smith *et al.*, 1993a; 1993b), and winter 1993 (Klinck and Smith, 1994).

3.1.2 Measurements of phytoplankton and zooplankton

Water was taken from discrete depths at each station with either Niskin or Go Flo bottles for phytoplankton determinations. The concentrations (mg m^{-3}) of selected chemotaxonomic pigments (B. Prézelin, unpublished data) were estimated using reverse-phase high-performance liquid chromatography (HPLC) procedures as described in Prézelin *et al.* (1992). Integrated pigment levels (mg m^{-2}) were determined at each location over the depth range 0-80 m. For the purposes of this study, the distribution and abundance of phytoplankton was described based on the concentration of three pigments: total chlorophyll-a, fucoxanthin, and hex-fucoxanthin. Fucoxanthin and hex-fucoxanthin were selected as chemotaxonomic markers for diatoms and prymnesiophytes, respectively, and were generally the most abundant markers among the larger group of pigments observed in the waters west of the Antarctic Peninsula (Prézelin *et al.*, 1992; B. Prézelin, unpublished data).

At each location, three zooplankton nets were towed obliquely through the water column, as described in Quetin *et al.* (1992), to collect zooplankton and micronekton. The samples (R. Ross and L. Quetin, unpublished data) from the 2-meter metro trawl (1000 μm mesh), towed in the upper 120 m, were used to identify the taxonomic groups

potentially responsible for acoustic scattering and to provide quantitative information on the demographic structure of the krill population.

Measurements of total length (mm), from the tip of the rostrum to the tip of the uropods, were made on krill collected by nets to obtain the length frequency distribution (LFD) of krill ($n=50-100$ individuals) at each location (R. Ross and L. Quetin, unpublished data). The observations from all locations, within a season, were visually examined and a composite LFD was created for groups of locations with similar LFDs. Locations, for which too few (<50) krill were caught to create a LFD, were assigned to a composite LFD group based on spatial patterns in LFD and environmental variables. A composite length-weight regression, representing a random selection of individuals from all locations, was generated for each cruise.

3.1.3 Habitat groups

Selected environmental variables were used to identify sub-regions (groups of stations) within each season which were similar in character. The mean salinity and temperature observed between 1 and 40 m was chosen to represent the hydrographic structure of the upper ocean. The local food conditions were represented by the concentrations of total chlorophyll, fucoxanthin, and hex-fucoxanthin, integrated over the upper 80 m. The depth range selected for the hydrographic parameters represented the vertical region most affected by variations in heat and buoyancy fluxes, whereas a deeper depth range was used for the integration of pigments to ensure that the chlorophyll maximum layer was included at all locations. The formation of initial habitat groups was guided by a subjective analysis of the similarity in these five variables. The presence of sea ice, proximity to the shelfbreak, distance from the coast or islands and hydrographic irregularities (e.g., upwelling) were also considered during the construction of final station groups. This systematic, yet subjective approach, was considered equivalent to the formation of habitat groups by hierarchical clustering packages which also suffer from the subjective choice

of distance metrics and linkage methods.

3.2 Acoustic sampling

3.2.1 Survey design

The spatial distribution of krill has historically been determined using conventional acoustic surveys in which continuous acoustic measurements are made while the ship rapidly transits predefined transects, and discrete sampling along the transect, of environmental conditions or biological communities, is infrequent or occurs after the acoustic survey (e.g., Miller and Hampton, 1989; Hewitt and Demer, 1993a). To provide better spatial and temporal coordination of acoustics data with other multidisciplinary data sets, a different sampling strategy was adopted by the Palmer LTER program (R. Ross and L. Quetin, personal communication) and used in this study. Acoustic measurements were made along several short (1-2 km) transects which were centered over a discrete location where other data sets were collected within four hours. The acoustic sampling effort is defined by the total linear distance traveled at each location, which generally ranged from 1-4 km.

3.2.2 Acoustic measurements

The acoustic system consisted of a BioSonics (BioSonics, Inc., Seattle, WA) Model 102 echo sounder connected to a downward looking 120-kHz transducer which was deployed in a dead-weight body and towed several meters below the surface. The sounder was operated using a $20 \log R$ (R = range in m) time-varied-gain (TVG) function to compensate for one-way acoustic spreading loss (MacLennan and Simmonds, 1992). Calibration of the acoustic system was performed once per year in a tank by the manufacturer (BioSonics, Inc.) and no significant changes were noted in the calibration coefficients during the time period of this study.

Echo integration of the returned acoustic energy (volts) was accomplished using the BioSonics Model 221 Echo Signal Processor (ESP, version 2.0) (BioSonics, 1990).

Table 2: Summary of acoustic processing parameters.

Parameter	Spring	Summer	Fall	Winter
Number of stations	15	40	81	25
Total acoustic sampling distance (km)	108	180	354	127
Ping rate (sec ⁻¹)	2	1	1	1
Pings per record	5-10	5 ^a ,3 ^b	3	3
Depth range (m)	17-190	12-196 ^a 5-189 ^b	15-189	5-189
Acoustic Matrix Cell Size				
Vertical (m)	2	2	2	2
Horizontal* (m)	6-13	3-9 ^a 2-5 ^b	2-7	2-8

^{a,b} Denotes values used in 1st and 2nd half of summer cruise, respectively.

* Cell length depends on ping rate, pings per integration record, and ship speed.

This system was configured to integrate voltage measurements over 2-m depth intervals and several pings. These integrated values were used to generate a two-dimensional (alongtrack, vertical) matrix of volume scattering data (VSD, m² m⁻³), for each acoustic transect, according to algorithms described in Appendix C of BioSonics (1990). The ship's position was time-keyed to the acoustics data and used to determine the total transect distance and mean horizontal resolution of cells in each acoustic data matrix (Table 2). The depth range over which acoustic observations were collected varied between cruises (Table 2) due to differences in ship configuration which affected the towed depth of the acoustic transducer. Each VSD acoustic matrix was post-processed to generate several derived data products as shown in Figure 10 and described below.

3.3 Post-processing of acoustic measurements

3.3.1 Noise removal

A background noise level of -81 decibels (dB) was removed from all acoustic observations during this study (step A, Figure 10). Based on the target strength of krill, this noise threshold was roughly equivalent to 0.05 g m⁻³ of krill biomass or 10 g m⁻² in-

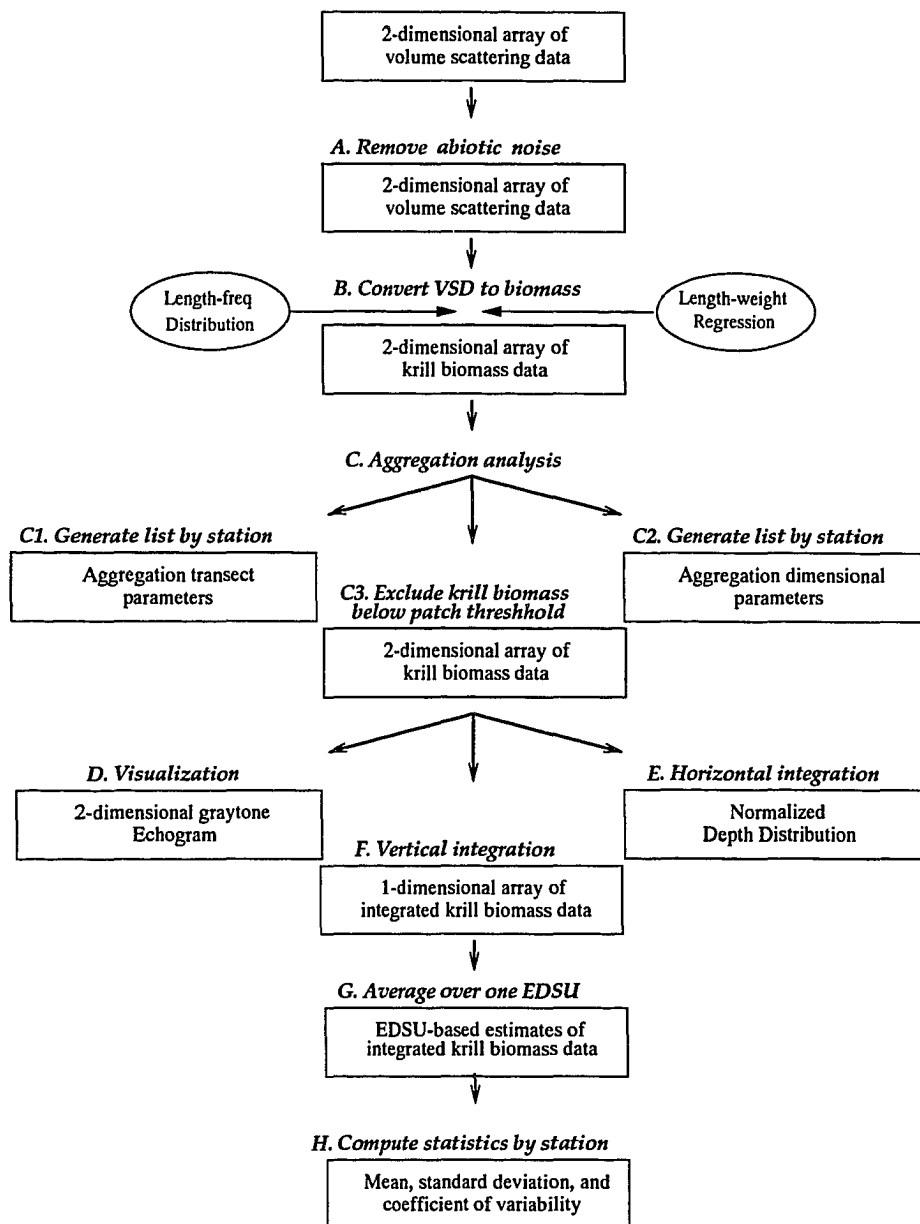


Figure 10: Schematic of acoustic post-processing steps. See text for details.

egrated over a depth of 200 m. Acoustic scattering produced by several abiotic factors including sea ice, air bubbles or the ocean bottom, as well as acoustic noise generated by shipboard electronic and mechanical equipment, were excluded from subsequent analysis by setting the VSD value to zero in the appropriate cells of the acoustic matrix.

3.3.2 Biomass conversion

The expression for krill target strength (TS, dB) used in this study was based upon the empirically derived linear regression equation of Wiebe *et al.* (1990) as modified by Greene *et al.* (1991) for 120 kHz:

$$TS = 10 \log \sigma_{bs} = -98.64 + 10.28 \log WW \quad (1)$$

where σ_{bs} is the weight specific backscattering cross section ($\text{m}^2 \text{mg}^{-1}$) and WW is krill wet weight (mg).

Using the krill length-weight regression determined for each cruise (Table 3) and krill length frequency distributions observed at each location, the σ_{bs} was estimated by equation 1 for each krill length size class at each location. Volume scattering data (VSD) was apportioned according to the observed σ_{bs} frequency distribution and converted to krill biomass (step B, Figure 10) with the relationship (MacLennan and Simmonds, 1992):

$$B_v = \sum_{i=1}^N \frac{(\text{VSD})(\Gamma_i)}{(\sigma_{bs})_i} \quad (2)$$

where B_v is the volumetric krill biomass (g m^{-3}), N is the number of σ_{bs} size classes, and Γ_i is the percentage of the total VSD represented by the i^{th} σ_{bs} class.

3.3.3 Aggregation analysis

Each two-dimensional matrix of krill biomass data was examined using an aggregation analysis procedure (Nero and Magnuson, 1989) designed to identify individual aggregations and quantify several aggregation parameters (step C, Figure 10). A patch or aggregation was defined as a contiguous group of cells in the acoustic matrix with biomass

Table 3: Summary of krill length-weight relationships by season. The coefficient (a) and exponent (b) are provided for the expression $W = aL^b$. Data provided R. Ross and L. Quetin (unpublished data).

Parameter	Spring	Summer	Fall	Winter
L-W regression				
Coefficient	0.0061	0.0040	0.0033	0.0093
Exponent	3.078	3.202	3.231	2.940

values exceeding a minimum defined threshold value. Cells within the data matrix with biomass values below this threshold were reset to zero and all subsequent processing thus represented only krill biomass associated with an aggregation.

Several threshold values (ranging from 0.05 to 5.0 g m⁻³) were examined and 0.5 g m⁻³ was chosen as it represented the lowest value which resulted in aggregations with lengths and heights similar in scale to those described for krill aggregations by other studies (Miller and Hampton, 1989; Kalinowski and Witek, 1985). At lower threshold values, numerous small aggregations were observed, as well as many horizontally and vertically extensive aggregations of low scattering intensity. These aggregations contributed very little (typically less than 5%) to the total krill biomass observed at a location and were excluded from analysis by the use of the 0.5 g m⁻³ threshold value.

The aggregation analysis procedure computed two variables, termed aggregation transect parameters (step C1, Figure 10), at each location. These parameters, the number of aggregations (no. km⁻¹) and total aggregation area (m² km⁻¹), are used as indices to describe the distribution and abundance of krill aggregations. The size, shape, and internal density of each krill aggregation (step C2, Figure 10) was also determined. These aggregation dimensional parameters (Table 4 and Figure 11) are used to characterize the structure of the krill aggregations. No assumptions were made concerning the extent of the unknown third dimension of each aggregation and thus total biomass (kg m⁻¹) was defined simply as mean biomass multiplied by aggregation area. Aggregations with a

Table 4: Definitions of dimensional parameters computed for each aggregation.

Parameter	Units	Definition
Length (L)	m	Intercepted length of aggregation along transect.
Height (H)	m	Distance from top to bottom of aggregation.
Area (A)	m^2	Cross-sectional area of aggregation in vertical plane Σ area for each matrix cell within the aggregation. Not equivalent to $L \times H$ for irregular aggregations.
Mean Biomass (B_v)	$g\ m^{-3}$	Mean volumetric biomass of the aggregation.
Total Biomass (B_t)	$kg\ m^{-1}$	Aggregation biomass estimated by $B_v \times A$

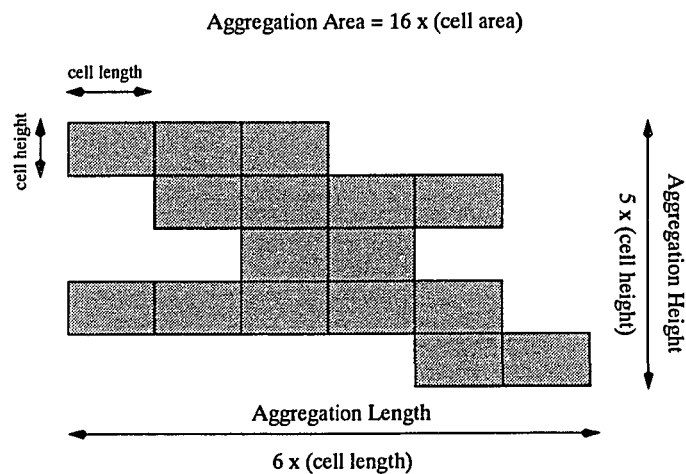


Figure 11: Schematic of krill aggregation size definitions. Figure adapted from Nero and Magnuson (1989).

total biomass exceeding 10 kg m^{-1} were classified as high-biomass (*HB*) aggregations and separate analyses are provided for all and *HB* aggregations.

3.3.4 Acoustic echograms

The analysis procedure used to identify aggregations also generated a two-dimensional matrix of krill biomass associated with aggregations (step C3, Figure 10). These matrices were visualized as acoustic echograms (step D, Figure 10) which were examined to identify patterns in the spatial arrangement of aggregations.

3.3.5 Horizontally-integrated krill biomass

The depth distribution of krill was determined for each location and by season. The volumetric biomass values (B_v) were horizontally integrated for each depth strata and normalized by the total biomass observed for that location (step E, Figure 10).

3.3.6 Vertically-integrated krill biomass

Individual estimates of krill biomass (B_a , g m^{-2}) were determined at each location by first integrating the volumetric biomass data (B_v , in g m^{-3}) over the entire acoustic depth range (step F, Figure 10) and then averaging these values over the horizontal distance defined by the elementary distance sampling unit (EDSU, MacLennan and Simmonds, 1992) (step G, Figure 10):

$$B_a = \frac{1}{I} \sum_{i=1}^{i=I} \left(\sum_{j=1}^{j=J} (B_v)_j \Delta z_j \right)_i \quad (3)$$

where I is the number of integration records in one EDSU, J is the number of depth strata, and Δz is the strata size in m. The EDSU is defined as the length (m) of the cruise track along which the acoustic measurements were averaged and a value of 750 m was used in this study based on the results described in Section 4.4.2.

The EDSU-based estimates of krill biomass (B_a) were used to generate a mean krill

biomass estimate at each location (step H, Figure 10) as:

$$\overline{B}_a = \frac{1}{K} \sum_{k=1}^{k=K} (B_a)_k \quad (4)$$

where K is the number of EDSUs for that station.

The reliability of acoustically-derived mean estimates is clearly an important issue particularly for aggregating species and several variance estimation methods are described in MacLennan and Simmonds (1992). Most methods, however, require numerous randomly positioned parallel transects. Given the simple sampling design employed in the current study and the small number of EDSUs obtained per location, a simple estimator of variance, the coefficient of variation (CV) (Snedecor and Cochran, 1978), was selected:

$$CV = \frac{\left(\frac{\sum_{k=1}^{k=K} ((B_a)_k - \overline{B}_a)^2}{K-1} \right)^{0.5}}{\overline{B}_a} \times 100\% \quad (5)$$

where K is the number of EDSU samples. Statistics were computed using different EDSU values (ranging from 50 to 1500 m) to examine the sensitivity of the variance estimate to the sample scale length.

RESULTS

This chapter is organized into five sections, of which the first four provide a description of the general and seasonal characteristics of the distribution of sea ice, hydrographic properties, phytoplankton concentration, and krill biomass and aggregation characteristics. The final section addresses spatial variability in these physical and biological distributions and explores mesoscale relationships between krill and local environmental conditions by season.

4.1 Sea ice

A description of sea ice conditions and the geographic extent of ice coverage during the four cruises is provided in this section based on the combination of shipboard observations and satellite-derived measurements. Using passive microwave satellite data, Stammerjohn and Smith (in press b) characterized the sea ice areal coverage (km^2) along the Antarctic Peninsula by month during the timeframe of this study. This analysis, which is summarized in Table 5, is based on a comparison of the 1991-1993 sea ice distribution with the mean winter maxima and mean summer minima in sea ice coverage derived from satellite-based measurements obtained over the period from January 1973 and August 1994 (Stammerjohn and Smith, in press b; Stammerjohn and Smith, in press a).

The classification of a winter as above average indicates that the maximum ice coverage observed during that winter exceeded the mean winter maximum value. Similarly, the classification of a summer as below average indicates that the minimum ice coverage observed during the summer was below the mean summer minimum value. The timing of the peaks is also compared to the mean month of maximum (August) and minimum (March) ice coverage. As described below the ship-based observations of sea ice conditions were generally consistent with the satellite-derived distribution of sea ice.

Sampling during spring 1991 followed an above average winter maximum in sea ice

Table 5: Summary of the magnitude and timing of peak sea ice coverage observed in winter and summer 1991-1993, relative to mean values derived over the time period, January 1973 through August 1994. This description is based on the analysis of surface sea ice concentrations derived from passive satellite data as presented in Stammerjohn and Smith (in press b). See text for definitions.

Year	Summer		Winter	
	Magnitude	Month of minimum	Magnitude	Month of maximum
1991	Below average	April	Above average	August
1992	Above average	March	Above average	July
1993	Below average	March	Below average	October

coverage (Stammerjohn and Smith, in press b) and sea ice was observed during the cruise to extend 80 km from the Peninsula over much of the area (Figure 8a). A compacted ice edge was encountered near the middle of the 500 and 600 lines and near the mouth of Dallman Bay on the 700 line (Lascara, personal observation). Snow covered, thick (1 m) pack ice prevented ship transit beyond the ice edge and thus acoustic sampling was limited primarily to the ice-free outer shelf region.

The entire region sampled during summer 1993 was essentially ice-free (Lascara, personal observation) (Figure 8b). Patches of thin, actively melting first year ice were observed only at the southern-most station. Bergy bits and larger glacier debris were frequently found along the inner shelf within 20 km of the Palmer LTER inshore baseline. These observations support the satellite-based characterization of this summer as below average in terms of minimum sea ice coverage (Table 5).

The ice conditions observed during fall 1993 were variable as expected for a cruise which covered 1000 km along the Peninsula over an eight week period. The northern portion (transects 600-900) of the study region was occupied during the first half of the cruise (late March thru mid April) and ice free conditions (E. Hofmann, personal communication) were observed throughout this area (Figure 9a). As the cruise progressed to the south, newly formed sea ice (including grease ice, pancake ice, and cake ice) was

encountered throughout most of the 000 line and the inner-shelf of the 100 line (Figure 9a), with some multi-year ice floes observed at the southern-most stations.

The winter of 1993 was considered below average based on maximum sea ice coverage and the maximum occurred later (October) than normal (August) based on satellite data (Table 5). During winter 1993, sea ice was encountered throughout the region (Klinck, personal communication) (Figure 9b). However, the sea ice observed along the northern transect lines (500 and 600) was characterized as relatively new pancake ice (30 to 70 cm thick) with young thin (10 cm) ice present on the outer ends of the transect lines. Sea ice was thicker (1 m) and more densely packed over most of the 200 and 300 lines and prevented acoustic sampling within this area.

4.2 Hydrography

Analyses of hydrographic data from the upper 500 m of the water column is used to characterize seasonal and mesoscale variability in the distribution of water masses within the study region. The data sets used for this analysis are described in the following technical reports: spring 1991 (Lascara *et al.*, 1993a), summer 1993 (Lascara *et al.*, 1993b; 1993c), fall 1993 (Smith *et al.*, 1993a; 1993b; 1993c) and winter 1993 (Klinck *et al.*, 1993). Some preliminary analyses of the hydrographic measurements from the fall and winter 1993 are given in Hofmann *et al.* (1993) and Smith *et al.* (in press).

4.2.1 Water mass thermohaline properties

Temperature–salinity (T–S) diagrams from each season (Figure 12) indicated the presence of two water masses, which are identified as Circumpolar Deep Water (CDW) and Antarctic Surface Water (AASW) according to the definitions given in Mosby (1934) and Deacon (1937). Within the range of T–S values defined for each water mass, distinct subregions were observed which represent either seasonal or geographic variability as described below.

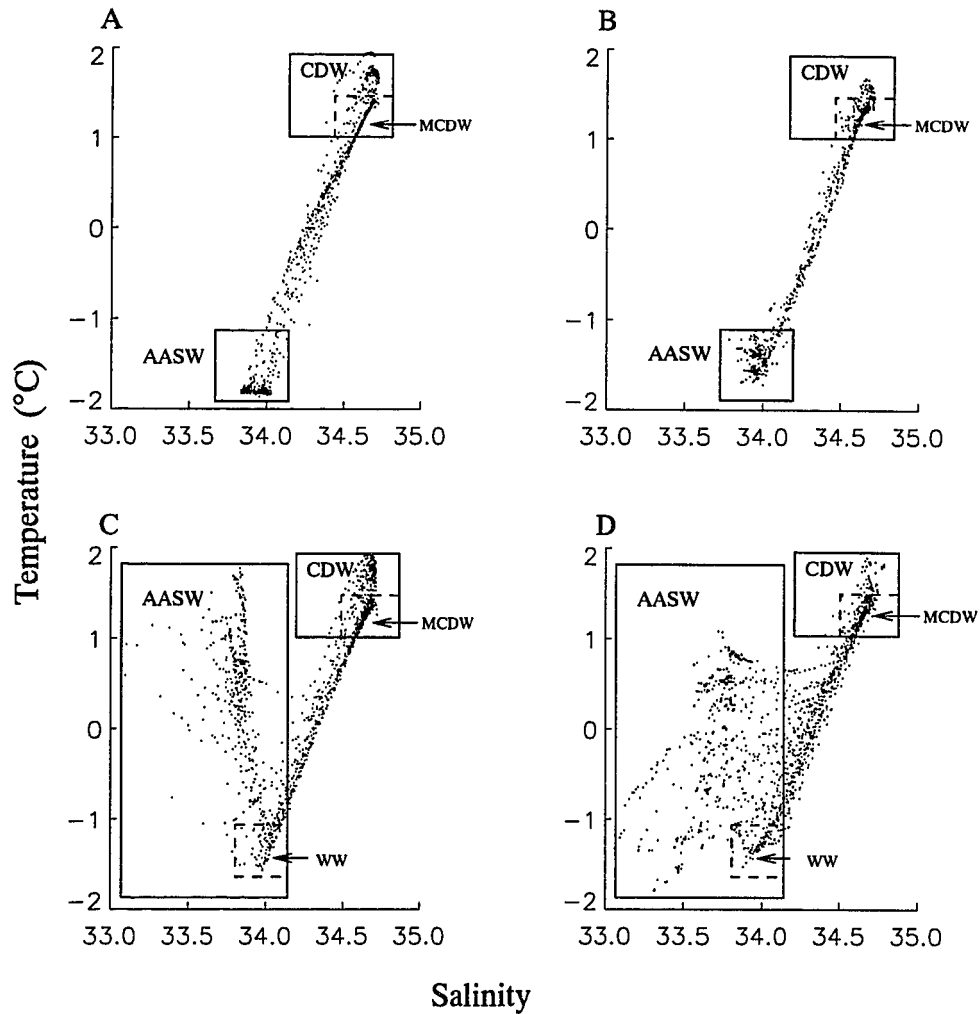


Figure 12: Temperature-salinity diagrams constructed for the upper 500 m: A) winter, B) spring, C) summer, and D) fall. The T-S space occupied by the two principal water masses, Circumpolar Deep Water (CDW) and Antarctic Surface Water (AASW), fall within the region enclosed by the solid lines. Similarly, the dotted lines enclose the T-S values for Modified Circumpolar Deep Water (MCDW) and Winter Water (WW). Analysis based on data sets in Lascara *et al.* (1993a; 1993b), Smith *et al.* (1993a; 1993b), and Klinck and Smith (1994).

CDW is characterized by relatively warm temperatures (>1.0 °C) and high salinities (>34.6) (Figure 12). Within this region of T-S space, two subregions which span similar salinity values but encompass different temperature ranges can be identified: one distinctly cooler ($1.0 - 1.4$ °C) than the other ($1.6 - 1.8$ °C) (e.g., Figure 12a). Though representing a single water mass, the term Modified-CDW (MCDW) is used to distinguish CDW water with cooler temperatures ($1.0 - 1.4$ °C) from CDW water with temperatures exceeding 1.5 °C. Both CDW and MCDW were observed during all cruises and their hydrographic character varied little between seasons (Figure 12) based on the analyzed data sets.

The second water mass, AASW, was distinctly fresher and cooler than CDW and its thermohaline character varied greatly between seasons (Figure 12). The winter hydrographic observations represented the coldest (<-1.7 °C), saltiest ($33.85 - 34.1$), and most homogeneous version of AASW (Figure 12a). The hydrographic observations in all seasons indicated the presence of water with the general T-S character (<-1.0 °C, $33.9-34.1$) observed for AASW during the winter, and water with this character is referred to as Winter Water (WW) (Mosby, 1934) (Figure 12c,d).

The range in AASW salinity observed during the spring (Figure 12b) was nearly identical to that in winter and temperatures were slightly warmer (-1.2 to -1.7 °C). In contrast, the summer and fall AASW observations (Figure 12c,d) were highly variable, spanning a wide range in salinity ($33.0 - 34.1$) and temperature (-1.8 to 1.8 °C). The minimum salinity observed during the winter was 33.8 and this value was used during other seasons to distinguish AASW which had been freshened by meltwater.

4.2.2 Vertical distributions

The vertical distribution of temperature and salinity from the winter show a relatively simple hydrographic structure with AASW overlying CDW (Figure 13). The two water masses are separated by a region of strong vertical gradients in hydrographic properties, which defines the permanent pycnocline (e.g., Figure 13a). This pycnocline is nearly

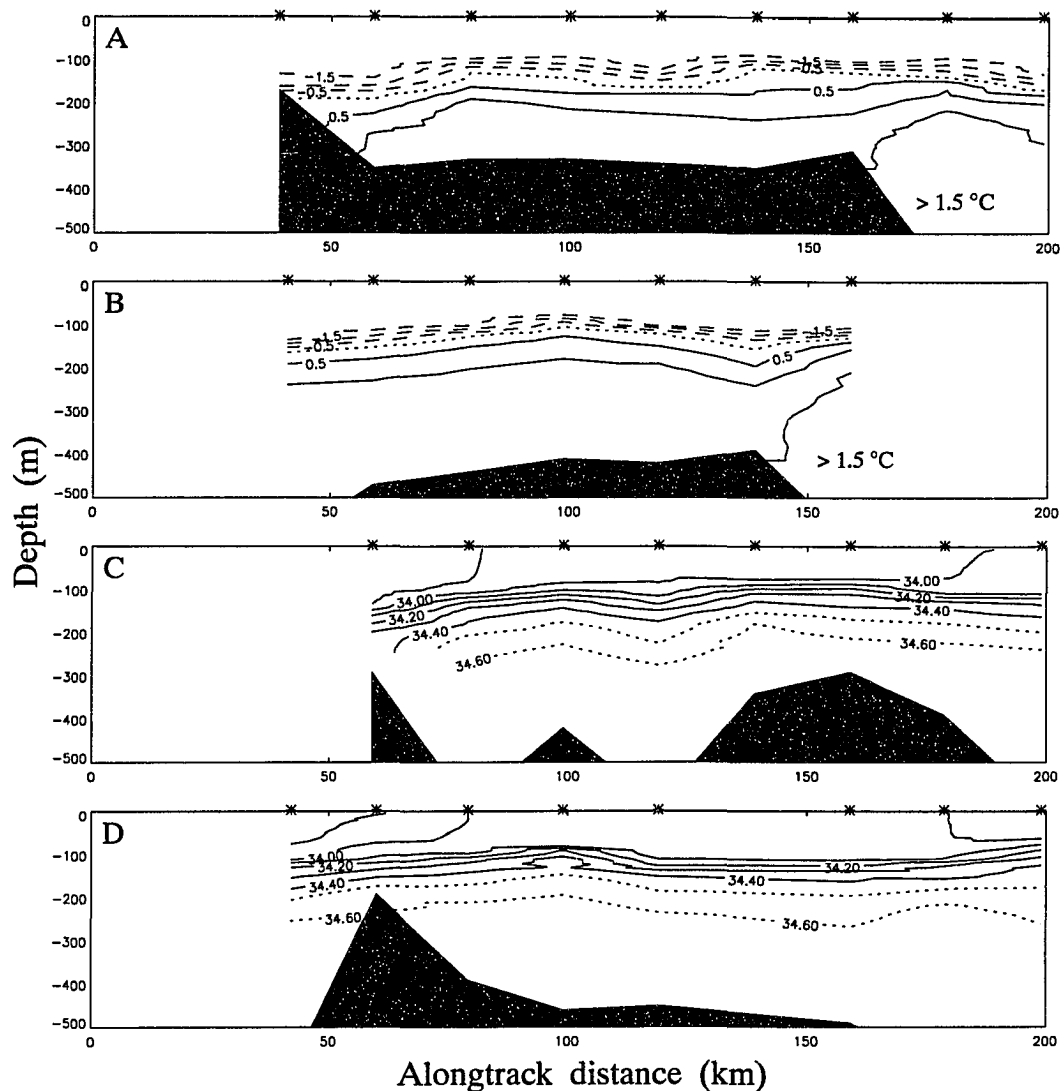


Figure 13: Vertical distribution of hydrographic variables observed in winter 1993: A) 400 Line (temperature), B) 200 Line (temperature), C) 500 Line (salinity), and D) 300 Line (salinity). Temperature contours range from -1.5 to $+1.5$ at $0.5\text{ }^{\circ}\text{C}$ intervals. Salinity contours range from 33.6 to 34.6 at 0.1 intervals. Station locations are indicated by asterisks. Analysis based on data sets in Klinck and Smith (1994).

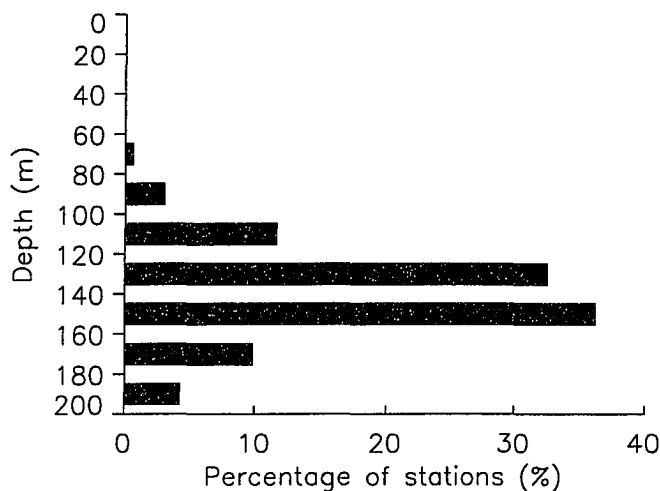


Figure 14: Frequency distribution of the depth of the 34.2 salinity isoline which was used as an index of the vertical location of the permanent pycnocline. Figure constructed using observations from all seasons and locations as provided in Lascara *et al.* (1993a; 1993b), Smith *et al.* (1993a; 1993b), and Klinck and Smith (1994).

100 m thick, throughout the west Antarctic continental shelf region. The depth of the 34.2 salinity isoline was chosen as an index of the vertical placement of the permanent pycnocline so that seasonal and geographic variations in the vertical distribution of water masses could be examined. This salinity is outside the range used to define the two primary water masses.

Permanent pycnocline depths, determined for all locations sampled during four seasons, ranged from 80 to 220 m. However, over 80% of the observations fell within the narrower depth range of 100 to 160 m (Figure 14). No consistent trends were found in comparisons of pycnocline depth made between seasons, between inshore and offshore stations, and between northern and southern transect lines (not shown). Examination of the vertical salinity distribution for across-shelf transects indicated that the relative flatness of the permanent pycnocline across the shelf, as shown in Figure 13c,d, was typical of all seasons.

The vertical range of AASW was relatively uniform as shown by analysis of the permanent pycnocline depth; however, seasonal changes in the thermohaline character of AASW (Figure 12) resulted in strong seasonal changes in the vertical structure of properties within AASW. During the winter, AASW was nearly isothermal and isohaline down to the permanent pycnocline (e.g., Figure 13). In contrast, during the summer and fall, vertical profiles of AASW salinity and temperature were highly variable, with AASW vertically partitioned into layers of warmer, fresher water overlying colder, saltier water (Figure 15). The introduction of heat and freshwater at the surface led to the formation of seasonal pycnocline(s) which separated the warm, fresh surface mixed layer from the WW form of AASW (Figure 15).

The seasonal dynamics of the mixed layer can be characterized by variations in the vertical profile of buoyancy frequency ($10^{-4} \text{ rad}^2 \text{ s}^{-2}$), in which maxima in buoyancy frequency are associated with regions of stability as occurs at a pycnocline. The simplest vertical profile was a well mixed layer of AASW overlying a single sub-surface maximum in buoyancy frequency, which represented the permanent pycnocline (Figure 16a). A second typical buoyancy frequency profile was a well mixed surface layer overlying a seasonal pycnocline(s), which was separated from the permanent pycnocline by another well mixed layer (Figure 16b). Simple forms were common during winter and spring, whereas complex profiles were restricted to summer and fall. The minimum depth at which the buoyancy frequency parameter exceeds $0.20 \times 10^{-4} \text{ rad}^2 \text{ s}^{-2}$ was chosen as an index of the surface mixed layer depth (Figure 16). This value was selected as being representative of the upper edge of the shallowest pycnocline based on review of all buoyancy frequency profiles.

The frequency distribution of the mixed layer depth by season (Figure 17) shows considerable variation for the study region. The vertical homogeneity of winter AASW resulted in a frequency distribution of the mixed layer depth (Figure 17a) which was similar in form, though 10-20 m shallower, to that of the permanent pycnocline (Figure 14). For

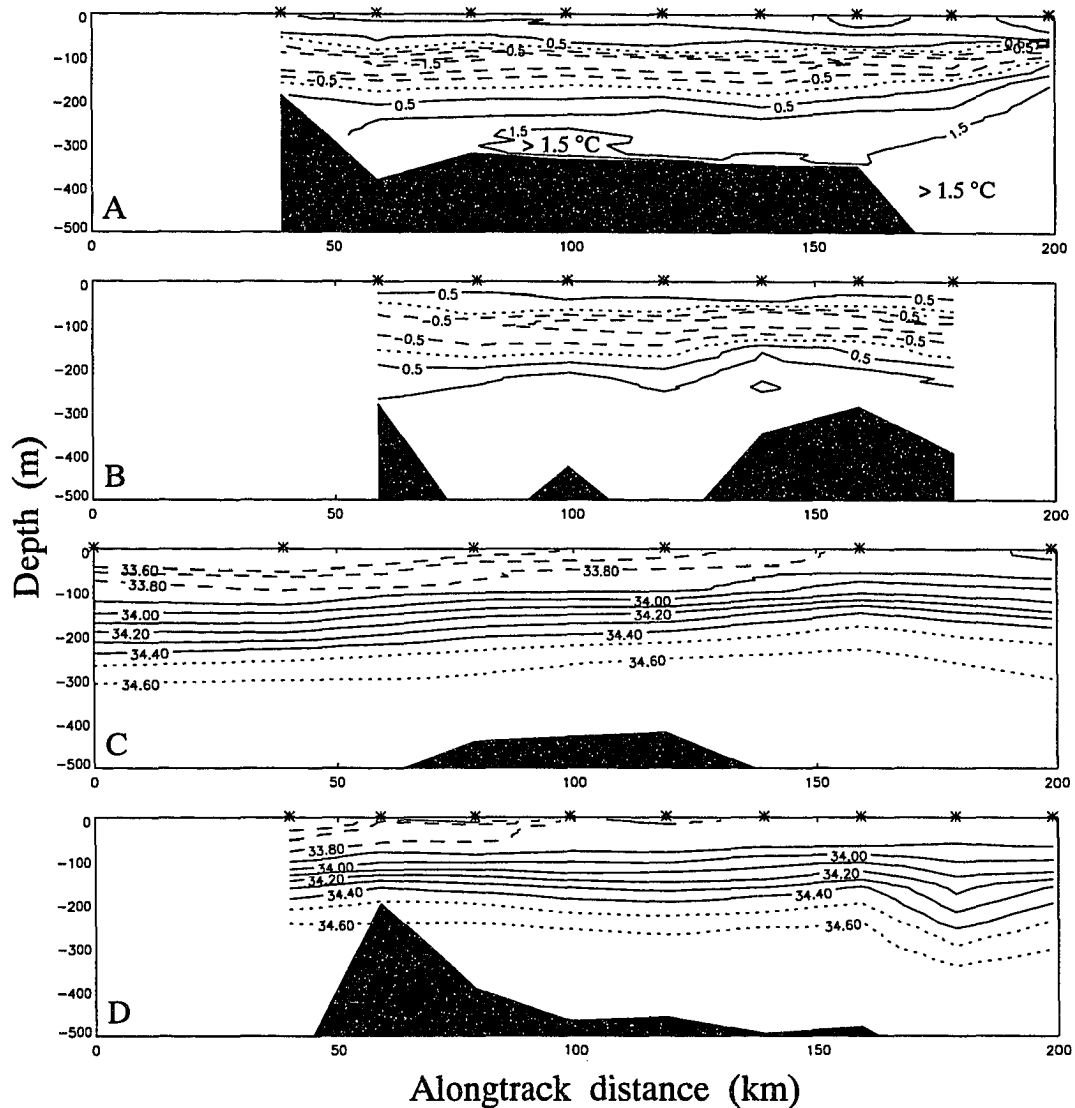


Figure 15: Vertical distribution of hydrographic variables observed in summer 1993: A) 400 Line (temperature), B) 500 Line (temperature), C) 200 Line (salinity), and D) 300 Line (salinity). Temperature contours range from -1.5 to +1.5 at 0.5 °C intervals. Salinity contours range from 33.6 to 34.6 at 0.1 intervals. Station locations are indicated by asterisk. Analysis based on data sets in Lascara *et al.* (1993a; 1993b).

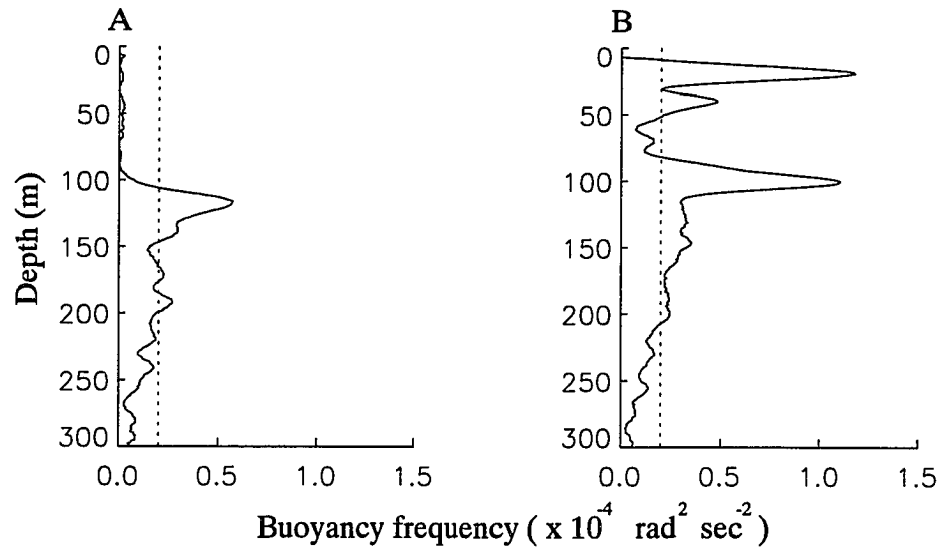


Figure 16: Example vertical profiles of buoyancy frequency: A) simple form observed in winter and B) complex form observed in summer. The dotted line indicates the buoyancy frequency value chosen to represent the depth of the mixed layer ($0.2 \times 10^{-4} \text{ rad}^2 \text{ s}^{-2}$).

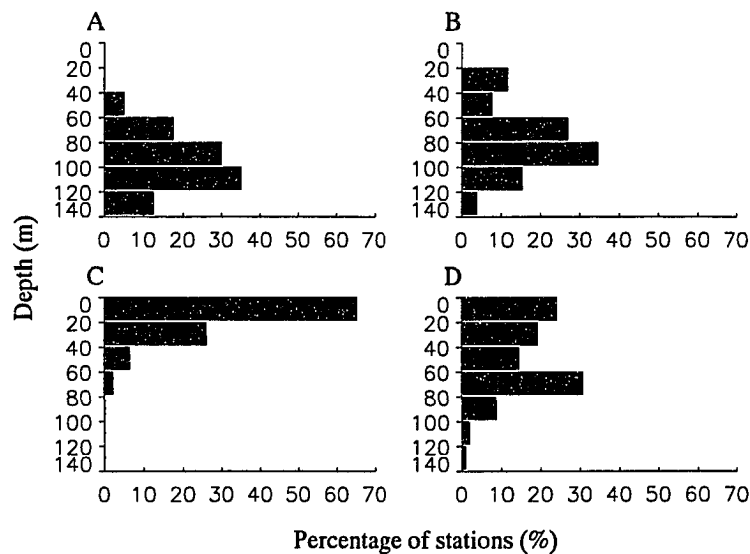


Figure 17: Frequency distribution of the mixed layer depth for stations sampled during A) winter, B) spring, C) summer, and D) fall. The depth of the mixed layer is defined as the shallowest depth at which the buoyancy frequency (N^2) exceeds $0.20 \times 10^{-4} \text{ rad}^2 \text{ s}^{-2}$. Analysis based on data sets in Lascara *et al.* (1993a; 1993b), Smith *et al.* (1993a; 1993b), and Klinck and Smith (1994).

most stations the mixed layer depth during the spring was only slightly shallower than that observed during the winter. However, the spring does show the occurrence of shallower mixed layers (<50 m) (Figure 17b) and these were associated with locations sampled near the ice edge (Figure 8a).

By summer, the depth of the surface mixed layer had clearly shoaled in comparison to that observed during the other seasons (Figure 17c). Over half of the stations sampled during the summer did not have a surface mixed layer, i.e., stratified conditions existed at the sea surface. The frequency distribution of mixed layer depths from the fall (Figure 17d) showed deepening of the surface mixed layer relative to summer values. The bimodal form of the fall frequency distribution reflected mesoscale variability in stratified and well-mixed conditions.

4.2.3 Horizontal distributions

A complete description of mesoscale distributional patterns for selected hydrographic properties is presented in section 4.5 by season. Two general features are described in this section, horizontal variations in the AASW salinity field and geographic separation of CDW and MCDW. Across-shelf gradients in AASW salinity were observed during all seasons (e.g., Figure 13 and 15). The difference between inshore and offshore surface salinities varied from a minimum of 0.30 during the winter (34.05-33.85) to a maximum of 0.85 during the summer (33.85-33.0). The lowest salinity values (<33.6) observed during the summer and fall were restricted to locations on the inner shelf (e.g., Figure 15c,d).

Across-shelf contours of temperature indicated that warm CDW (1.6 to 1.8 °C) was geographically separated from cooler MCDW (1.0 to 1.3 °C) (e.g., Figure 13 and 15). The maximum temperature observed below the permanent pycnocline at each location from all cruises was used to construct a composite view of the geographic distribution of CDW (>1.5 °C) and MCDW (<1.5 °C) (Figure 18). The general pattern was that of CDW

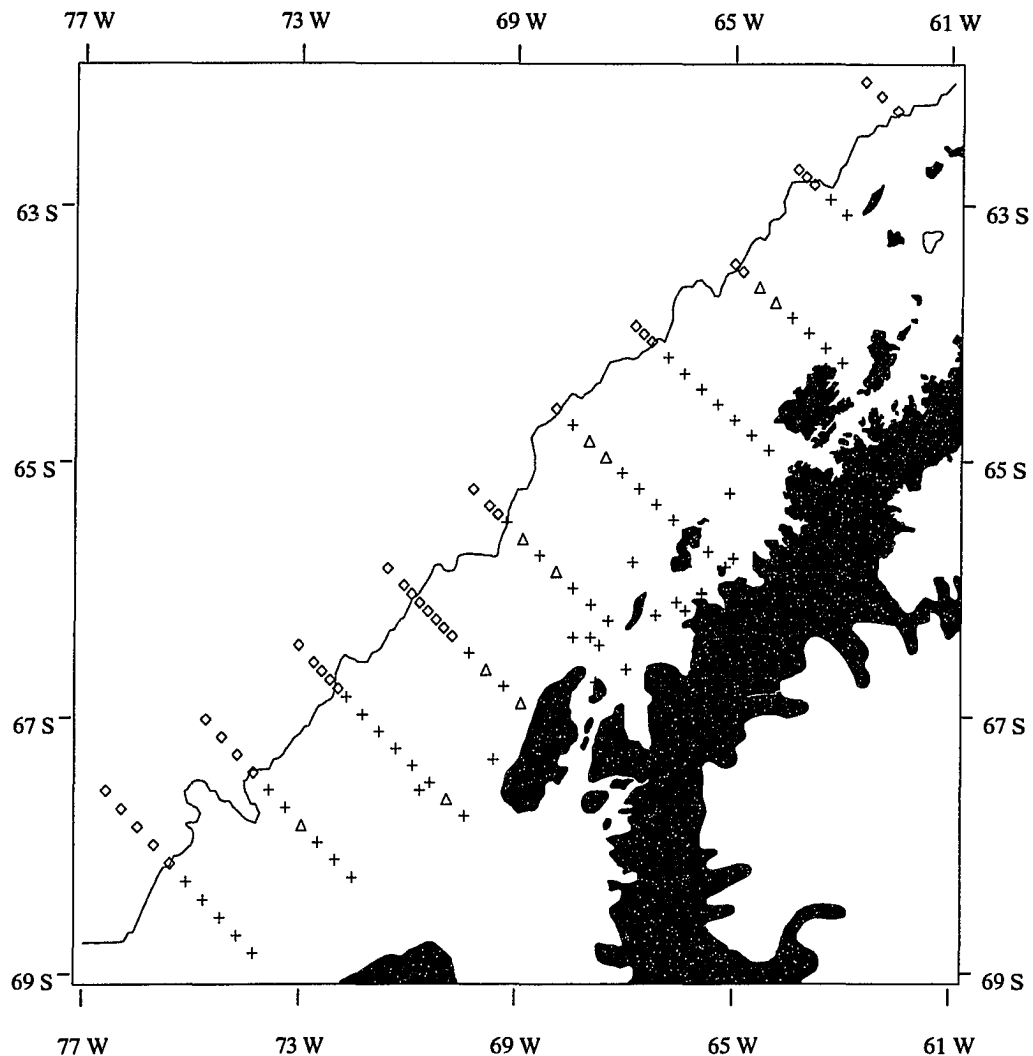


Figure 18: Composite distribution of CDW and MCDW along the west coast of the Antarctic Peninsula based on the maximum temperature observed below the permanent pycnocline. Locations where CDW (>1.5 °C) and MCDW (1.0-1.5 °C) were observed in all cruises are denoted by the \diamond and \times , respectively. Locations where CDW was observed on a single cruise are indicated by the (\triangle). The solid line denotes the 1000-m isobath. Analysis based on data sets in Lascara *et al.* (1993a; 1993b), Smith *et al.* (1993a; 1993b), and Klinck and Smith (1994).

located beyond the shelfbreak and MCDW positioned over the shelf (Figure 18). The across-shelf gradient in CDW temperature was not uniform and a peak in the magnitude of the gradient was typically located in the vicinity (within 20 km) of the shelfbreak (not shown).

Variability in the distribution of CDW generally reflected variability in the alongshelf placement of the shelfbreak. One consistent exception to this generality, occurred along the 300 line where CDW (>1.5 °C) was observed during all cruises to intrude inshore of the shelfbreak by about 60 km (Figure 18). This penetration of CDW onto the shelf may have resulted from the presence of a deeper shelf in this region (450-500 m) relative to the adjacent transect lines (400 m). CDW was also infrequently observed at locations on the middle or inner shelf (indicated by \triangle in Figure 18). There was no seasonal or geographic pattern to the observation of these features which were generally 20-40 km in across-shelf width and were bordered offshore and inshore by MCDW (e.g., Figure 15a).

4.3 Phytoplankton

Vertically-integrated concentrations (mg m^{-2}) of total chlorophyll-a (Figure 19a), fucoxanthin, (Figure 19b), and hex-fucoxanthin (Figure 19c) observed throughout this study were generally low (<60 mg m^{-2}). Seasonal variability in all three pigment levels was apparent with summer mean concentrations roughly two- to three-fold higher than winter values (Figure 19). The highest winter measurements did, however, overlap with the lowest observations for all other seasons. The pattern of seasonal change was dissimilar between fucoxanthin and hex-fucoxanthin (Figure 19) with higher fucoxanthin to hex-fucoxanthin ratios observed during the fall and winter.

4.4 Krill

4.4.1 Verification of acoustic targets

Several taxa were considered potential acoustic scatterers as they have theoretical

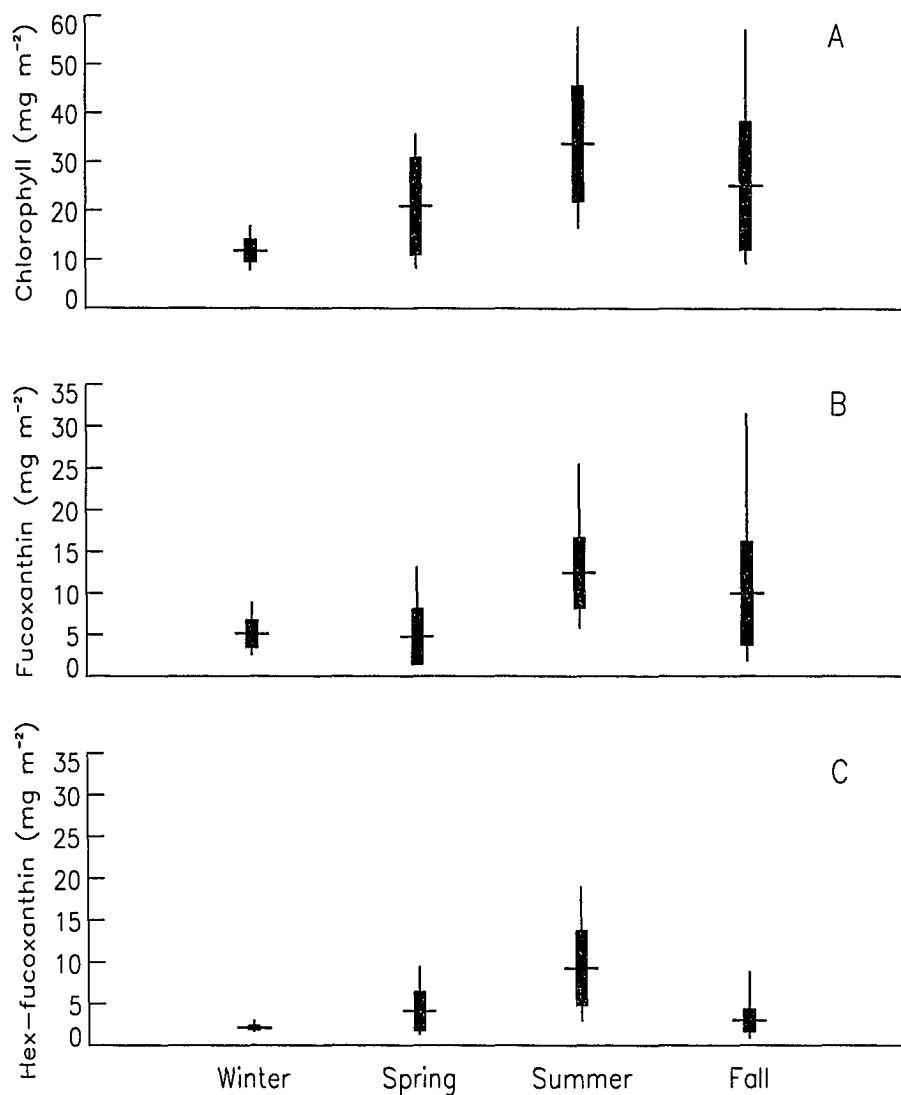


Figure 19: Spatially-averaged estimates of pigment concentrations integrated over the upper 80 m (mg m^{-2}): A) chlorophyll-a, B) fucoxanthin, and C) hex-fucoxanthin. The thin vertical line indicates the full range in observations and the horizontal cross-line indicates the mean value. The thick vertical line denotes the range between the mean value \pm one standard deviation. Data provided by B. Prézelin (unpublished data).

target strengths similar to krill and historically have been shown to occur at times in aggregations. During this study, pteropods, amphipods, salps and other euphausiids (*E. crystallorophias* and *Thysanoessa*), were collected by nets in addition to krill. The net collections associated with locations where aggregations were not detected acoustically were considered representative of the non-aggregated community and were characterized by low densities (<10 ind. per 1000 m^3) of the potential scattering taxa.

Comparisons between paired net/acoustic observations were used to identify locations where krill was the dominant scatterer. The validity of this analysis depends upon the degree to which the net collections can be considered representative of the aggregated community and so comparisons were restricted to locations where the total aggregation area (AA-index) was high ($>2000\text{ m}^2\text{ km}^{-1}$). Locations with a high AA-index were observed during each cruise and were typically associated with high net catches of krill (100-1000 ind. per 1000 m^3) and low catches of the other potential scatterers (0-10 ind. per 1000 m^3). The echogram scattering signatures observed at these locations (e.g., Figure 20a and b) were consistent with historical accounts describing acoustic traces of krill aggregations as cohesive structures with distinct edges (Kalinowski and Witek, 1985; Miller and Hampton, 1989a).

Not all locations with a high AA-index, however, exhibited high net-derived estimates of krill density. Specifically several locations, sampled during summer 1993 on the outer shelf and slope, were characterized by a high AA-index; however, net-derived estimates of krill density were low to moderate (0-100 ind. per 1000 m^3). The density estimates of salps, pteropods, and *Thysanoessa* at these locations were higher (10-100 ind. per 1000 m^3) than values observed for these taxa at locations characterized by zero acoustic scattering. In addition, small mesh nets towed in this region became clogged by dense concentrations of phytoplankton (B. Prézelin, personal communication). The acoustic traces observed at these locations were distinctly different with horizontally extensive layer-like structures or groups of vertically aligned patches (Figure 20c and d). The

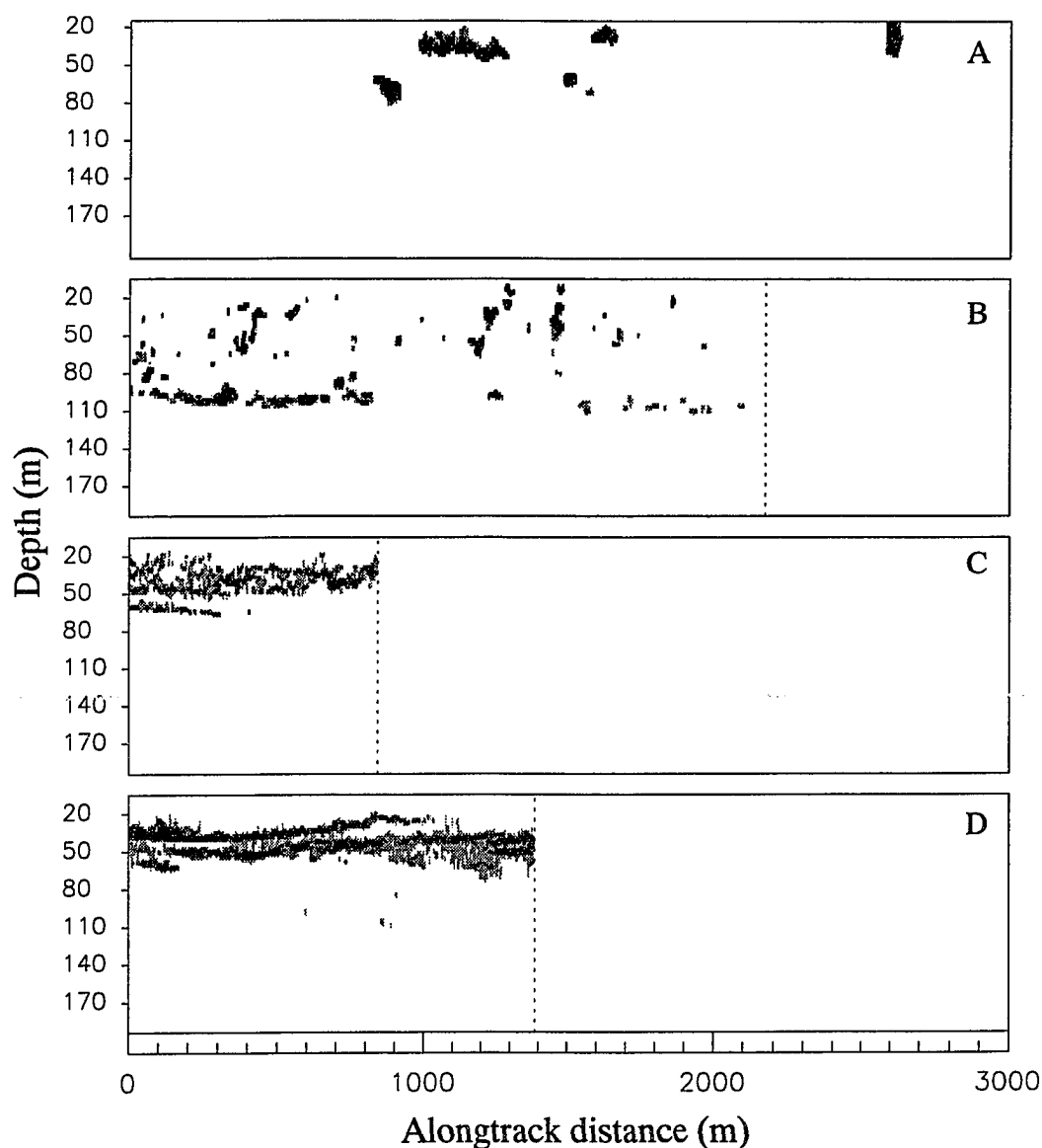


Figure 20: Example acoustic echograms observed in this study. Panels A and B are representative of locations where large densities of krill ($>100\text{-}1000$ ind. per 1000 m^3) were collected by nets which sampled concurrently with acoustic measurements. Panels C and D are representative of acoustic observations made during the summer at locations where other taxa, such as salps, pteropods, other euphausiids, and dense phytoplankton concentrations, potentially represented a significant portion of the acoustic backscatter signal. The dotted line denotes the end of the acoustic transect. Differences in the graylevel tones reflect the relative strength of the acoustic scattering.

volume scattering strength associated with these echograms was highly variable, however low values predominated. Moreover, the presence of small cohesive dense areas within larger lighter structures, indicative of patches within patches, was also noted. The net observations combined with the atypical character of the acoustic signature suggest that aggregations at these locations may represent multi-species assemblages.

Most of the locations sampled during this study exhibited a low AA-index and direct correlations between acoustic scattering strength and net-derived estimates of organism density were not attempted. The density of krill and alternate scatterer taxa collected by nets at these locations were generally similar to those observed at locations where aggregations were not acoustically detected (zero AA-index). The acoustic signatures of individual aggregations detected at the low AA-index locations were similar in character to that described above for locations where high densities of krill were collected by net.

In this study, krill was assumed to be the sole acoustic scatterer and thus estimates of krill biomass were generated using the entire acoustic VSD signal. This assumption resulted in an unquantifiable overestimate of krill biomass for locations where scattering by non-krill taxa was important. For the majority of observations, this overestimate was considered negligible due to the predominance of krill throughout the study region and the cohesive character of the scattering signal observed on most echograms. The overestimate of krill biomass was potentially highest for those locations during the summer with a high AA-index, low net-based krill densities, and high alternate scatterer densities (i.e., potential multi-species assemblages). Therefore, the estimates of krill biomass and aggregation characteristics obtained for these locations will be highlighted in all subsequent analyses.

4.4.2 Variability of krill biomass estimates

Most of the analyses presented in this study are based upon comparisons of mean krill biomass between seasons or between locations within a season. The mean krill biomass is determined by averaging several estimates of krill biomass obtained at the

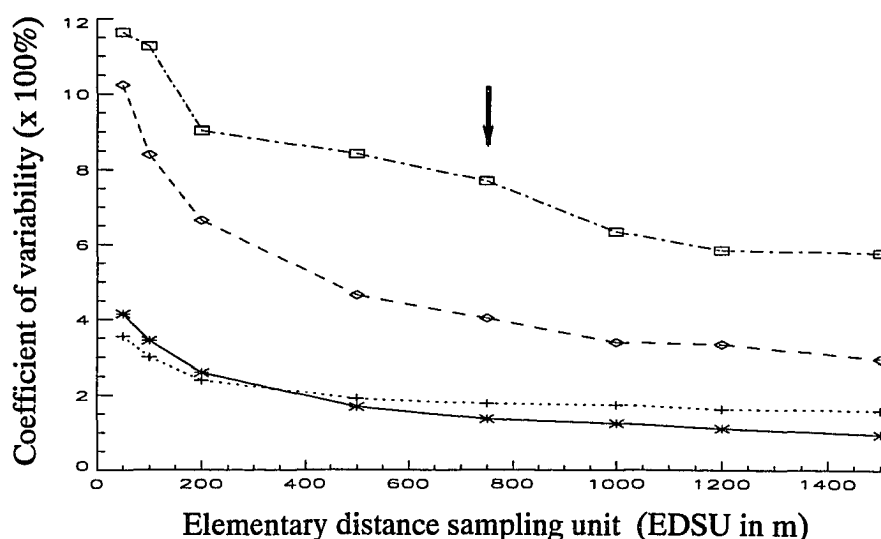


Figure 21: Coefficient of variability ($\frac{\text{StdDev}}{\text{Mean}} \times 100\%$) in krill biomass estimates as a function of the elementary distance sampling unit (EDSU). The solid, dotted, dashed, and dash-dotted lines represent observations from spring, summer, fall and winter, respectively. The arrow indicates the EDSU value (750 m) chosen for subsequent analyses.

scale of the elementary distance sampling unit (EDSU). The variability associated with the EDSU-based estimates of krill biomass are described in this section first by season and then by location.

The coefficient of variation (CV) determined from krill biomass samples grouped by season was sensitive to the EDSU length, e.g., variability decreased as EDSU length increased (Figure 21). The highest CV values were associated with biomass estimates computed over distances smaller than the length scale of most krill aggregations (<200 m). A standard EDSU value of 750 m was selected for all further biomass analyses and this scale was chosen as a compromise between reduced variance and increased sample count. The highest CV values were observed during winter (800%) and fall (400%), which are seasons that were characterized by the absence of krill from a majority of the EDSU samples.

Individual estimates of krill biomass, as well as the mean value, are shown in

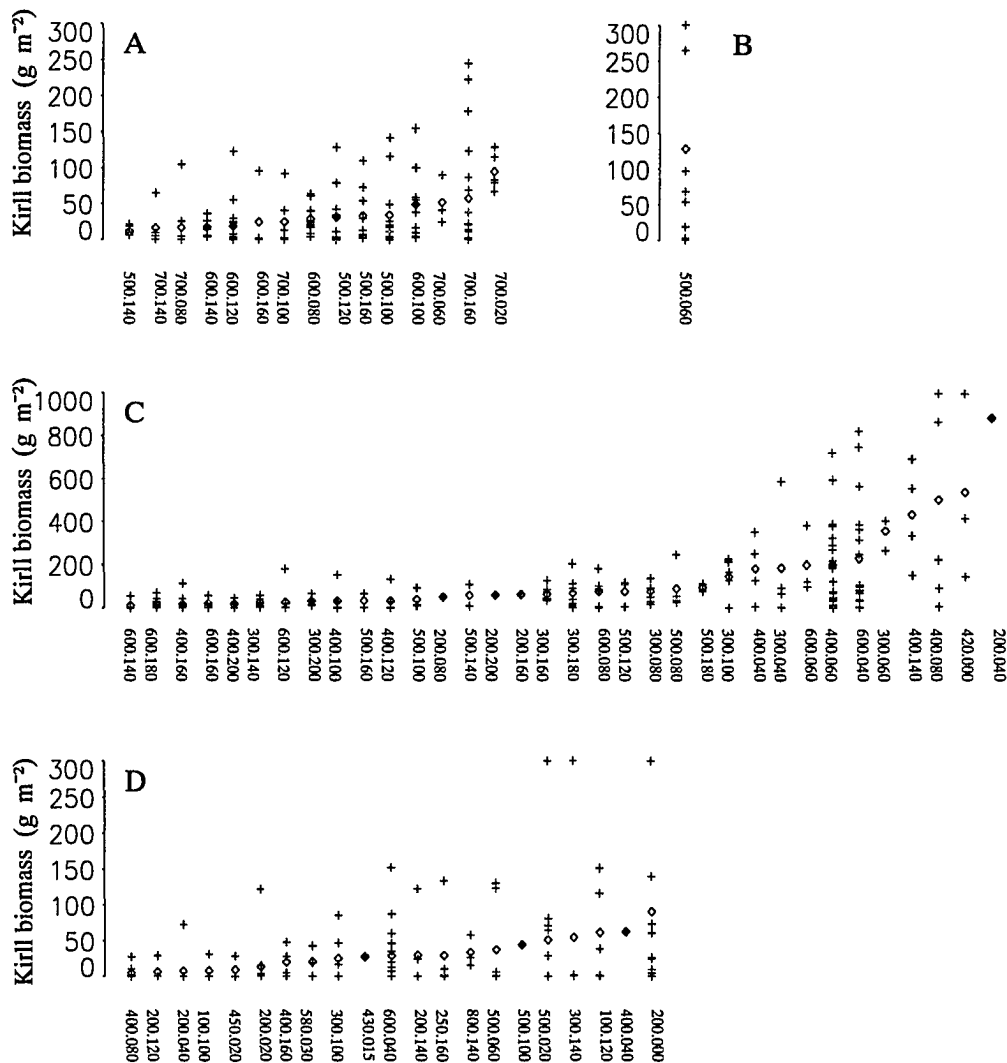


Figure 22: Estimates of krill biomass computed from acoustic observations averaged over one elementary distance sampling unit (EDSU, 750 m): A) spring, B) winter, C) summer, and D) fall. Individual EDSU-based estimates of krill biomass are shown as (+) and the mean for each station is indicated by ◇. The stations are sorted in order of increasing mean krill biomass and only stations with a mean value exceeding 5 g m⁻² are included.

Figure 22 for each location where acoustic observations were made. The EDSU-based estimates of krill biomass were variable and ranged over one to two orders of magnitude at several locations (Figure 22). Furthermore, locations with similar mean krill biomass values may be represented by different distributions of EDSU-based estimates (Figure 22). A more detailed description of krill biomass variability is presented in the section 4.5. The purpose of the brief analysis presented here is to establish the magnitude of the seasonal (within-cruise) and local (within-station) variability in krill biomass estimates observed during this study and to suggest a conservative approach to the interpretation of distribution patterns derived from the mean krill biomass values.

4.4.3 Seasonality of vertically-integrated krill biomass

The vertically-integrated krill biomass estimates from all locations were averaged by season as a first attempt at characterizing seasonal variations in krill abundance (Figure 23). Spatially-averaged estimates of krill biomass increased three-fold from spring to summer (34 to 110 g m⁻²) and then decreased an order of magnitude to the low values (<10 g m⁻²) observed during fall and winter (Figure 23a). The dramatic decrease in krill biomass from summer to fall occurred over a two to three month period in 1993.

Since the sampling intensity and region occupied differed between cruises, mean krill biomass was also determined by averaging the acoustic data for selected subsets of stations. Only nine stations were common to the sampling done during all four seasons primarily because of the ice conditions (Figure 8) encountered during spring 1991 which limited acoustic sampling for this season. Based on this subset, which encompassed locations on the mid- and outer-shelf of the 500 and 600 lines, the summer mean krill biomass value was greatly reduced from that obtained for all locations and was similar in magnitude to that observed during the spring (Figure 23b). The mean krill biomass (<1 g m⁻²) and variance were lower for observations from the winter and fall compared to the full data set. However, the basic pattern of higher krill biomass in summer and

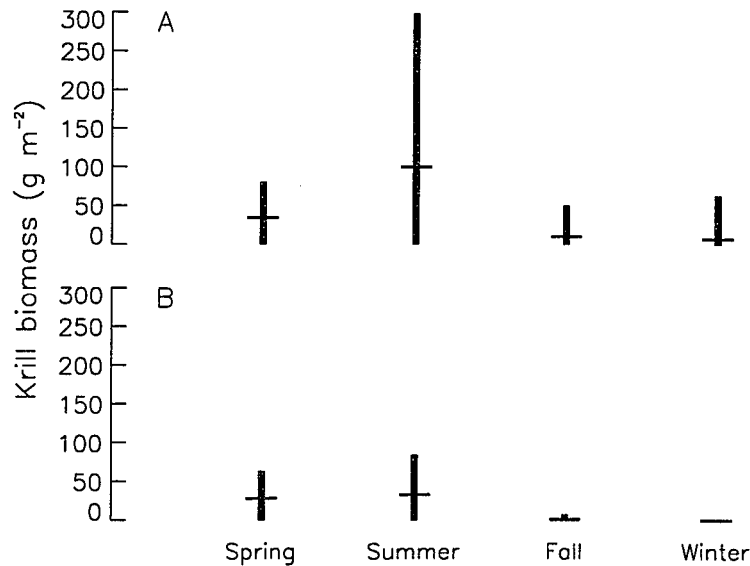


Figure 23: Seasonal changes in spatially-averaged, vertically-integrated krill biomass (g m^{-2}) for: A) all locations, and B) nine locations that were sampled during all four seasons. The mean of the EDSU-based estimates of krill biomass for each season is denoted by the horizontal line. The vertical bar indicates \pm one standard deviation about the mean.

spring relative to fall and winter is apparent even in this reduced data set.

A third comparison was made using spatially-averaged krill biomass values for 22 stations that were sampled during summer, fall, and winter (not shown). The fall decline, by an order of magnitude, in krill biomass was clearly evident for this data set and the level of krill biomass was similar to that noted using all acoustic observations (Figure 23a).

4.4.4 Aggregation transect parameters

In total, over 3000 krill aggregations were acoustically-detected during this study and seasonal changes in the abundance of these aggregations is described in terms of two variables: number of aggregations (km^{-1}) and total aggregation area ($\text{m}^2 \text{km}^{-1}$). A summary of these aggregation transect parameters determined for all and high-biomass aggregations (*HB*, defined as aggregation with total biomass exceeding 10 kg m^{-1}) is provided in Table 6. Consistent with the seasonal pattern in mean vertically-integrated

Table 6: Summary of the abundance of krill aggregations, as defined by transect parameters, observed for all and high-biomass (*HB*, $> 10 \text{ kg m}^{-1}$) aggregations. The total number of aggregation detected in a season and the number and total area (m^2) of aggregations per unit of sampling effort (km) is provided. The percent contribution by *HB* aggregations to the total number, total area, and total biomass of all aggregations is also presented.

Category	Parameter	Spring	Summer	Fall	Winter
All Aggregations	Total detected	519	2186	354	56
	Number (km^{-1})	4.8	12.1	0.9	0.4
	Total area ($\text{m}^2 \text{ km}^{-1}$)	1770	3345	450	1715
<i>HB</i> Aggregations	Total detected	86	299	61	5
	Number (km^{-1})	0.8	1.7	0.17	0.03
	Total area ($\text{m}^2 \text{ km}^{-1}$)	780	1960	300	1660
	Percent by Number	17	14	20	9
	Percent by Area	44	59	67	97
	Percent by Biomass	80	92	93	99

krill biomass (Figure 23), the abundance of aggregations, increased 2.5-fold from spring to summer (4.8 to 12.1 km^{-1}) and then decreased by an order of magnitude to the low values ($<1 \text{ km}^{-1}$) observed during the winter and fall. The second index used to describe aggregation abundance, total area ($\text{m}^2 \text{ km}^{-1}$), followed the same trend as observed for number of aggregations over the time period spring to summer to fall (Table 6). However, the total aggregation area increased from fall to winter to a value which was nearly identical to that observed during the spring ($1700 \text{ m}^2 \text{ km}^{-1}$). The increase in total aggregation area between fall and winter was accompanied by a decrease in number of aggregations and a decrease in mean vertically-integrated krill biomass suggesting a seasonal change in the character of aggregations which will be described in a later section.

The seasonal change in the number and total area of the *HB* aggregations was consistent with that described above for all aggregations (Table 6). The percent contribution by *HB* aggregations to the total number of aggregations was low (10-20%) and similar between all seasons. However, a characteristic feature observed in all seasons was that

HB aggregations accounted for a disproportionately large percentage of the total biomass (80-99%) and total aggregation area (44-97%).

4.4.5 Aggregation dimensional parameters

The dimensional parameters (Table 4) were quantified for the 3000 aggregations and used to describe the size, shape, and density of aggregations observed in continental shelf waters west of the Antarctic Peninsula. The general form of the distribution of the aggregation dimensional parameters was similar during all seasons and can be illustrated using a reduced data set that includes aggregations from all seasons. As such, a composite data set of 950 aggregations was constructed by randomly selecting 300 aggregations each from the spring, summer, and fall cruises and 50 aggregations from the winter cruise. Aggregations from the locations during the summer which were identified as problematic due to alternate scatterers were excluded from the composite data set.

The frequency distributions, based on percentage by number, of aggregation length, height, area, and mean biomass were skewed, generally resembling a negative exponential distribution (solid lines in Figure 24). None of the aggregation parameters were normally or log-normally distributed (χ^2 statistic, $p=0.01$). Fifty percent of all the aggregations were <24 m in horizontal length, <6 m in vertical height, covered <120 m², and had mean biomass values <4 g m⁻³. In contrast, frequency distributions, based on percentage by biomass, indicated that most of the total biomass was not associated with the most frequently observed aggregations but rather with a small number of aggregations which were two- to four-fold larger and an order of magnitude more dense (dotted lines in Figure 24).

The seasonal distributions of each dimensional parameter (not shown) were similar in form to those generated using the composite data set. Simple statistics were computed for each of the dimensional parameters and are provided in (Table 7) by season. Given the skewed nature of these distributions (e.g., Figure 24), simple statistics such as those

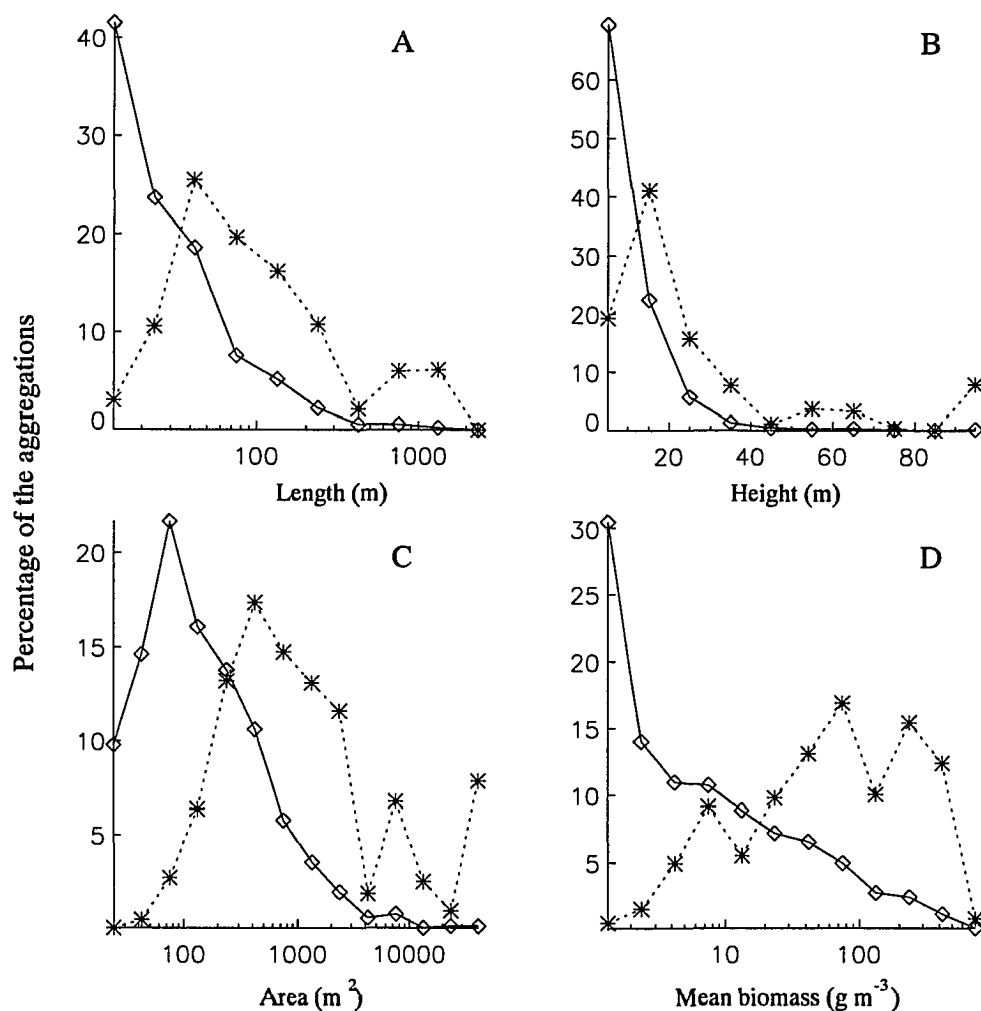


Figure 24: The frequency distribution of aggregation dimensional parameters, in terms of number (solid line) and total biomass (dotted line), obtained using the composite data set of aggregations ($n=950$) from all seasons: A) length, B) height, C) cross-sectional area, and D) mean biomass.

Table 7: Summary of statistics used to describe the mean, median, 90th percentile, and maximum values observed for the dimensional parameters measured for each krill aggregation.

Parameter	Season	Mean	Median	90 th %	Maximum
Length (m)	Spring	52	32	120	620
	Summer	30	17	60	860
	Fall	45	21	100	1100
	Winter	83	13	72	1270
Height (m)	Spring	8	6	14	44
	Summer	8	6	16	76
	Fall	10	6	22	62
	Winter	15	8	20	158
Area (m ²)	Spring	370	180	830	6200
	Summer	240	90	480	10300
	Fall	510	100	1230	10800
	Winter	3800	60	810	106400
Mean Biomass (g m ⁻²)	Spring	14	5	40	120
	Summer	47	6	160	840
	Fall	19	3	45	350
	Winter	1	1	2	10
Total Biomass (kg m ⁻¹)	Spring	7	1	17	180
	Summer	15	0.7	40	560
	Fall	12	0.4	34	310
	Winter	18	0.1	3	480

reported in Table 7 were considered inappropriate as a basis by which to make seasonal comparisons. The purpose of presenting the statistics here is for comparison to other studies where these statistics represent the only analysis of aggregation size and shape.

The seasonal differences in the dimensional character of aggregations is described in this study by comparing plots of aggregation length with aggregation height (Figure 25) and plots of aggregation area with aggregation mean biomass (Figure 26). In all seasons, the most frequently observed aggregations were represented by small length and height measurements, with low volumetric biomass estimates as described above for the composite data set. The dimensional character of these aggregations did not vary between seasons however these aggregations accounted for little (<20%) of the total biomass in each season. Comparisons between seasons were thus focused on *HB* aggregations as this subset represented the bulk of the total biomass observed each season and differences between seasons were noted for aggregation length, height, area, and mean biomass as described next.

Aggregations with horizontal lengths ranging from 50-200 m and vertical heights ranging from 4-20 m represented the majority of the *HB* aggregations in spring (Figure 25a). In contrast, summer observations indicated that most of the *HB* aggregations were smaller in horizontal length with 68% ranging from 10-50 m (Figure 25b). The proportion of *HB* aggregations that exceeded 20 m in height was higher during the fall (45%) and winter (100%) in comparison to spring (11%) and summer (22%) (Figure 25). All five of the winter *HB* aggregations exceeded 300 m in length and 60 m in height (Figure 25d), representing some of the longest and thickest aggregations observed during this study.

During the spring, 70% of the *HB* aggregations were characterized by a cross-sectional area of 300–2000 m², with mean biomass values <100 g m⁻³ (Figure 26a). The distribution of measurements in summer for *HB* aggregations was shifted towards smaller areas (<300 m²) but higher mean biomass (>150 g m⁻³) (Figure 26b). By fall, the

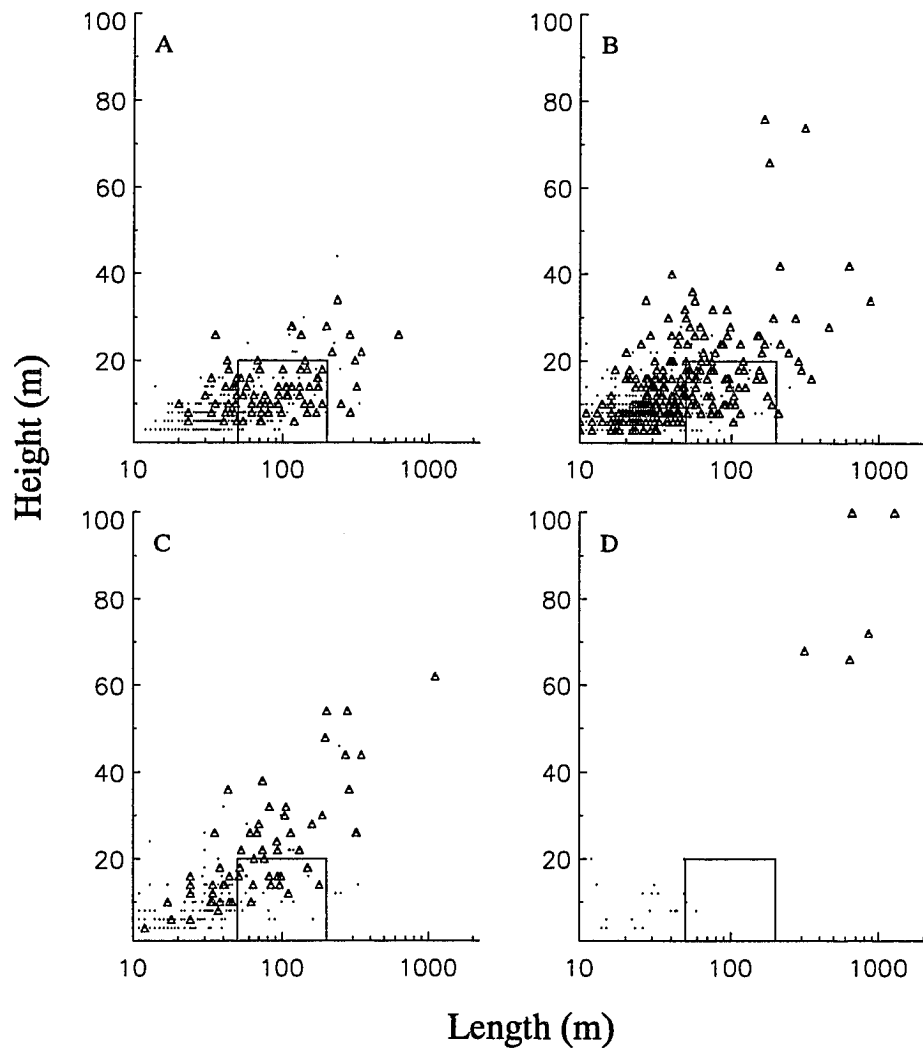


Figure 25: Aggregation length versus height by season: A) spring, B) summer, C) fall, and D) winter. *HB* and all other aggregations are represented by \triangle and dots, respectively. The solid lines provide a point of reference for comparisons described in the text.

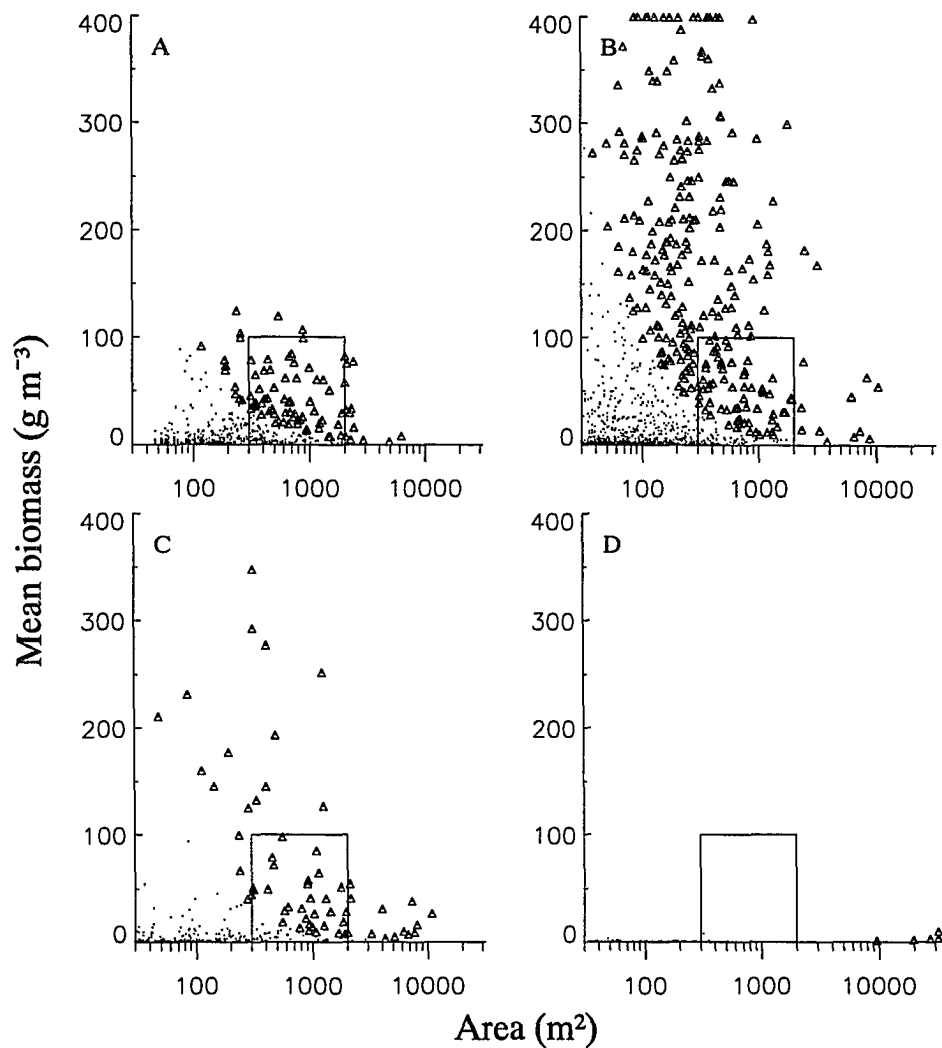


Figure 26: Aggregation area versus mean biomass by season: A) spring, B) summer, C) fall, and D) winter. *HB* and all other aggregations are represented by \triangle and dots, respectively. The solid lines provide a point of reference for comparisons described in the text.

range of mean biomass values were similar to that observed during the summer but with a distinctly lower proportion of aggregations exceeding 150 g m^{-3} (Figure 26). Also the fall observations were characterized by proportionately more *HB* aggregations exceeding 2000 m^2 ($>20\%$ compared to 10% for spring and summer). The winter *HB* aggregations exhibited high cross-sectional area ($>10^4 \text{ m}^2$) and low mean biomass ($<10 \text{ g m}^{-3}$) values (Figure 26d).

4.4.6 Depth distribution of krill

Seasonal differences in the depth distribution of spatially-averaged estimates of krill biomass are illustrated in Figure 27. During the winter, krill were distributed deeper than any other season, with only 10% of the total biomass located in the upper 70 m of the water column (Figure 27). By spring, over 60% of the biomass was present in the upper 70 m , but with 20% still deeper than 100 m . The summer distribution was skewed towards the ocean surface, and only 10% of the biomass was positioned deeper than 50 m . The fall profile was intermediate between the shallow summer and the deeper spring distributions.

The seasonal change in the depth distribution of krill was consistent with the seasonal change in the depth of the mixed layer, which was defined according to the vertical profiles of buoyancy frequency (Figure 27). Krill predominantly occupied the upper portion of AASW during the summer and fall which was characterized by elevated temperatures and reduced salinities compared to the cold, saltier AASW located below the seasonal pycnocline (e.g., Figure 15). These two seasons were also characterized by complicated vertical profiles of chlorophyll, fucoxanthin, and hex-fucoxanthin. During the winter and spring, krill occupied the lower portion of AASW and frequently extended down into the permanent pycnocline separating AASW and CDW (e.g., Figure 13). These two seasons were characterized by predominantly unstructured vertical pigment profiles.

The depth distribution of krill was also examined with respect to time of day and surface irradiance for spring, summer, and fall. Analyses using all acoustic observations

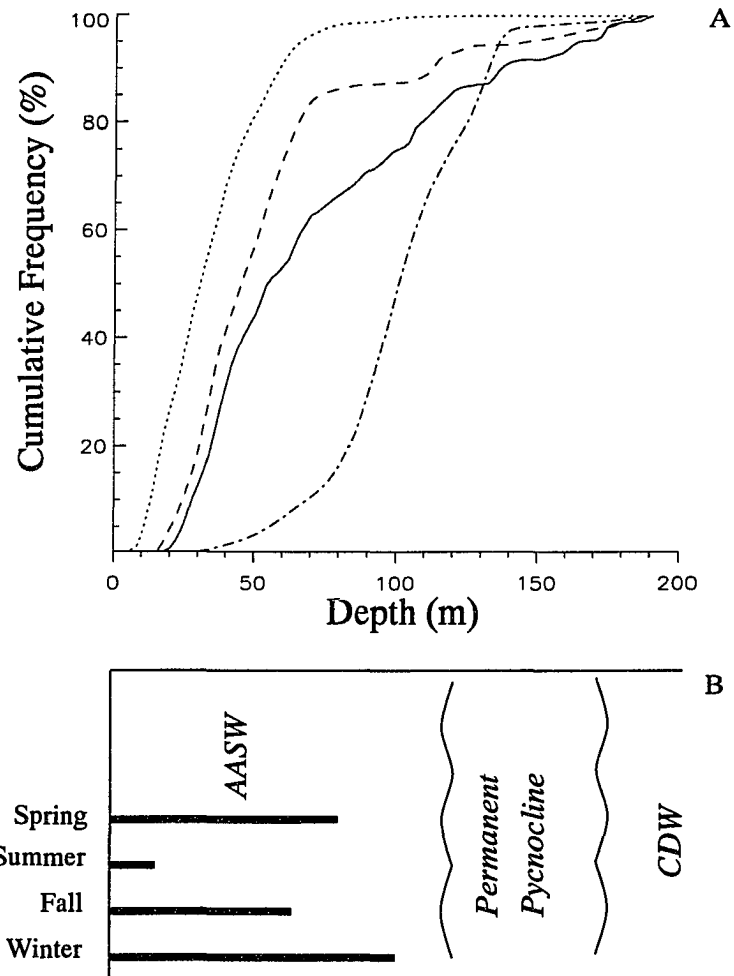


Figure 27: A) Cumulative frequency of krill biomass as a function of depth by season: spring (solid), summer (dotted), fall (dashed), and winter (dash-dotted). B) The approximate depth distribution of Antarctic Surface Water (AASW), Circumpolar Deep Water (CDW), and the mixed layer (heavy solid lines) for each season.

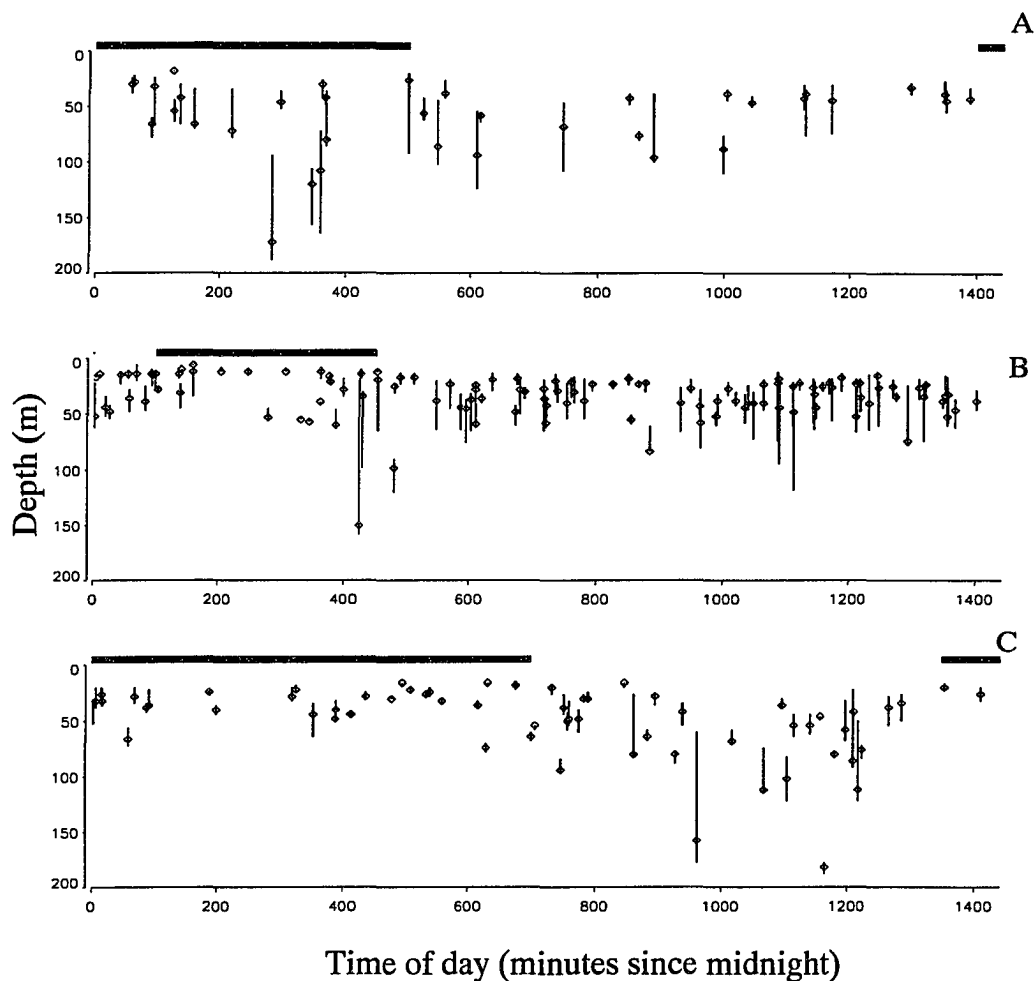


Figure 28: Krill depth distribution as a function of time of day by season: A) spring, B) summer, and C) fall. The horizontal bar indicates night hours based on measurements of surface irradiance (R. Smith, unpublished data). Depth distribution profiles are derived from individual acoustic transects. The depth range over which 80% of the krill biomass resides is denoted by the vertical line (with 10% above and below) and the median depth is indicated by a \diamond . The depth axis is relative to the sea surface and the depth range of acoustic sampling for each season is provided in Table 2.

for spring and summer (Figure 28a and b) showed no evidence of a clearly defined diel migration pattern. There was some indication of shallower distributions during the night for fall 1993 (Figure 28c), however, the difference in the median depth observed between day and night were not large. Given the degree of horizontal and vertical variability observed during this study in other environmental properties (e.g., hydrographic conditions and food concentrations) which are also thought to have an affect on krill distributions (e.g., Miller and Hampton, 1989a; Daly and Macaulay, 1991), it is not surprising that distinct patterns of diel migration were not observable when examinations included all acoustic measurements.

Acoustic measurements, which were collected at locations with similar habitat properties and were obtained over a short time period (24-30 hours), were also analysed in an attempt to reduce the impact of other environmental factors on variations in the vertical distributions of krill. Two examples or subsets of acoustic measurements satisfying these conditions, are provided in Figure 29 and diel changes in the krill depth distribution were apparent. The depth above which 50% of the krill biomass was observed during the night was typically shallower than daytime observations (by 20-50 m) with most of the krill biomass at night restricted to the upper twenty meters. The greatest vertical ranges were observed during the day and though variability in the depth profiles was high during daylight hours, it was not correlated with the magnitude of daytime surface irradiance (not shown). In all seasons several echograms collected at night indicated the presence of surface aggregations for which only the bottom edge was acoustically detected (Figure 30) and consequently the integrated krill biomass was underestimated by an unquantifiable factor.

4.5 Mesoscale Relationships

This section focuses on spatial distributions and mesoscale relationships between physical and biological variables. Selected environmental variables were used to iden-

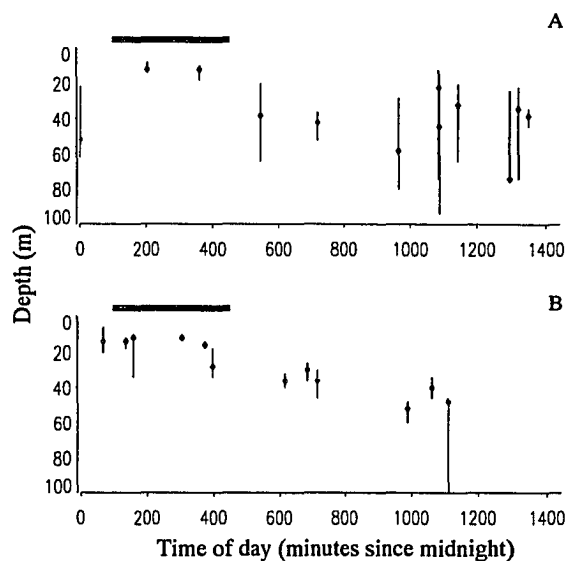


Figure 29: Same as Figure 28 for subset of acoustic transects collected: A) over a 24-hour period at station 400.060 during the summer, and B) from several locations on the inner shelf of the 300 line during the summer. The depth axis is relative to the sea surface and the depth range of acoustic sampling was 5-189 m.

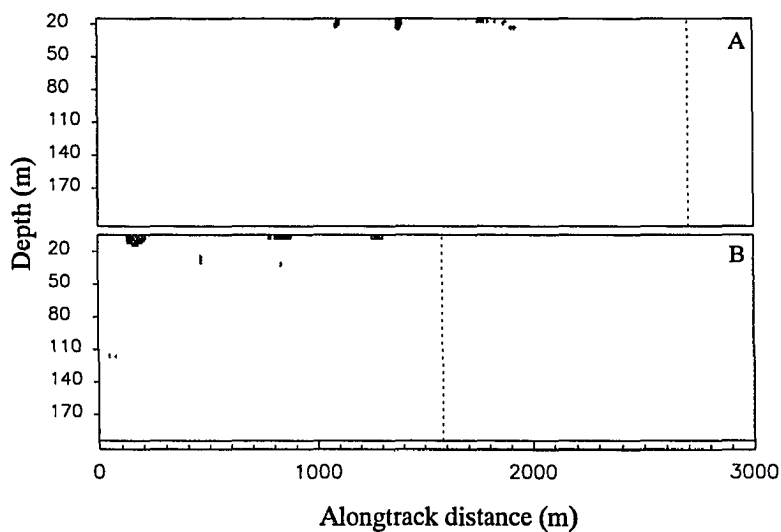


Figure 30: Example acoustic echograms illustrating surface aggregations observed during night: A) station 400.100 in summer and B) station 400.120 in fall. The dotted line denotes the end of the acoustic transect. Differences in the graylevel tones reflect the relative strength of the acoustic scattering.

tify locations within each season which were similar in character. These habitat groups were based on geographic variability in the surface salinity and temperature fields and the vertically-integrated concentrations of total chlorophyll, fucoxanthin, and hex-fucoxanthin. Geographic variability in the distribution of krill, in terms of vertically-integrated krill biomass, aggregation transect parameters, aggregation dimensional parameters, acoustic echogram patterns and vertical profiles, is also described and comparisons are made between discrete locations and between habitat groups.

4.5.1 Spring (November 1991)

4.5.1.1 Environmental conditions

The main feature of the hydrographic observations collected during the spring cruise (November 1991) was the relative uniformity of the upper ocean, in terms of thermohaline character, throughout the study region (Figure 31a and b). The difference between inshore and offshore surface salinities was small, <0.15 , (33.85 compared to 33.97). Similarly, temperature variability was small, ranging from -1.32°C on the middle shelf of the 600 line to -1.64°C near the ice edge on the 500 line (Figure 31b). Elevated chlorophyll concentrations were observed in two areas (Figure 31c), the outer shelf of the 500 line and the inner shelf of the 700 line (Figure 32). Based on the maximum temperature observed below the permanent pycnocline (not shown), MCDW was present at all stations with the exception of the outer-most station of the 500 and 700 lines, where CDW was present.

The fifteen stations occupied during spring 1991 were partitioned into seven habitat groups based on environmental conditions (Figure 31d). Groups A, B, and C were characterized by AASW salinity values typical of winter conditions and were positioned on the middle and outer shelf, with each group along a single transect line (Figure 31d). There was a general trend of decreasing chlorophyll, increasing salinity, and increasing temperature (Figure 32) from habitat group A to B to C. The highest hex-fucoxanthin concentrations were observed at locations associated with group A (Figure 32b).

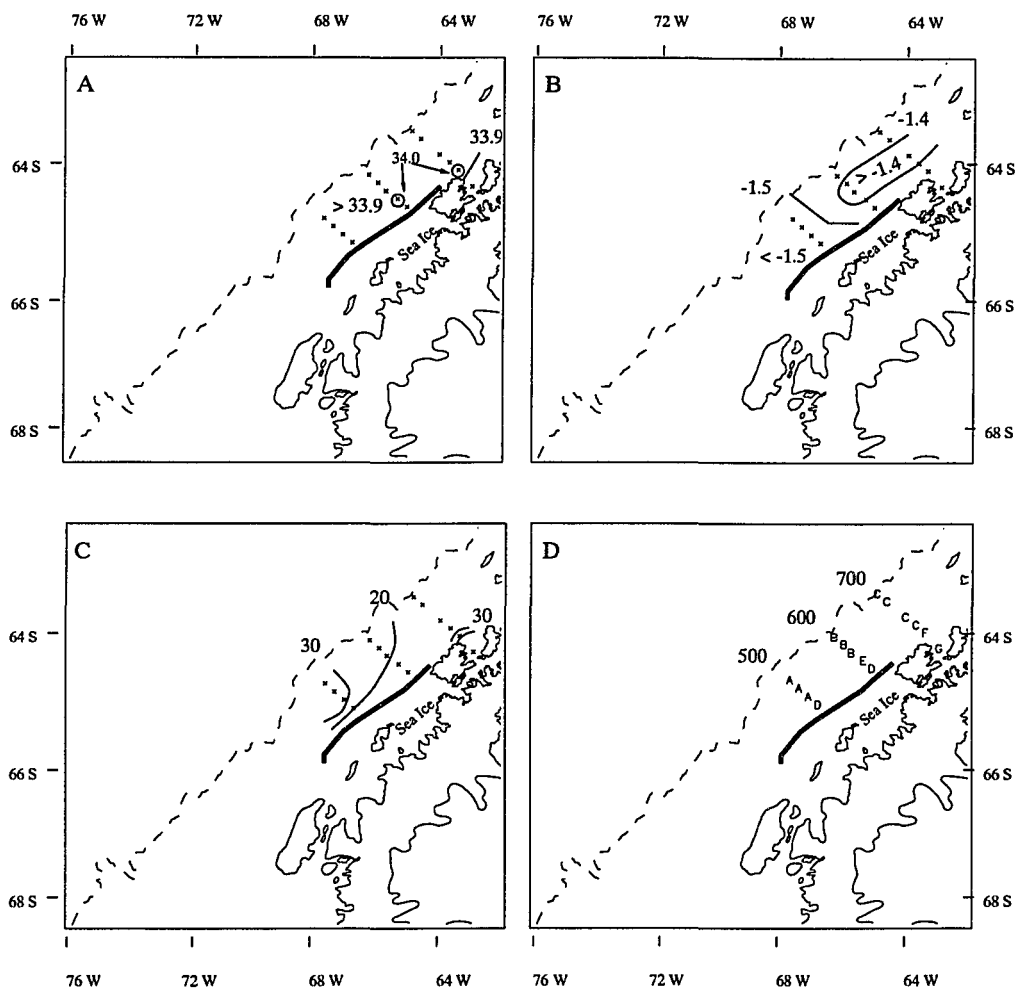


Figure 31: Distribution of A) salinity, B) temperature ($^{\circ}\text{C}$), C) chlorophyll-a concentration (mg m^{-2}), and D) habitat groups (A-G, see text for definitions) observed in spring 1991. Hydrographic measurements were averaged over the upper 40 m and pigment concentrations integrated over the upper 80 m of the water column. Station locations are denoted by an X. Dashed line is the 1000-m isobath and the thick solid line represents the ice edge. Transect line numbers are provided with habitat groups. Data sources: hydrographic observations (Lascara *et al.*, 1993a) and pigment concentrations (B. Prézelin, unpublished data).

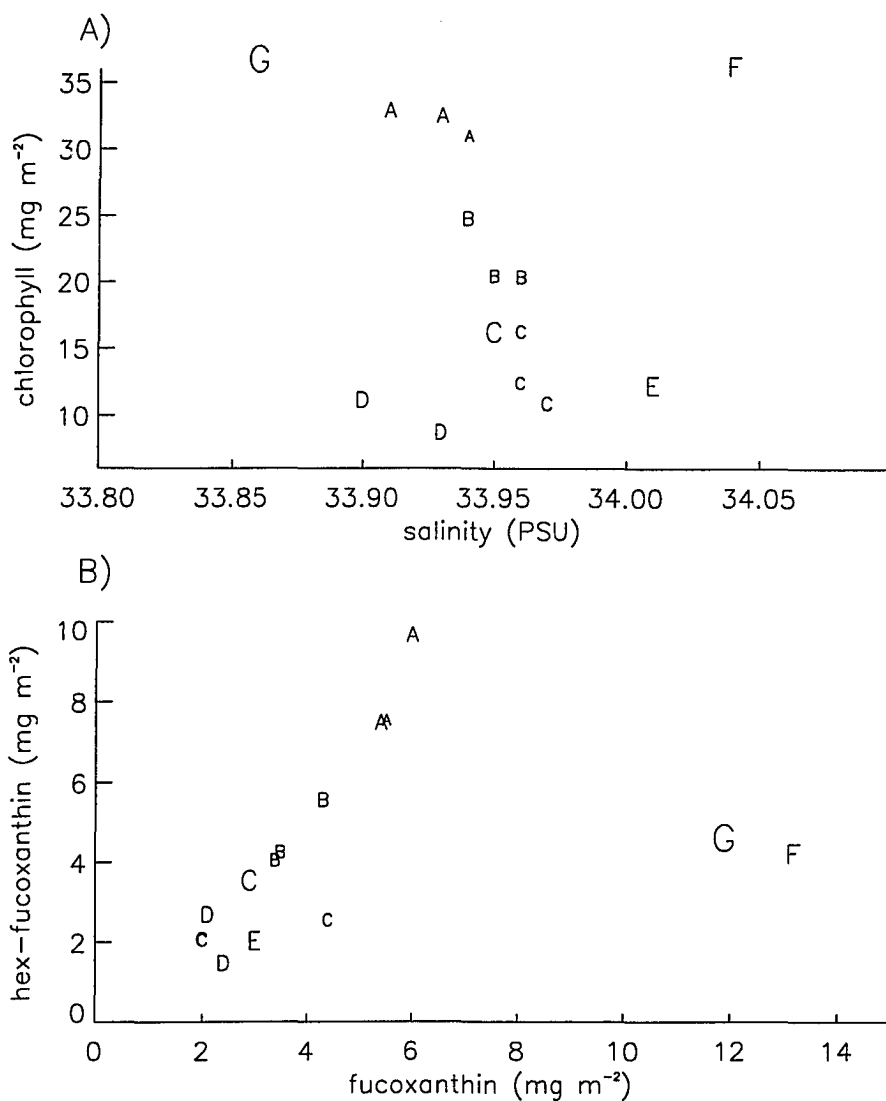


Figure 32: Correlations between selected environmental variables used to partition the locations occupied during spring 1991 into habitat groups: A) salinity and total chlorophyll, and B) fucoxanthin and hex-fucoanthin. Pigment concentrations (mg m^{-2}) were integrated over the upper 80 m and salinity was averaged over the upper 40 m. The size of the letter designating each station's habitat group is scaled by the magnitude of the mean krill biomass observed at that location, with the minimum and maximum letter size corresponding to 11 and 96 g m^{-2} , respectively. Data sources: hydrographic observations (Lascara *et al.*, 1993a) and pigment concentrations (B. Prézelin, unpublished data).

The fourth group (D) included the two stations positioned in open water just offshore (within a few km) of the marginal ice zone on the 500 and 600 lines (Figure 31d). Extensive freshening by recent meltwater was not present at these stations as salinity values were only slightly lower (33.90) than observed further offshore (Figure 32a). These ice edge stations were characterized by the lowest levels of all three pigments observed during spring 1991 (Figure 32b).

The three remaining habitat groups were each represented by a single unique station. Group G was characterized by the lowest salinity (33.86) and the highest vertically-integrated chlorophyll and fucoxanthin levels (Figure 32). This station (700.020) was situated in the protected waters of Dallman Bay between Anvers and Brabant Islands (Figure 31d). Two stations with elevated surface salinities indicative of upwelling activity were observed (>34.0). One of these (Group F) was located on the inner shelf of the 700 line off the northern tip of Anvers Island (Figure 31d). This station, though hydrographically distinct, was similar, in terms of very high chlorophyll and fucoxanthin levels, to the group G station located nearby, in Dallman Bay (Figure 32). The second upwelling station (Group E) was located offshore of the ice edge station on the 600 line (Figure 31d) where very low pigment levels were observed (Figure 32).

4.5.1.2 Krill population structure

Three groups were formed, based on similarities in krill length frequency distributions (LFD), observed during spring 1991 (Figure 33). Small (10-20 mm) krill, which were spawned the previous summer (age class 0), numerically dominated the net samples for two of the LFD groups (Figure 33a,b). Group 1, was comprised exclusively of this small size class (Figure 33a); whereas, the LFD of group 2 was bimodal with the primary peak at 15 mm and a secondary peak between 32-36 mm (Figure 33b). In contrast, large individuals, between 40-50 mm, dominated the LFD of group 3 (Figure 33c).

Group 2 was observed at all locations sampled along the 600 line, near Dallman Bay

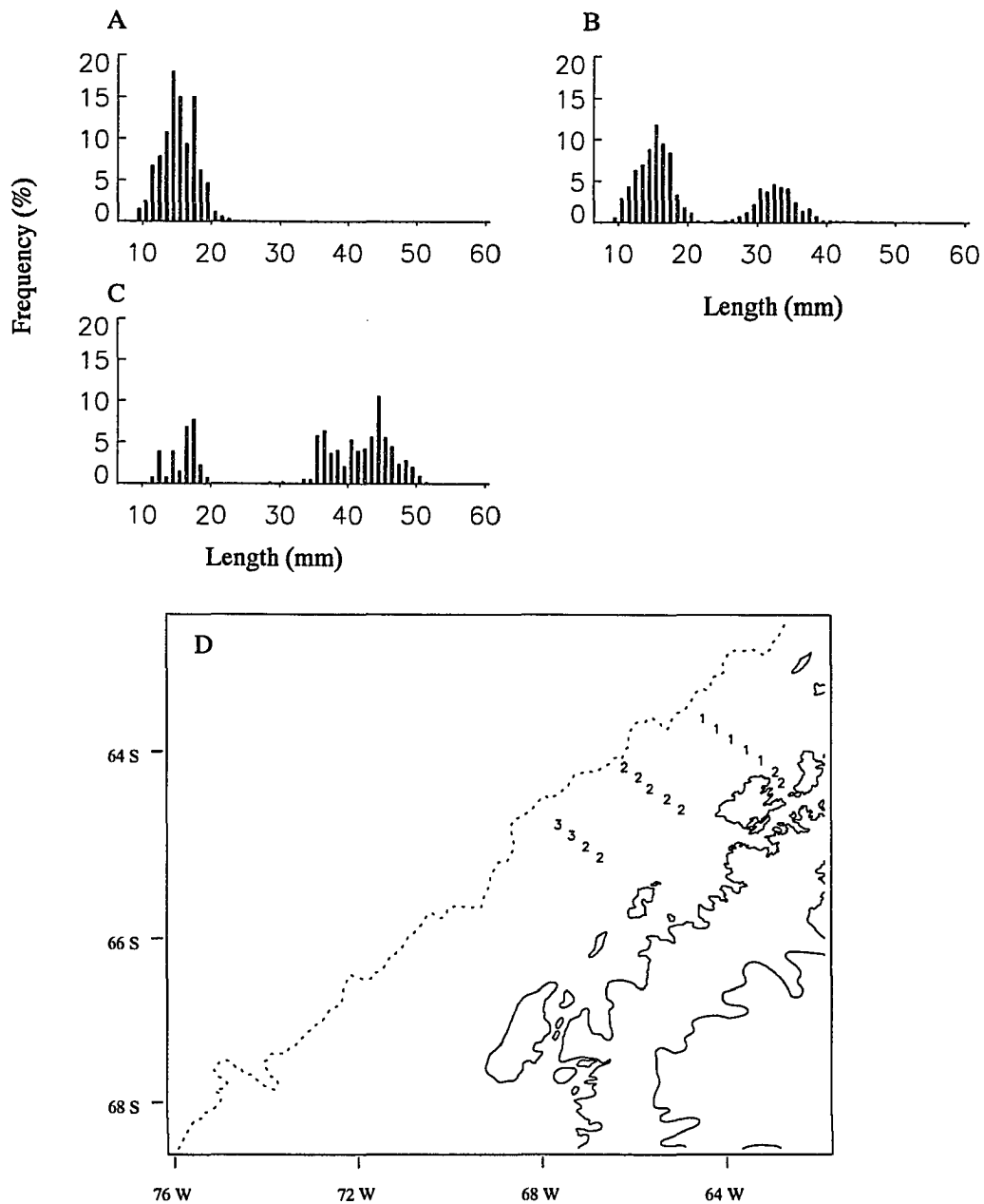


Figure 33: Length frequency distribution (LFD) of krill individuals (1 mm resolution) collected in net samples during spring 1991: A) group 1, B) group 2, C) group 3, and D) mesoscale distribution of LFD groups. The composite LFD for each group was derived from all krill collected at locations with similar station-based LFD. The dashed line indicates the 1000-m isobath. Data from net collections provided by R. Ross and L. Quetin (unpublished data).

on the 700 line, and within 40 km of the ice edge on the 500 line (Figure 33d). Samples collected along the rest of the 700 line were characterized by the small individuals of group 1. Large individuals, group 3, were restricted to two locations on the outer shelf of the 500 line (Figure 33d).

Spring 1991 was the only time period during which small (<20 mm) krill were collected. The backscattering cross-section of a 17 mm krill is roughly an order of magnitude lower than that derived for a 35 mm krill (-82 dB compared to -72 dB, using equation 1 of the Methods section). The acoustic measurements made at locations associated with LFD group 1 were generally characterized by aggregations with strong backscattering strengths. The net-based density estimates, however, indicated low abundance of krill in the area (10-70 ind. per 1000 m³). Given the target strength relationship, the character of the acoustic signature, and the low net-based density estimates, LFD group 2 was used to compute krill biomass for all stations from LFD group 1 as it was assumed that small krill (<20 mm) were not the primary scatterer.

4.5.1.3 Krill biomass distribution

Krill were detected acoustically at all 15 locations sampled during spring 1991 and mean station biomass values ranged from 10–96 g m⁻² (Table 8 and Figure 34). Eleven stations exhibited mean biomass values between 10-35 g m⁻² and the local variability at these stations was also similar, as illustrated by the distribution of individual EDSU estimates (Figure 22). These stations were located over the middle and outer shelf region, including the ice edge (Figure 34), spanned a broad range in environmental conditions (Figure 32), and accounted fully for groups A, B, D, and all but one station of group C. Slightly higher mean biomass values (50-54 g m⁻²) were observed at both of the upwelling stations (group E and F, Table 8); however, the distribution of EDSU estimates were similar to those observed at the eleven stations with lower mean krill biomass (Figure 22).

The highest mean krill biomass (96 g m⁻²) and the lowest coefficient of variability

Table 8: Acoustically-derived values of krill abundance observed in spring 1991. The mean (g m^{-2}) and coefficient of variability (CV, %) of krill biomass were computed using the number (n_E) of EDSU-based estimates of krill biomass obtained for each station. The transect parameters, number (km^{-1}) and total area ($\text{m}^2 \text{km}^{-1}$), of all and *HB* aggregations are also given. Stations sampled at night designated by #.

Group	Station	Estimates of krill biomass			Transect Parameters			
		Mean	CV	n_E	All Aggregations		<i>HB</i> Aggregations	
					Number	Area	Number	Area
A	500.120#	32	130	13	2.7	879	1.0	560
	500.140	11	50	10	6.0	1786	0.1	54
	500.160	33	120	9	4.2	1648	0.7	503
B	600.120#	19	170	16	3.2	756	0.6	323
	600.140	17	70	6	5.7	4345	0.4	1232
	600.160#	24	200	4	0.9	339	0.3	293
C	700.080	17	220	8	1.3	715	0.5	508
	700.100	25	150	6	2.0	715	0.4	406
	700.140#	16	180	5	1.2	270	0.5	147
	700.160	58	140	18	1.4	1564	0.7	1374
D	500.100	34	140	12	7.0	2739	1.1	1198
	600.080	29	70	12	13.4	3409	0.5	822
E	600.100#	50	100	10	9.5	2653	1.5	1173
F	700.060#	53	60	3	2.8	2176	2.0	1821
G	700.020#	96	30	5	6.9	2373	2.6	1593

(30%) was found on the inner shelf within Dallman Bay (station 700.020, Figure 34), and was represented by habitat group G with elevated fucoxanthin levels and low surface salinities (Figure 32). The second highest mean krill biomass (58 g m^{-2}) was observed at the only station (700.160, group C) located near the shelfbreak (Figure 34). The local variability at this station was affected by the three highest EDSU estimates observed during spring (Figure 22).

4.5.1.4 Aggregation characteristics

Despite the similarity in integrated krill biomass levels, the aggregation transect parameters based on all aggregations were different between locations (Table 8), i.e., stations with nearly identical mean krill biomass values exhibited different combinations

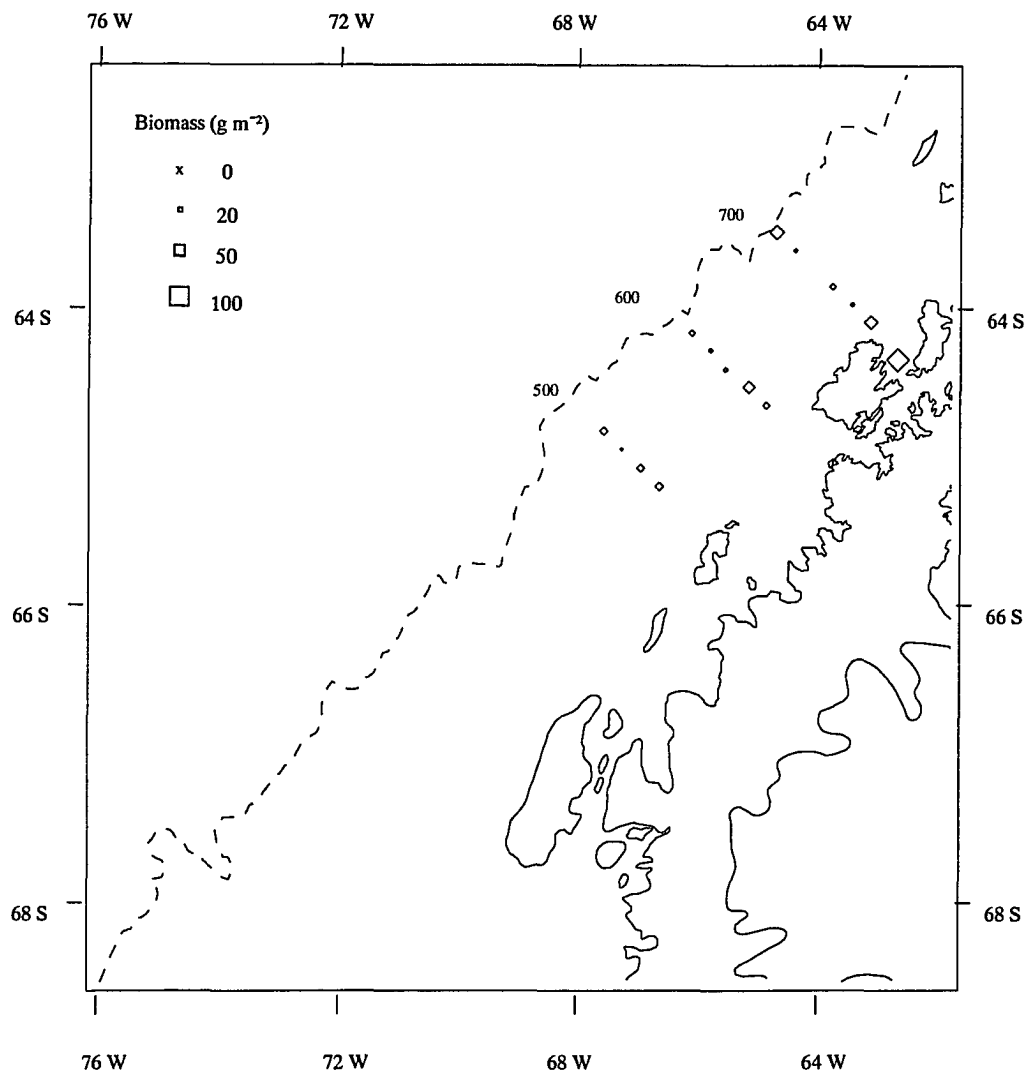


Figure 34: Distribution of vertically-integrated krill biomass (g m^{-2}) observed at locations sampled during spring 1991. The 1000-m isobath is indicated by the dashed line.

of number and total area of aggregations. The abundance of aggregations, in terms of number and total area detected per kilometer of acoustic transect, was lowest for habitat group C. The locations sampled near the ice edge (habitat group D) exhibited the highest abundance of aggregations (Table 8), although total krill biomass was similar to that observed further from the ice edge (Figure 34). The transect parameters based on *HB* aggregations were less variable (Table 8) and better correlated with krill biomass based on comparisons made between stations.

Within each habitat group, the dimensional parameters of the *HB* aggregations covered a broad range which was similar between groups (Figure 35). The most frequently observed *HB* aggregations were characterized by mean volumetric biomass values between 10 and 50 g m⁻³ and covered between 300 and 1000 m² in area. Large aggregations, exceeding 1000 m², were observed for all habitat groups but occurred most frequently for groups C and D (Figure 35c,d). The dimensional parameters of the aggregations observed at the station with the highest mean biomass (700.020, group G, Figure 35f) were not uniquely different from the other stations. The elevated biomass observed at this station was due to a higher abundance, i.e., number and total area, of *HB* aggregations (Table 8).

Over 17% of the total biomass observed during spring 1991 was contained within three large (>2000 m²), dense (>70 g m⁻³) aggregations located near the shelfbreak at station 700.160, each of which exhibited a total biomass value exceeding 150 kg m⁻¹. Despite the presence of these large aggregations the mean vertically-integrated krill biomass at this location (Table 8) was only slightly higher than surrounding stations due to the absence of aggregations throughout much of the acoustic transect.

Visual examination of the echograms from the acoustic observations showed that most of the detected aggregations could be grouped into two pattern types. The first type was characterized by solitary aggregations or small groups of aggregations that were irregularly spaced along the acoustic transect (Figure 36a). The second type was similar

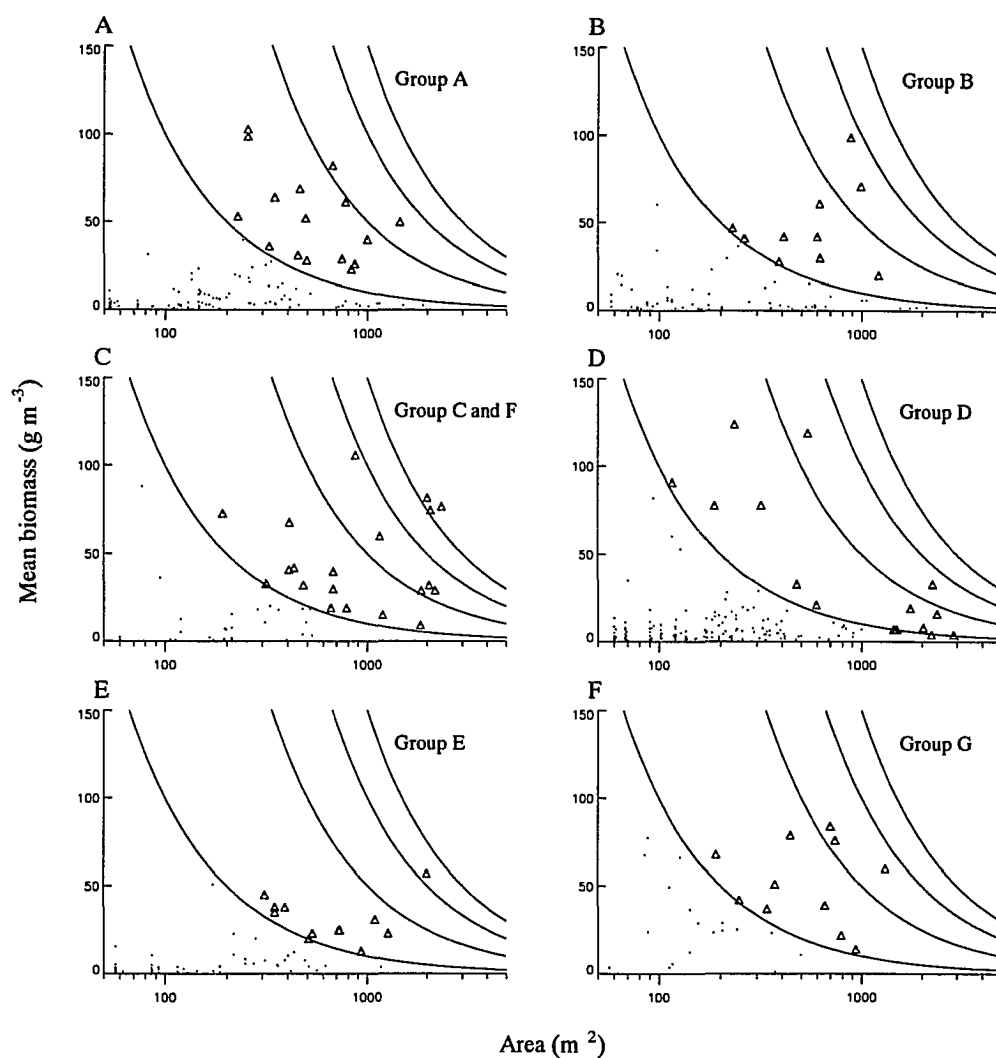


Figure 35: Relationship between cross-sectional area (m^2) and mean biomass (g m^{-3}) for aggregations observed during spring 1991 at locations associated with each habitat group. The Δ and dots, indicate *HB* and all other aggregations, respectively. The solid lines represent the 10, 50, 100, and 150 isolines of total krill biomass (kg m^{-1}), from left to right, respectively. Total krill biomass is computed as aggregation area \times mean biomass.

to the first but with many small, low density aggregations (total aggregation biomass $<10 \text{ kg m}^{-1}$) also observed (not shown).

Exceptions to these basic pattern types were observed at three locations. The acoustic signature, observed at the high biomass ($>95 \text{ g m}^{-2}$) station within Dallman Bay, was characterized by a series of closely spaced aggregations which were aligned in a layer-like or chain-like fashion within the upper 30 m of the water column (Figure 36b). A similar pattern of aggregation arrangement was also observed at one of the ice edge stations (600.080), however, here the aggregations were not as dense and multiple layer-like structures were observed over two depth strata, near 50 and 100 m depth (Figure 36c). Another unique echogram signature was observed at one of the upwelling stations, 600.100 (group E), where the aggregations were numerous, distributed somewhat evenly throughout the transect line, and the majority were positioned deeper than 100 m (Figure 36d). It should, however, be noted that the pattern of aggregation arrangement observed at the second upwelling station (700.060) and second ice-edge station (500.100) was similar to the standard pattern type described above for the rest of the study region.

4.5.1.5 Krill depth distribution

The most frequently observed depth distribution of krill in spring 1991 was characterized by a uni- or multi-modal peak in krill biomass in the upper 80 m of the water column (e.g., Figure 37a). For 12 of the 15 stations the maximum depth range of krill was restricted to the surface mixed layer. At most of these stations, the primary or a secondary peak in biomass was observed coincident with the upper edge of the permanent pycnocline (indicated by subsurface maximum in buoyancy frequency), which separated AASW from CDW (e.g., Figure 37a).

Deeper distributions of krill were observed at the remaining three stations. Most of the krill biomass at the station positioned near the shelfbreak (700.160) was located within the stratified waters of the permanent pycnocline between 100 and 170 m depth (not

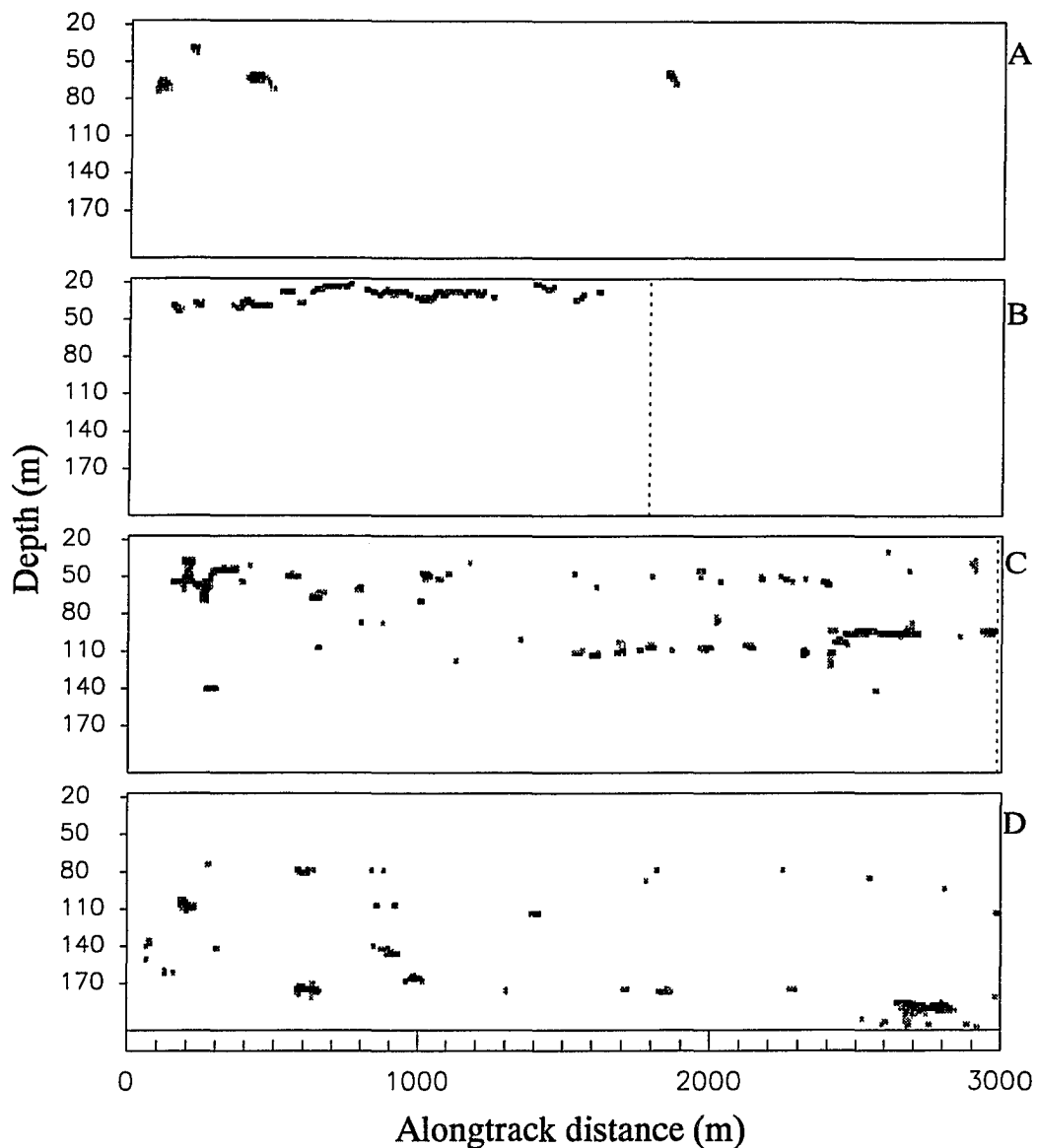


Figure 36: Echograms illustrating different aggregation patterns observed during spring 1991: A) typical pattern of solitary or small groups of aggregations irregularly spaced along the acoustic transect (500.160); B) vertically restricted layer observed in Dallman Bay (700.020); C) vertical alignment observed near ice edge (600.080); and D) deeper distribution observed at upwelling station (600.100). The dotted line denotes the end of the acoustic transect. Differences in the graylevel tones reflect the relative strength of the acoustic scattering.

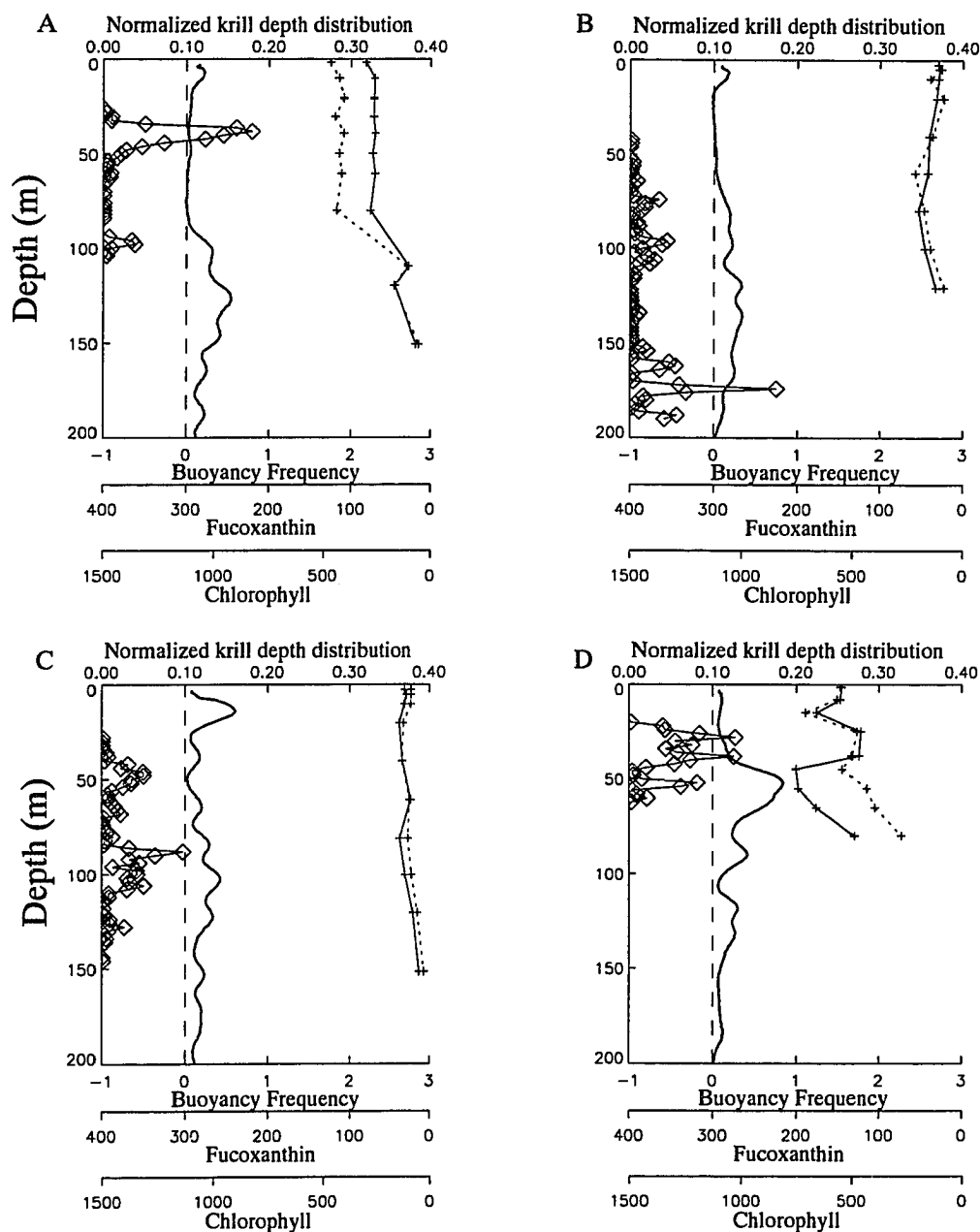


Figure 37: Vertical distribution of normalized krill biomass (\diamond), buoyancy frequency ($10^{-4} \text{ rad}^2 \text{ s}^{-2}$, solid black line), chlorophyll (mg m^{-2} , dashed line with + symbols), and fucoxanthin (mg m^{-2} , solid line with + symbols) observed during spring 1991 at stations: A) 500.160, B) 600.100, C) 600.080, and D) 700.020. The vertical dashed line represents zero buoyancy frequency. Data sources: hydrographic observations (Lascara *et al.*, 1993a) and pigment concentrations (B. Prézelin, unpublished data).

shown). This depth distribution coincided with the vertical placement of the three biggest *HB* aggregations ($>150 \text{ kg m}^{-1}$) observed during spring. The other two stations with deeper depth distributions (600.100, 600.080) were characterized by unique aggregation patterns as described above (Figure 36c,d) and by atypical buoyancy frequency profiles (Figure 37b,c). At the upwelling station, 600.100, over 65% of the biomass was positioned deeper than 150 m, and the depth profile of buoyancy frequency was relatively flat over the depth range of the permanent pycnocline (Figure 37b). At the ice edge station, 600.080, krill were distributed in several broad multi-modal peaks over the depth range 40–120 m and the vertical scale of the layer-like arrangement of krill aggregations was similar in magnitude to the vertical scale ($<10 \text{ m}$) of the multiple peaks observed in the complex profile of buoyancy frequency (Figure 37c).

The vertical distribution of phytoplankton in the upper 100 m was relatively uniform at most locations sampled during spring 1991 and was similar to the vertical profile shown in Figure 37b,c. However, a subsurface maximum in pigment concentration (Figure 37d) was observed at the station within Dallman Bay (700.020), which was characterized by high vertically-integrated levels of chlorophyll and fucoxanthin (Figure 32). This location also had the highest krill biomass observed during spring (Table 8). The presence of dense vertically, restricted aggregations (Figure 36b) which were vertically coincident with reduced pigment levels (Figure 37d) suggests that krill grazing may have affected the distribution and abundance of pigments at this location.

4.5.2 Summer (January-February 1993)

4.5.2.1 Environmental conditions

The hydrographic structure of the upper water column observed during the summer cruise (January-February 1993) was characterized by vertical stratification and across-shelf gradients. As described in a previous section (4.2.2), AASW was vertically partitioned during summer 1993 into layers of warmer, fresher water overlying a sub-surface

region of water which retained the cold temperatures ($<-1.0^{\circ}\text{C}$) and higher salinities observed vertically throughout AASW during the winter (e.g., Figure 15). The introduction of freshwater into the study region was not uniform and an across-shelf gradient in surface salinity was apparent (Figure 38a), with the lowest salinities (<33.6) found on the inner shelf near the Antarctic Peninsula. Over the outer shelf and beyond the shelfbreak, the surface salinities were relatively uniform, varying between 33.81-33.87.

The across-shelf gradient in salinity was used to partition the shelf region into two hydrographic regimes. The 33.8 salinity isoline was chosen as the transition value distinguishing the inner shelf regime from that of the outer shelf. This salinity value represents the freshest AASW observed during the winter (e.g., Figure 12a) and thus it is assumed that waters exhibiting lower salinity values (inner shelf regime) have been modified by fluxes of freshwater. The inner shelf hydrographic regime extended out 120-140 km from the inshore grid baseline on the 200, 400, and 600 lines (Figure 38a). The offshore excursion of the 33.8 isohaline was reduced on the 300 and 500 lines, extending offshore only 100 and 60 km, respectively. Most of the stations with surface salinities of 33.8 or greater were located over CDW; whereas, stations associated with the inner shelf regime were located over MCDW. The position of CDW and MCDW was determined by variations in the maximum temperature observed below the permanent pycnocline (Figure 18).

Surface temperatures within the upper ocean of the outer shelf hydrographic regime were geographically variable (Figure 38b), which was due in part to the direction and timing of the sampling (Figure 8b). The highest surface values ($>1.0^{\circ}\text{C}$) were observed on the southern three transect lines (200-400) which were sampled three weeks later than the two northern lines. The inner shelf regime surface temperatures were generally lower (Figure 38b) than those observed offshore and this distribution may have been due in part to the cold temperatures of the meltwater responsible for reducing the salinity in these areas.

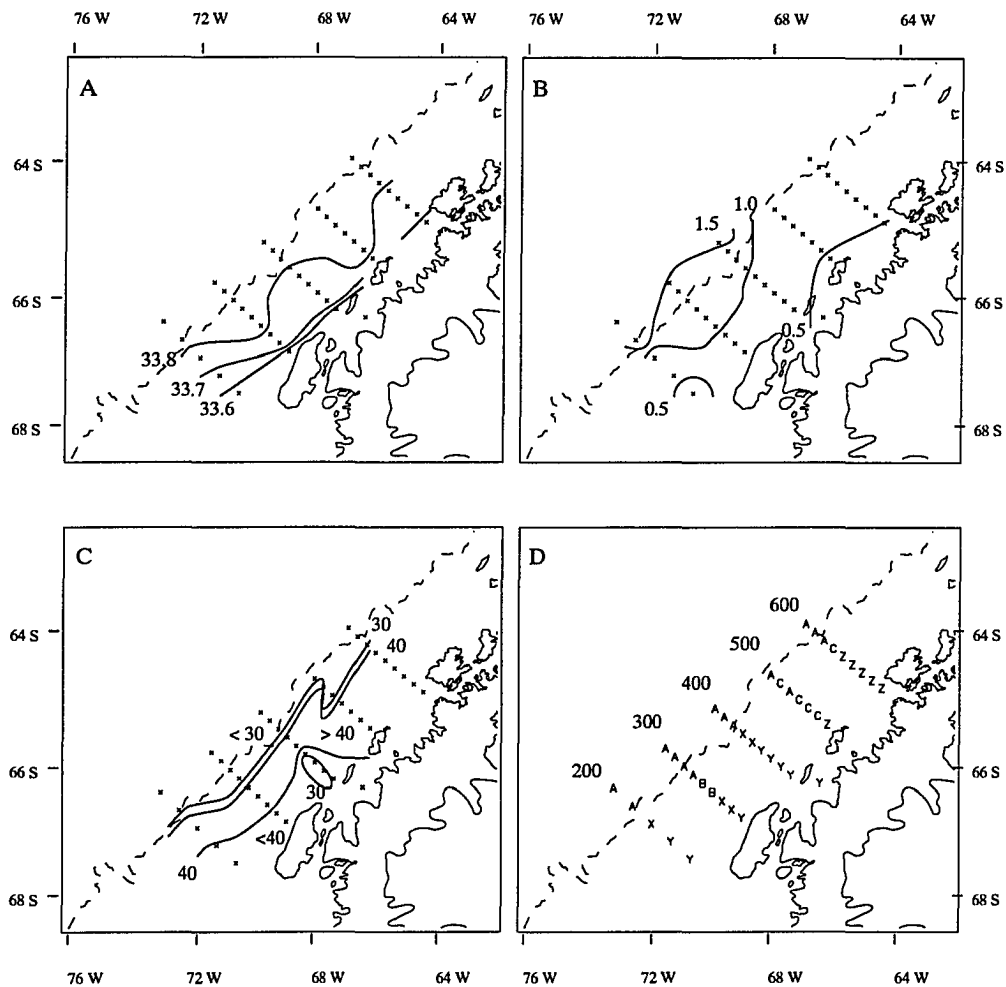


Figure 38: Distribution of A) salinity, B) temperature ($^{\circ}\text{C}$), C) chlorophyll-a concentration (mg m^{-2}), and D) habitat groups (A-C, X-Z, see text for definitions) observed in summer 1993. Hydrographic measurements were averaged over the upper 40 m and pigment concentrations integrated over the upper 80 m of the water column. Station locations are denoted by an X. Dashed line is the 1000-m isobath. Transect line numbers are provided with habitat groups. Data sources: hydrographic observations (Lascara *et al.*, 1993b) and pigment concentrations (B. Prézelin, unpublished data).

The concentration of chlorophyll integrated over the upper 80 m of the water column ranged from 17 to 58 mg m⁻² (Figure 38c). All of the locations sampled near or beyond the shelfbreak were characterized by low chlorophyll values (<30 mg m⁻²). Higher chlorophyll concentrations (>40 mg m⁻²) were observed throughout the middle shelf region and extended onto the inner shelf of the 500 and 600 lines (Figure 38c). The inner shelf of the southern three transect lines exhibited low chlorophyll concentrations (20-40 mg m⁻²).

The 40 locations sampled during summer 1993 were combined into six habitat groups (Figure 38d) based on environmental observations. The pigment correlations were useful in separating locations into habitat groups within each hydrographic regime, however, pigment concentrations observed within a group were variable and some overlap between groups was observed (Figure 39).

Three of the habitat groups (A, B, and C) included locations from the outer shelf hydrographic regime. Habitat group A was characterized by the lowest chlorophyll and lowest hex-fucoxanthin levels of any group (Figure 39) and was restricted to the outer shelf and slope waters, encompassing stations from all transect lines (Figure 38d). Group B was represented by two locations positioned midway along the 300 transect line (Figure 38d), which were characterized by high (>18 mg m⁻²) fucoxanthin concentrations (Figure 39b). The final group, C, associated with the outer shelf hydrographic regime, included several locations on the middle shelf of the northern two transect lines (Figure 38d). This habitat group was differentiated by high chlorophyll and hex-fucoxanthin concentrations (Figure 39).

The inner shelf hydrographic regime was partitioned into three habitat groups (X, Y, Z) (Figure 38d). Group Z was characterized by the lowest observed fucoxanthin concentrations of all groups (Figure 39) and was positioned along the 500 and 600 lines. Habitat group Y exhibited higher fucoxanthin but lower hex-fucoxanthin concentrations

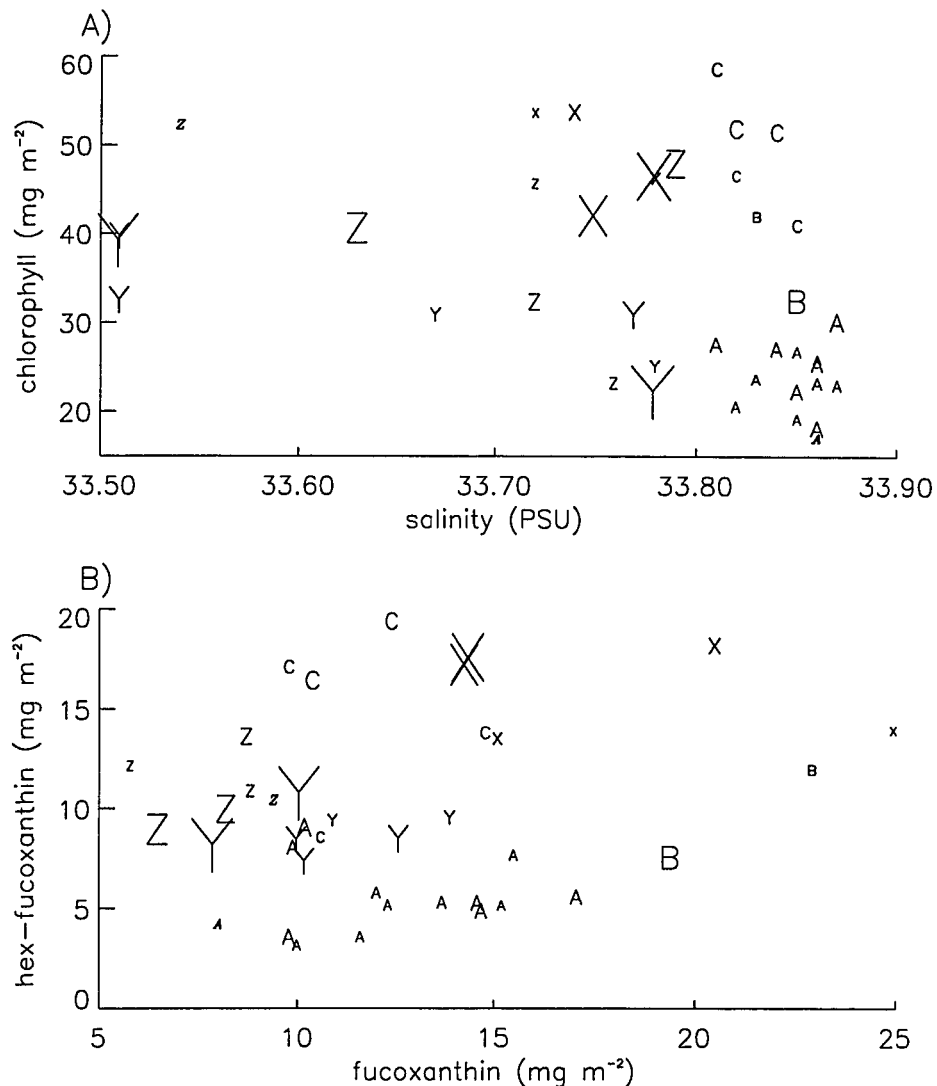


Figure 39: Correlations between selected environmental variables used to partition the locations occupied during summer 1993 into habitat groups: A) salinity and total chlorophyll, and B) fucoxanthin and hex-fucoanthin. Pigment concentrations (mg m^{-2}) were integrated over the upper 80 m and salinity was averaged over the upper 40 m. The size of the letter designating each station's habitat group is scaled by the magnitude of the mean krill biomass observed at that location, with the minimum and maximum letter size corresponding to 1 and 539 g m^{-2} , respectively. Italics indicate stations where krill were not detected acoustically. Data sources: hydrographic observations (Lascara *et al.*, 1993b) and pigment concentrations (B. Prézelin, unpublished data).

compared to group Z and was observed throughout the inner shelf of the southern three transect lines sampled during summer 1993 (Figure 38d). Group X, which was positioned offshore of group Y, had high concentrations of both fucoxanthin and hex-fucoxanthin.

4.5.2.2 Krill population structure

Four groups were formed, based on similarities in krill length frequency distributions (LFD), observed during summer 1993 (Figure 40). Groups 1 and 2 were characterized by individuals smaller than 40 mm, with the mode of group 1 (32-35 mm) being slightly smaller than that of group 2 (34-38 mm). In contrast, groups 3 and 4 were dominated by large individuals, >40 mm (Figure 40c,d). The mode of group 4 (49-52 mm) was larger than the broad mode observed for group 3 (40-50 mm).

Spatial separation of the LFD groups was apparent (Figure 40e). Groups 3 and 4 which represented primarily large, mature adults were restricted to locations associated with the outer shelf hydrographic regime, i.e., seaward of the 33.8 isohaline (Figure 40e). This region also coincided with the presence of CDW, with maximum temperatures exceeding 1.5°C, below the permanent pycnocline. All but two of the locations representing the smaller krill individuals of LFD groups 1 and 2 were located within the inner shelf hydrographic regime.

4.5.2.3 Krill biomass distribution

The abundance of krill was highly variable during summer 1993 (Table 9). Biomass values exceeding 180 g m⁻² were observed at ten of the nineteen stations within the inner shelf hydrographic regime and most of these were located within 60 km of the Antarctic Peninsula (Figure 41). The region of high krill biomass included all three inner shelf habitat groups and so spanned the full range of environmental conditions observed within this regime.

Krill biomass values at the remaining inner shelf sampling locations ranged from 0-78 g m⁻² (Table 9). The transition from high (>180 g m⁻²) to low (<100 g m⁻²)

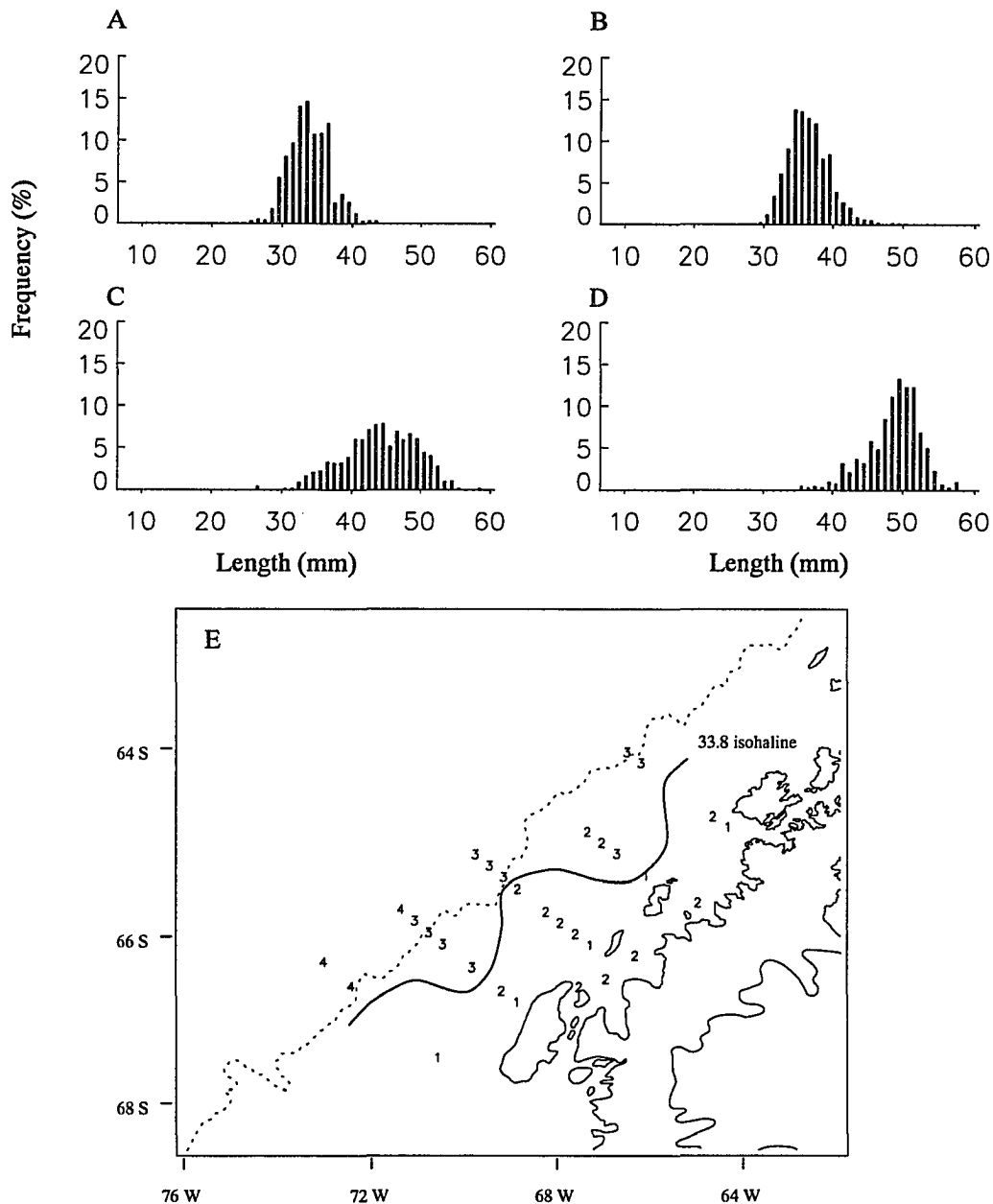


Figure 40: Length frequency distribution (LFD) of krill individuals (1 mm resolution) collected in net samples during summer 1993: A) LFD group 1, B) LFD group 2, C) LFD group 3, D) LFD group 4, and E) mesoscale distribution of LFD groups. The composite LFD for each group was derived from all krill collected at locations with similar station-based LFD. The dashed line indicates the 1000-m isobath and the solid line represents the 33.8 salinity isohaline. Data from net collections provided by R. Ross and L. Quetin (unpublished data).

Table 9: Acoustically-derived values of krill abundance observed in summer 1993. The mean (g m^{-2}) and coefficient of variability (CV, %) of krill biomass were computed using the number (n_E) of EDSU-based estimates of krill biomass obtained for each station. The transect parameters, number (km^{-1}) and total area ($\text{m}^2 \text{km}^{-1}$), of all and *HB* aggregations are also given. Stations sampled at night designated by # and those identified as problematic due to alternate scatterers are designated by *.

Group	Station	Estimates of krill biomass			Transect Parameters			
		Mean	CV	n_E	All Aggregations		<i>HB</i> Aggregations	
					Number	Area	Number	Area
A	200.160*	64	-	1	17.8	17748	2.4	15353
	200.200	60	-	1	20.5	3258	1.1	1432
	300.140*	25	90	8	16.5	7028	0.8	5733
	300.160*	64	50	7	36.4	15056	1.6	8343
	300.180*	67	110	7	22.5	4091	0.9	1700
	300.200#	32	80	4	4.6	454	0.6	117
	400.160*	17	160	17	15.5	6725	0.2	3655
	400.180*	3	160	8	18.5	808	0.0	0
	400.200*,#	20	100	4	11.7	2150	0.3	821
	500.180*	96	20	4	7.3	6582	1.7	5992
	500.140	57	120	2	12.9	2112	1.0	316
	600.160*	19	100	6	6.4	1857	0.4	128
	600.180*	14	150	12	8.4	2019	0.2	349
	600.200#	0	-	1	0.0	0	0.0	0
B	300.100	151	60	5	15.7	3269	3.6	2405
	300.120#	5	210	6	5.3	205	0.2	17
C	500.080	92	110	4	8.3	879	2.7	386
	500.100	39	120	3	13.5	4252	1.0	1390
	500.120	77	80	3	12.2	3131	1.2	1103
	500.160#	32	140	2	2.6	337	0.5	227
	600.140	12	210	5	2.9	271	0.5	74
X	200.120#	1	-	1	1.1	49	0.0	0
	300.060	360	20	3	27.4	4979	8.2	3512
	300.080	78	70	6	5.3	608	1.2	298
	400.120#	32	180	5	1.8	220	0.5	151
	400.140	434	60	4	11.1	2332	4.9	1888
Y	200.040	886	-	1	13.1	16323	2.9	15682
	200.080#	53	-	1	6.5	756	1.3	588
	300.040#	189	140	4	10.5	2023	3.2	1591
	400.040	185	80	4	14.0	5493	2.7	2557
	400.060	202	100	25	16.2	3038	3.2	1599
	400.080	504	110	5	8.7	6369	3.1	5735
	400.100#	32	190	6	4.2	611	0.9	139
	420.000	539	90	3	17.7	4043	7.8	3393
Z	500.060#	2	190	4	4.7	471	0.0	0
	600.040	231	110	18	12.3	4249	2.8	2787
	600.060	200	80	3	19.0	4016	3.7	1491
	600.080	76	90	6	7.3	1009	1.7	462
	600.100#	0	0	6	0.0	0	0.0	0
	600.120	26	250	8	1.4	186	0.3	63

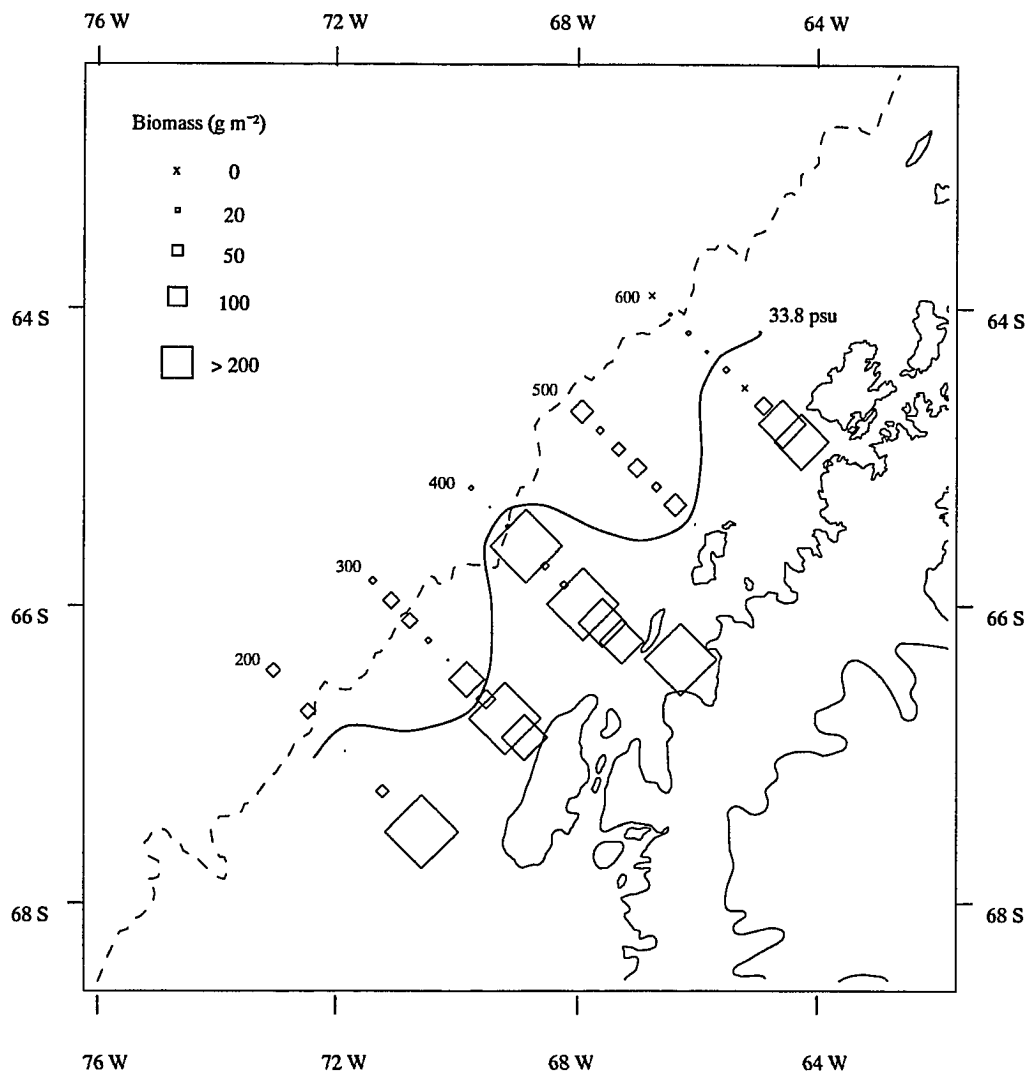


Figure 41: Distribution of vertically-integrated krill biomass (g m^{-2}) observed at locations sampled during summer 1993. The 1000-m isobath is indicated by the dashed line. The 33.8 surface salinity isoline is represented by the thick solid line.

krill biomass within the inner shelf hydrographic regime was not correlated with salinity, temperature, total chlorophyll, specific pigment levels, stratification parameters, or bottom depth (not shown). However, six of the low krill biomass stations were sampled during the night (Table 9) and the reduced level of acoustically-detected krill biomass at these locations may represent an artifact of diel migration by krill into surface waters and out of the acoustic detection range. Also several of the locations with reduced krill biomass within the inner shelf hydrographic regime were positioned on the middle shelf and this area may represent a variable transition region between high krill biomass inshore and lower values offshore (Figure 41).

The sampling stations that comprised habitat group A were primarily located offshore of the shelfbreak and were characterized by krill biomass values ranging from 0 to 96 g m^{-2} . This group included all of the acoustic transects that were identified as problematic due to the presence of alternate scatterers (Table 9) and, hence, many of these krill biomass values may represent overestimates.

The highest krill biomass observed within the outer shelf hydrographic regime (150 g m^{-2}) was located on the middle shelf of the 300 line (Figure 41) in a region of elevated fucoxanthin concentration (300.100, group B). This location was in proximity (within 5 km) to the inner shelf hydrographic regime based on the salinity values measured by the alongtrack thermosalinograph (R. Smith, unpublished data). The other group B station exhibited very low krill biomass, however it was sampled at night. Krill biomass values ranging from 0 to 92 g m^{-2} were found at all habitat group C locations (Table 9). These stations, which were located over the outer and middle shelf of the 500 line, represented the most inshore placement of the outer shelf hydrographic regime (Figure 41).

Spatially-averaged estimates of krill biomass were also computed for each habitat group and for both hydrographic regimes (Table 10). The mean krill biomass observed within the inner shelf hydrographic regime was 183 g m^{-2} , with a higher value of 227

Table 10: Acoustically-derived values of krill abundance observed for each habitat group and hydrographic regime in summer 1993. The mean (g m^{-2}) and coefficient of variability (CV, %) of krill biomass were computed using the number (n_E) of EDSU-based estimates of krill biomass obtained for each habitat group.

Group(s)	Krill biomass		
	Mean	CV	n_E
A	31	130	82
B	70	136	11
C	49	133	17
A,B,C (all)	38	137	110
A,B,C (day only)	41	134	93
X	182	114	19
Y	241	126	49
Z	121	161	45
X,Y,Z (all)	183	139	113
X,Y,Z (day only)	227	118	86

g m^{-2} (Table 10) obtained using day-only collections. Using day/night and day-only acoustic measurements collected within the outer shelf regime, resulted in mean krill biomass values of 38 and 41 g m^{-2} , respectively. The inner shelf regime was thus characterized by a 5-fold higher estimate of krill biomass compared to the outer shelf regime with a coefficient of variation <140% observed for both estimates (Table 10). The length frequency distributions observed at locations within the inner shelf hydrographic regime were dominated by small adults (<38 mm) and thus this size class represented the bulk of the krill biomass observed during summer 1993.

4.5.2.4 Aggregation characteristics

A wide range in aggregation transect and dimensional parameters were observed for discrete locations within each habitat group (Table 9 and Figure 42). The distribution of the dimensional parameters of *HB* aggregations observed for each of the three inner shelf habitat groups (X, Y, Z) were similar (Figure 42b,d,f). Though the abundance of

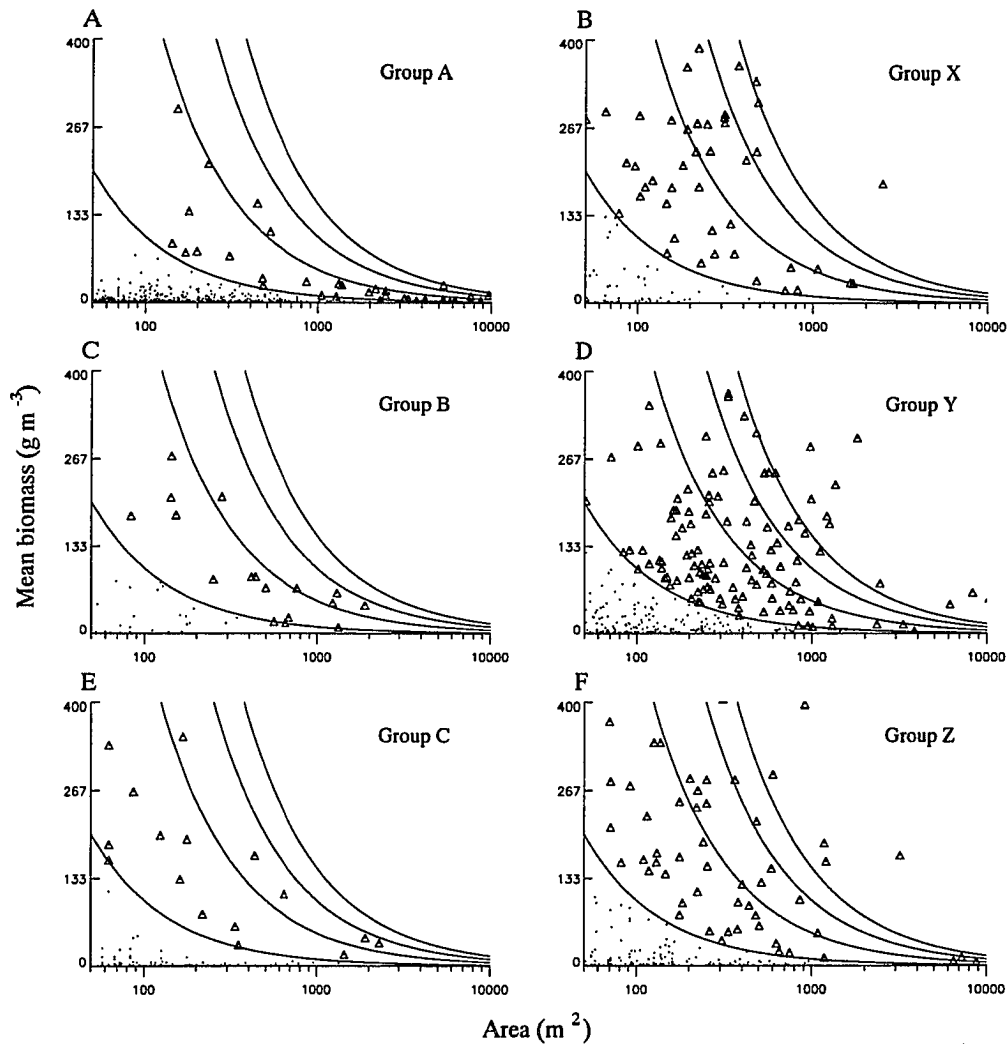


Figure 42: Relationship between cross-sectional area (m²) and mean biomass (g m⁻³) for aggregations observed during summer 1993 at locations associated with each habitat group. The Δ and dots, indicate *HB* and all other aggregations, respectively. The solid lines represent the 10, 50, 100, and 150 isolines of total krill biomass (kg m⁻¹), from left to right, respectively. Total krill biomass is computed as aggregation area \times mean biomass.

aggregations was lower, the dimensional parameters observed for *HB* aggregations within habitat group B and C were also similar to those of the inner shelf regime (Figure 42a,c,e).

Habitat group A was most dissimilar from the others, being characterized by a large number of small aggregations with very low mean volumetric biomass values (Figure 42a). Aggregations exceeding 1000 m² in area, were also more abundant for group A (0.73 per km) compared to all other groups (0.13 per km). The net samples collected at the group A locations were characterized by the presence of several alternate scatterer taxa as described previously (see section 4.4.1). The net observations combined with the atypical character of the aggregations (Figure 20c,d) suggests that many of the aggregations located in habitat group A may represent multi-species assemblages.

Of the 2186 aggregations detected during summer 1993, roughly 32% of the total krill biomass was associated with 22 aggregations, each of which contained over 150 kg m⁻¹ (Figure 42b,d,f). The dimensional characteristics of these aggregations were variable and included relatively small (400-500 m²) and dense (>300 g m⁻³) structures as well as large (>5000 m²) but less dense (<70 g m⁻³) structures. All of these aggregations were observed in the inner shelf hydrographic regime and all but two were found within 80 km of the Antarctic Peninsula.

The acoustic signature for those locations with integrated krill biomass levels below 100 g m⁻², (excluding habitat group A echograms) was similar to that typically observed during spring 1991, i.e., solitary aggregations or small groups of aggregations that were irregularly spaced along the acoustic transect (Figure 43a). Acoustic echograms from transects made within the inner shelf hydrographic regime, that were associated with high vertically-integrated krill biomass estimates, showed the presence of numerous, closely-spaced aggregations (Figure 43b,c) with some single aggregations potentially representing a clustered group of smaller aggregations. In particular, the visual appearance of the three largest aggregations, in terms of areal coverage (5000-10000 m²), observed during summer

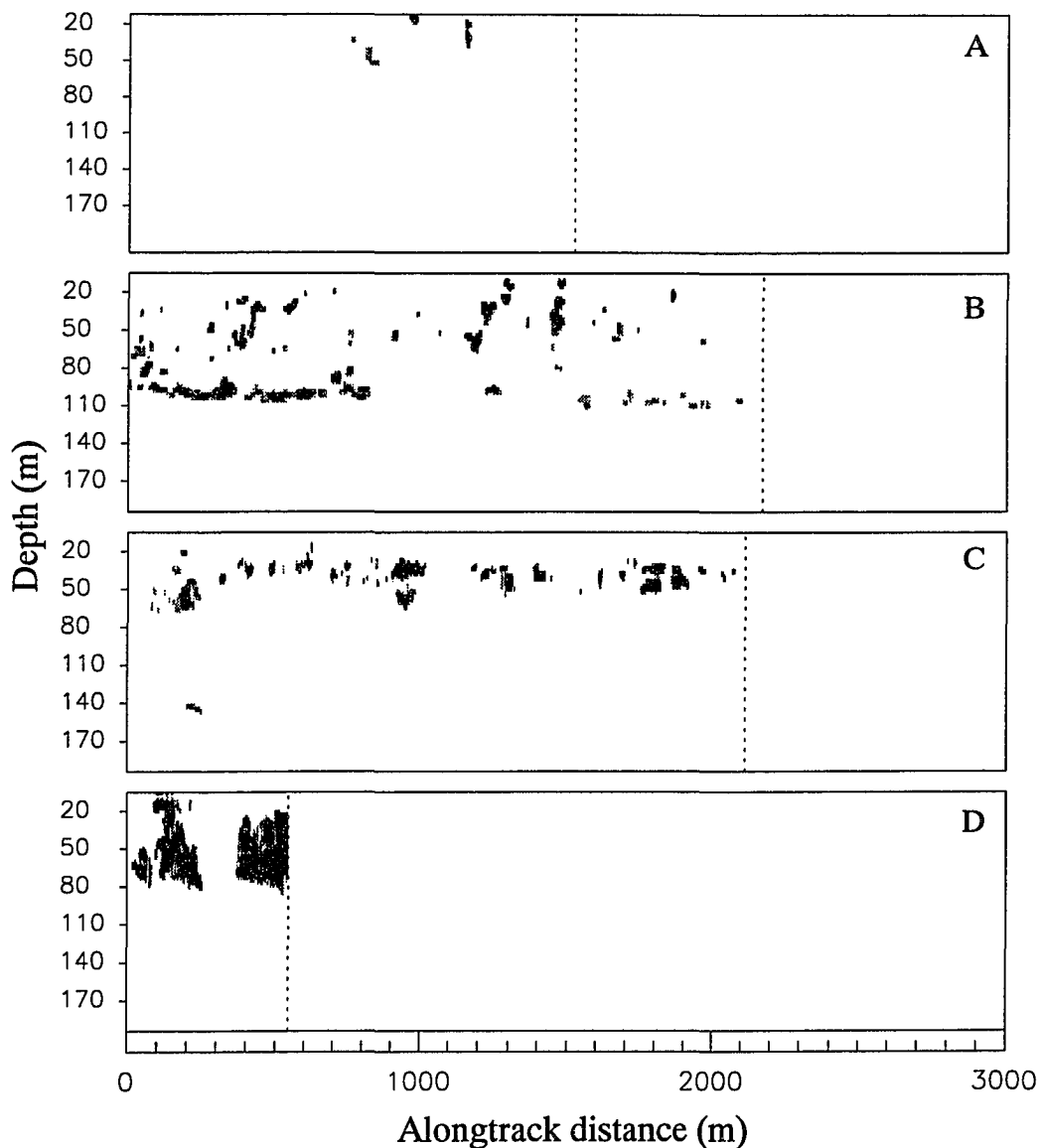


Figure 43: Echograms illustrating different aggregation patterns observed during summer 1993: A) typical pattern observed for stations with krill biomass $<100 \text{ g m}^{-2}$ (600.080); B) closely packed dense aggregations observed at station on the inner shelf (400.060); C) same as B) at station 300.100 on the middle shelf; D) very large ($>5000 \text{ m}^2$) aggregations observed at station 400.080. The dotted line denotes the end of the acoustic transect. Differences in the graylevel tones reflect the relative strength of the acoustic scattering.

1993, suggested that they resulted from the merging of smaller aggregations (Figure 43d). Large aggregations ($>5000 \text{ m}^2$) were found at only two locations on the inner shelf (400.080, 200.040), and the environmental conditions were not uniquely different from those observed at other inner shelf stations.

4.5.2.5 Krill depth distribution

The depth distribution of krill biomass at individual locations was similar throughout the study region during summer 1993. Of the 38 stations at which krill aggregations were detected, 90% were characterized by 90% of the krill biomass positioned shallower than 50 m (Figure 44). Thus most of the krill during summer were located within the lower salinity, stratified waters of the seasonal pycnocline and were coincident with waters exceeding 0°C (Figure 15). Krill aggregations were also routinely detected between 50 and 100 m (e.g., Figure 44); however, their contribution to the total krill biomass was generally quite low ($<10\%$). This deeper depth coincided with the cold waters resident within the unmodified region of AASW (Winter Water in Figure 12c).

The general form of the vertical distribution of pigment concentrations (mg m^{-3}) observed during summer 1993 was variable (e.g., Figure 44). The depths of the maximum concentration of chlorophyll, hex-fucoanthin, and fucoanthin were averaged over all locations, giving median values of 37, 40, and 50 m for these pigments, respectively. Most of the krill biomass was thus positioned shallower than the subsurface maximum for these pigments (not shown). However, at some locations, krill were distributed vertically such that most of the krill biomass was coincident with the maximum or on the upper edge of the maximum in chlorophyll concentration (e.g., Figure 44c,d). Correlation with environmental conditions or time of sampling was not apparent for the limited set of observations which were characterized by vertically coincident distributions of krill biomass and pigment concentrations.

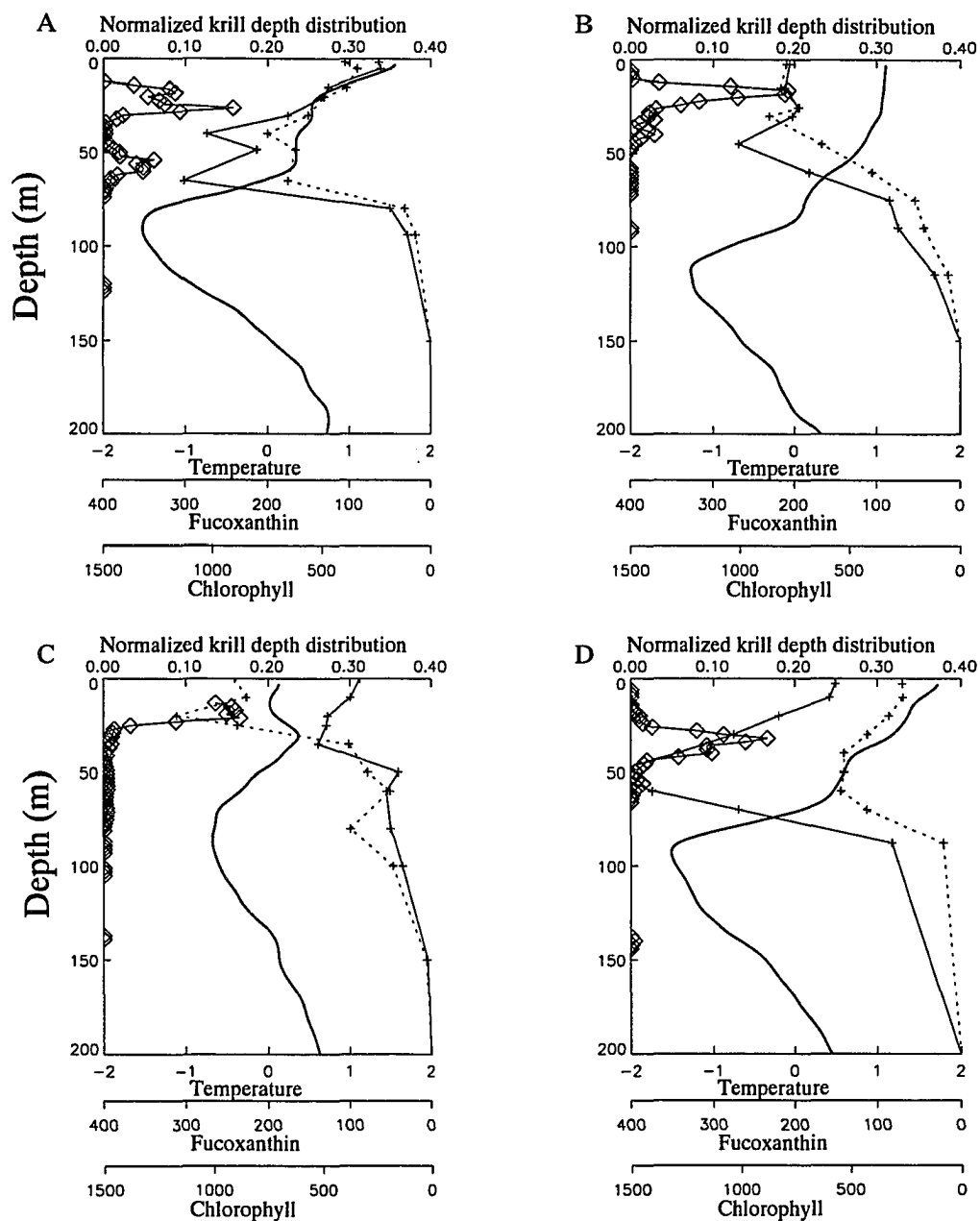


Figure 44: Vertical distribution of normalized krill biomass (\diamond), temperature ($^{\circ}\text{C}$, solid black line), chlorophyll (mg m^{-2} , dashed line with + symbols), and fucoxanthin (mg m^{-2} , solid line with + symbols) observed during summer 1993 at stations: A) 300.060, B) 400.140, C) 600.040, and D) 300.100. Data sources: hydrographic observations (Lascara *et al.*, 1993b) and pigment concentrations (B. Prézelin, unpublished data).

4.5.3 Fall (March-May 1993)

4.5.3.1 Environmental conditions

Mesoscale variations in the hydrographic and pigment distributions observed during the fall sampling period (March-May 1993) were evident (Figure 45). Salinity values over the upper 40 m were lower (Figure 45a) than observed during the preceding summer (Figure 38a), suggesting additional inputs of freshwater between the two sampling periods. Surface salinities exceeding 33.8, which typified the outer shelf and slope regions during summer 1993, were restricted to a few stations located beyond the shelfbreak north of the 700 line during fall 1993 (Figure 45a). Lower salinity water, similar to the inner shelf hydrographic regime of the summer, extended from the Peninsula offshore beyond the shelfbreak throughout most of the study region (Figure 45a). The 33.8 isohaline, which was located on the middle shelf during the summer, was observed generally beyond the shelfbreak by fall, representing an offshore movement of 50-100 km depending on transect line (compare Figure 45a and Figure 38a).

Temperatures observed within the upper 40 m of the water column (Figure 45b) were cooler by 0.5 to 1.5°C than those observed during the previous summer (Figure 38b). Surface temperatures above 0°C and elevated chlorophyll concentrations were observed along the northern transect lines (Figure 38b,c). In contrast, sub-zero temperatures and low pigment levels prevailed along the southern-most grid lines, with lower temperatures and higher chlorophyll levels located on the inner portion of the transects (Figure 45b,c). The apparent north to south gradient in surface temperature and pigment concentrations was due in part to the north to south progression of the cruise track (Figure 9a) over the ten-week sampling period.

As described in section 4.2.2, mixed layer depths were deeper during fall 1993 and the intense vertical stratification, which characterized the summer observations, was seen infrequently. Typically, shallower mixed layer depths were observed at locations with

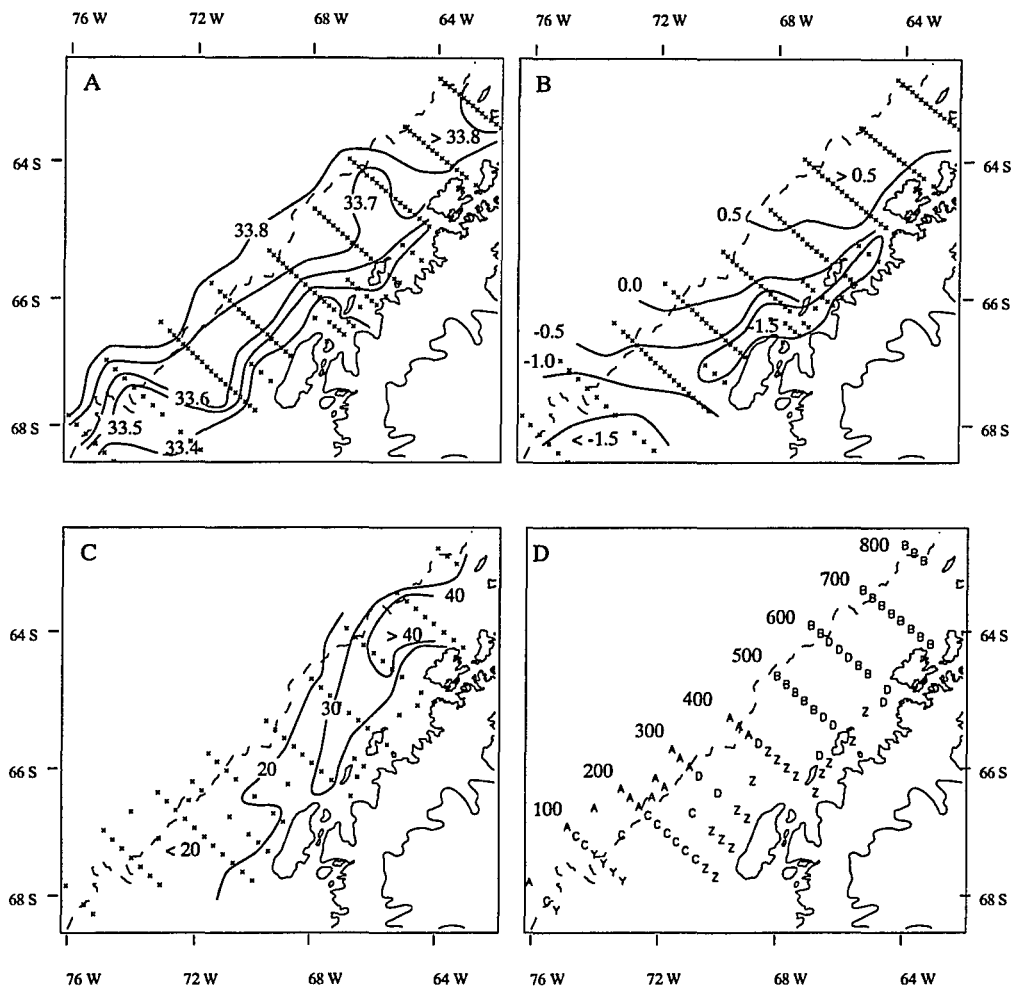


Figure 45: Distribution of A) salinity, B) temperature ($^{\circ}\text{C}$), C) chlorophyll-a concentration (mg m^{-2}), and D) habitat groups (A-C, X-Z, see text for definitions) observed in fall 1993. Hydrographic measurements were averaged over the upper 40 m and pigment concentrations integrated over the upper 80 m of the water column. Station locations are denoted by an X. Dashed line is the 1000-m isobath. Transect line numbers are provided with habitat groups. Data sources: hydrographic observations (Smith *et al.*, 1993a; 1993b) and pigment concentrations (B. Prézélin, unpublished data).

lower surface salinities resulting in an across-shelf pattern to the mixed layer depths (not shown) which was similar to the surface salinity distribution (Figure 45a).

The surface salinity structure was used to partition the study region into three sub-areas (>33.7 , <33.5 , $33.5-33.7$). These salinity definitions, combined with chlorophyll concentrations, were used as a basis for forming six habitat groups (Figure 46). This combination of environmental conditions generally resulted in a north (high chlorophyll) to south (low chlorophyll) geographic split of stations within the three sub-areas defined by salinity (Figure 45d).

4.5.3.2 Krill population structure

Four LFD groups were formed based on analysis of net samples collected during fall 1993 (Figure 47). Groups 1 and 2 were dominated by individuals 34-38 mm in length (Figure 47a,b) with animals >40 mm more prevalent in Group 2. Larger individuals, primary mode between 46-52 mm, dominated groups 3 and 4, with animals <40 mm rare in group 4 (Figure 47c,d). Spatial separation of different sized individuals was apparent during fall (Figure 47e); however, the region dominated by large adults (Figure 47e) was positioned much further inshore than observed during the preceding summer (Figure 40e). Furthermore locations at which groups 1 and 2, characterized by small individuals, were found were primarily restricted to the portion of the inner shelf with low surface salinity values (<33.5) (Figure 47e).

4.5.3.3 Krill biomass distribution

No krill were detected acoustically at over half of the locations sampled during fall 1993, and biomass values $<10 \text{ g m}^{-2}$ were observed at 40% of the remaining stations (Table 11). The distribution of krill was patchy (Figure 48) and showed no apparent correlation with the habitat groups defined by environmental conditions (Figure 45d). Six of the sixteen stations exhibiting biomass values exceeding 10 g m^{-2} were located within 20 km of the shelfbreak and seven were located on the inner shelf within 40 km of the

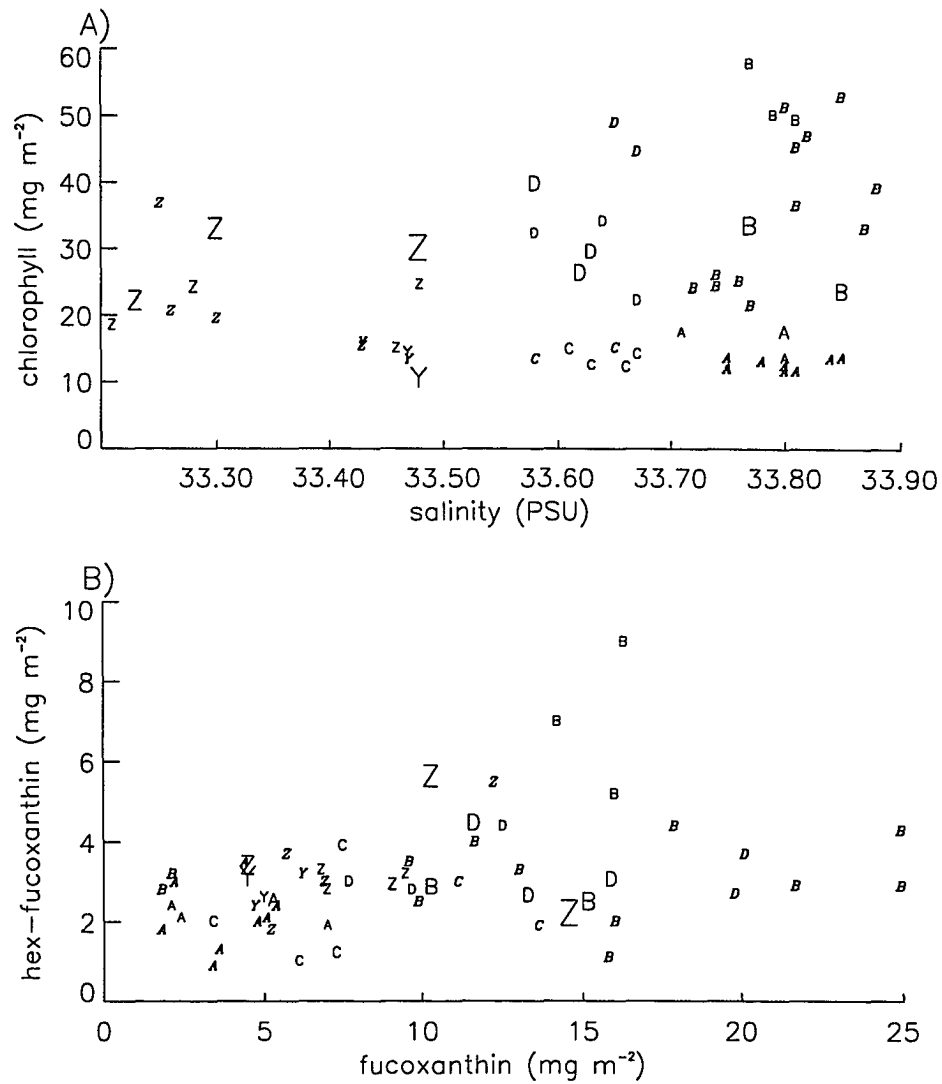


Figure 46: Correlations between selected environmental variables used to partition the locations occupied during fall 1993 into habitat groups: A) salinity and total chlorophyll, and B) fucoxanthin and hex-fucoanthin. Pigment concentrations (mg m^{-2}) were integrated over the upper 80 m and salinity was averaged over the upper 40 m. The size of the letter designating each station's habitat group is scaled by the magnitude of the mean krill biomass observed at that location, with the minimum and maximum letter size corresponding to 1 and 91 g m^{-2} , respectively. Italics indicate stations where krill were not detected acoustically. Data sources: hydrographic observations (Smith *et al.*, 1993a;1993b) and pigment concentrations (B. Prézelin, unpublished data).

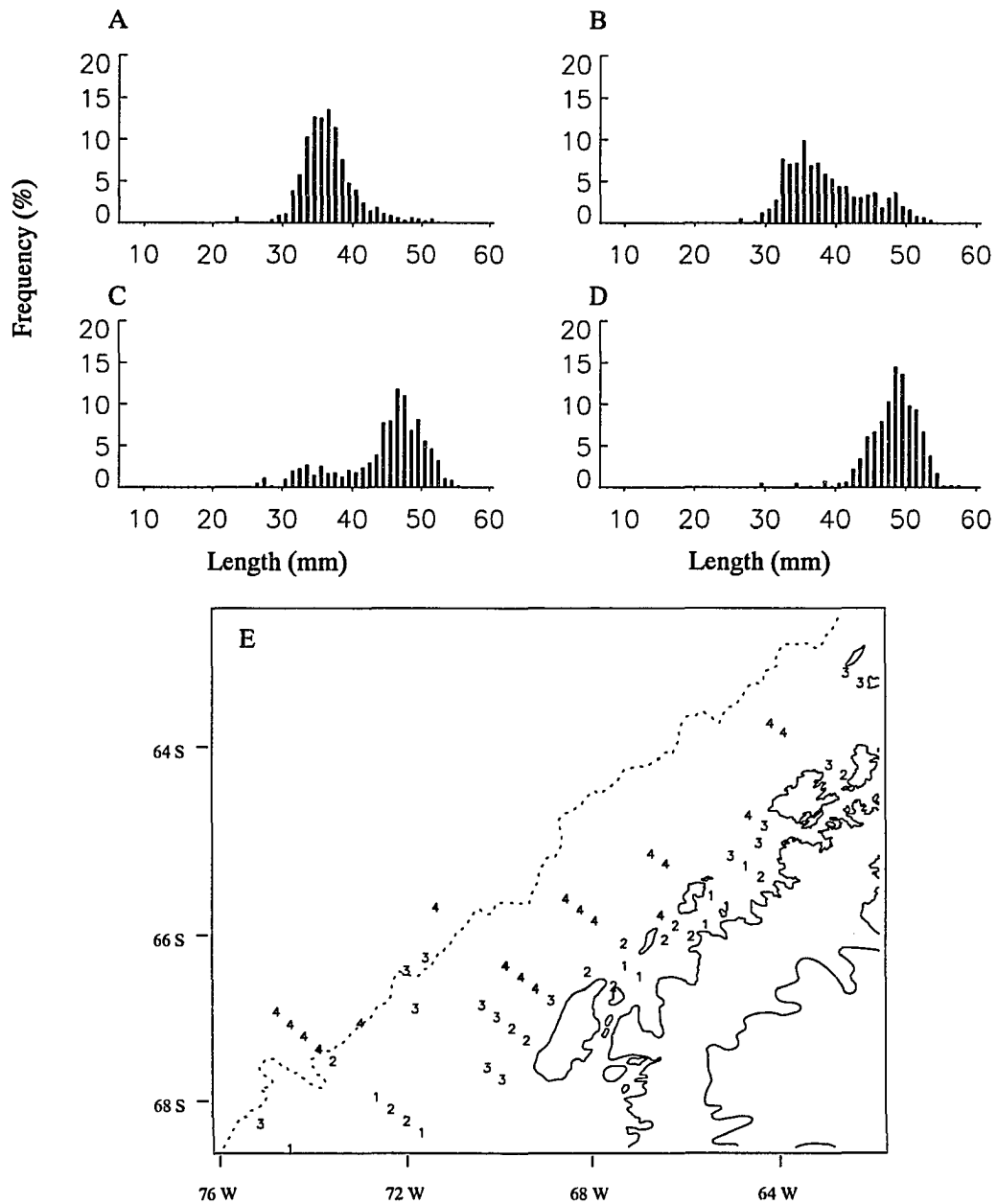


Figure 47: Length frequency distribution (LFD) of krill individuals (1 mm resolution) collected in net samples during fall 1993: A) LFD group 1, B) LFD group 2, C) LFD group 3, D) LFD group 4, and E) mesoscale distribution of LFD groups. The composite LFD for each group was derived from all krill collected at locations with similar station-based LFD. The dashed line indicates the 1000-m isobath. Data from net collections provided by R. Ross and L. Quetin (unpublished data).

Table 11: Acoustically-derived values of krill abundance observed in fall 1993. The mean (g m^{-2}) and coefficient of variability (CV, %) of krill biomass were computed using the number (n_E) of EDSU-based estimates of krill biomass obtained for each station. The transect parameters, number (km^{-1}) and total area ($\text{m}^2 \text{km}^{-1}$), of all and *HB* aggregations are also given. Stations sampled at night designated by #. The 42 stations characterized by zero krill biomass were excluded.

Group	Station	Estimates of krill biomass			Transect Parameters			
		Mean	CV	n_E	All Aggregations		<i>HB</i> Aggregations	
					Number	Area	Number	Area
A	100.200	<1	70	10	3.1	220	0.0	0
	150.200	2	140	4	1.4	79	0.0	0
	250.160	29	200	5	5.8	4148	0.7	3491
	250.180	<1	0	3	0.4	20	0.0	0
	400.140 [#]	<1	230	3	1.2	131	0.0	0
	400.160	20	110	4	1.9	380	0.8	249
	400.180	<1	300	4	0.8	65	0.0	0
B	500.100 [#]	44	-	1	0.8	1082	0.8	1082
	700.040 [#]	<1	210	5	0.5	218	0.0	0
	700.060	2	100	2	0.9	106	0.0	0
	700.080	4	240	7	0.4	123	0.2	109
	800.140	33	70	3	3.6	1087	1.8	601
C	100.180 [#]	4	70	3	0.7	221	0.0	0
	150.140 [#]	2	160	4	0.6	283	0.0	0
	200.040 [#]	7	320	10	0.1	73	0.1	73
	200.060	<1	70	6	1.5	143	0.0	0
	200.120 [#]	6	220	5	0.2	217	0.2	217
	200.140 [#]	29	180	5	0.7	264	0.7	264
D	300.100 [#]	25	140	6	2.4	1302	0.7	840
	300.140	54	240	6	1.2	446	0.6	387
	400.120 [#]	3	230	7	1.3	174	0.2	55
	450.040 [#]	2	-	1	6.2	773	0.0	0
	500.060	37	170	7	2.0	851	0.4	249
	500.080 [#]	2	320	13	0.4	128	0.1	101
	580.030 [#]	21	100	3	0.7	4109	0.7	4109
	600.040	28	150	15	3.9	1654	0.3	984
	600.160 [#]	<1	40	4	0.6	129	0.0	0
Y	100.100	8	200	4	1.0	370	0.3	277
	100.120	61	110	5	1.6	680	0.9	642
	100.140 [#]	<1	90	3	1.3	110	0.0	0
Z	500.020	51	180	11	1.7	2116	0.6	1825
	450.020 [#]	9	170	3	1.1	1146	0.4	343
	430.015 [#]	27	-	1	1.4	1728	1.4	1728
	400.100 [#]	2	210	5	1.7	889	0.0	0
	400.040 [#]	62	-	1	14.2	11594	0.8	5143
	300.060 [#]	2	150	6	1.8	735	0.0	0
	200.020 [#]	13	290	11	0.0	0	0.0	0
	200.000	91	150	12	1.7	2611	1.1	2332
	400.080	5	190	8	1.9	92	0.2	13

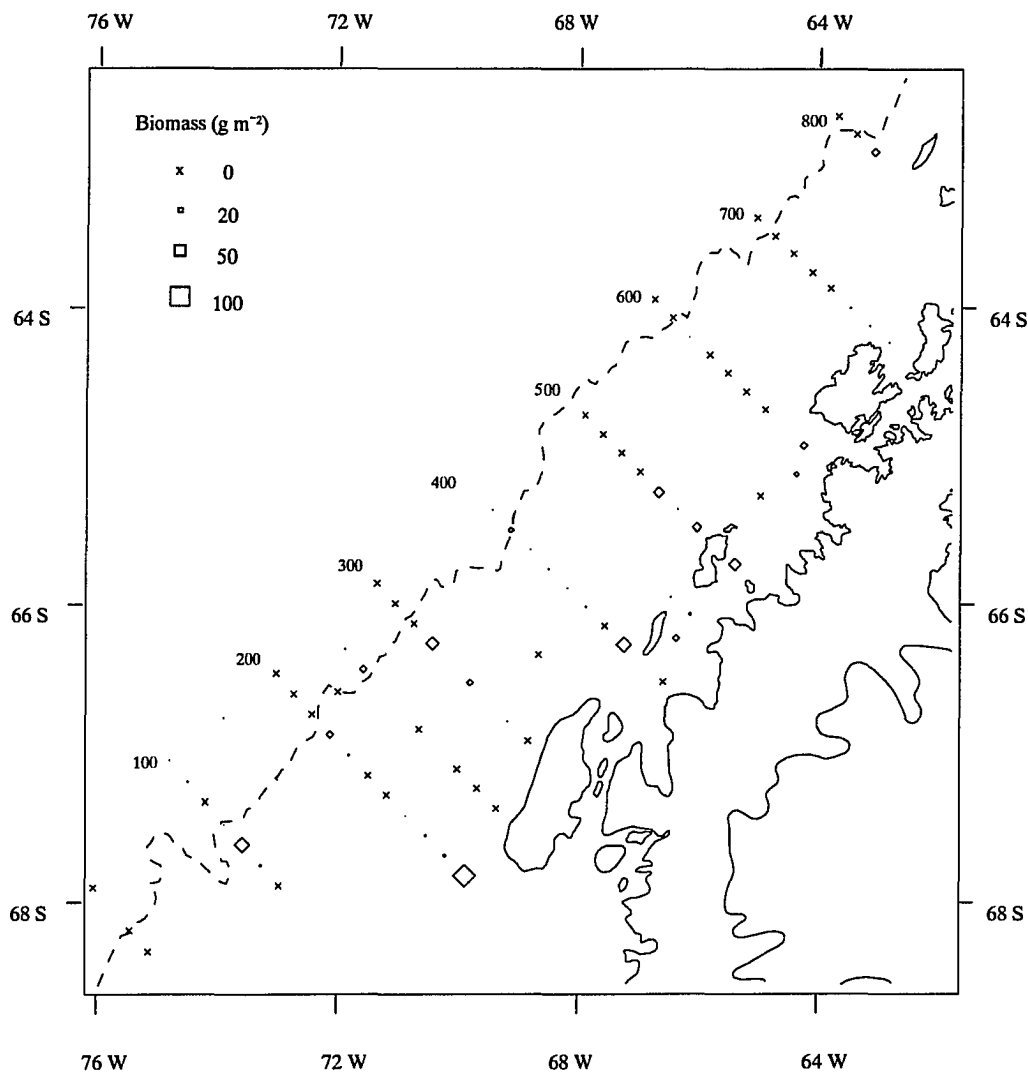


Figure 48: Distribution of vertically-integrated krill biomass (g m^{-2}) observed at locations sampled during fall 1993. The 1000-m isobath is indicated by the dashed line.

inshore grid baseline defined for the study region (Table 11 and Figure 48). These stations thus spanned a broad range in hydrographic and pigment parameters (Figure 46). The magnitude of the highest (50-90 g m⁻²) estimates of krill biomass observed during the fall were similar to the maximum values found during spring 1991 (Table 8) and to the maximum observed within the outer shelf hydrographic regime of summer 1993 (Table 9).

4.5.3.4 Aggregation characteristics

In general, the aggregation transect parameters derived from the fall acoustic observations were low (Table 11). Locations at which the number of aggregations exceeded 2 km⁻¹ or total aggregation area exceeded 1000 m² km⁻¹ were rare.

The dimensional parameters were compared for three groups of aggregations, which were formed based on the location of the aggregation and the mean vertically-integrated krill biomass observed at that location. The distribution of cross-sectional area (m²) and mean volumetric biomass (g m⁻³) of aggregations was similar between inner shelf stations (Figure 49a), shelfbreak stations (Figure 49b), and all other stations (Figure 49c), with the exception that *HB* aggregations exceeding 5000 m² were most frequently observed on the inner shelf.

Consistent with observations from the other seasons, 45% of the krill biomass observed during the fall was contained within eight aggregations each of which exhibited total aggregation biomass values >100 kg m⁻¹ (Figure 49a,b). Four of these were characterized by large areas (>2000 m²) and four exhibited high volumetric biomass (>100 g m⁻³). Several of these *HB* aggregations, which exhibited a variety of sizes and shapes, are illustrated in the echograms provided in Figure 50.

4.5.3.5 Krill depth distribution

The depth distribution profile was similar for most stations during fall 1993 with peaks in krill biomass generally occurring over the depth range between 30 and 80 m (e.g., Figure 50a,b). There were two stations during the fall which exhibited a much

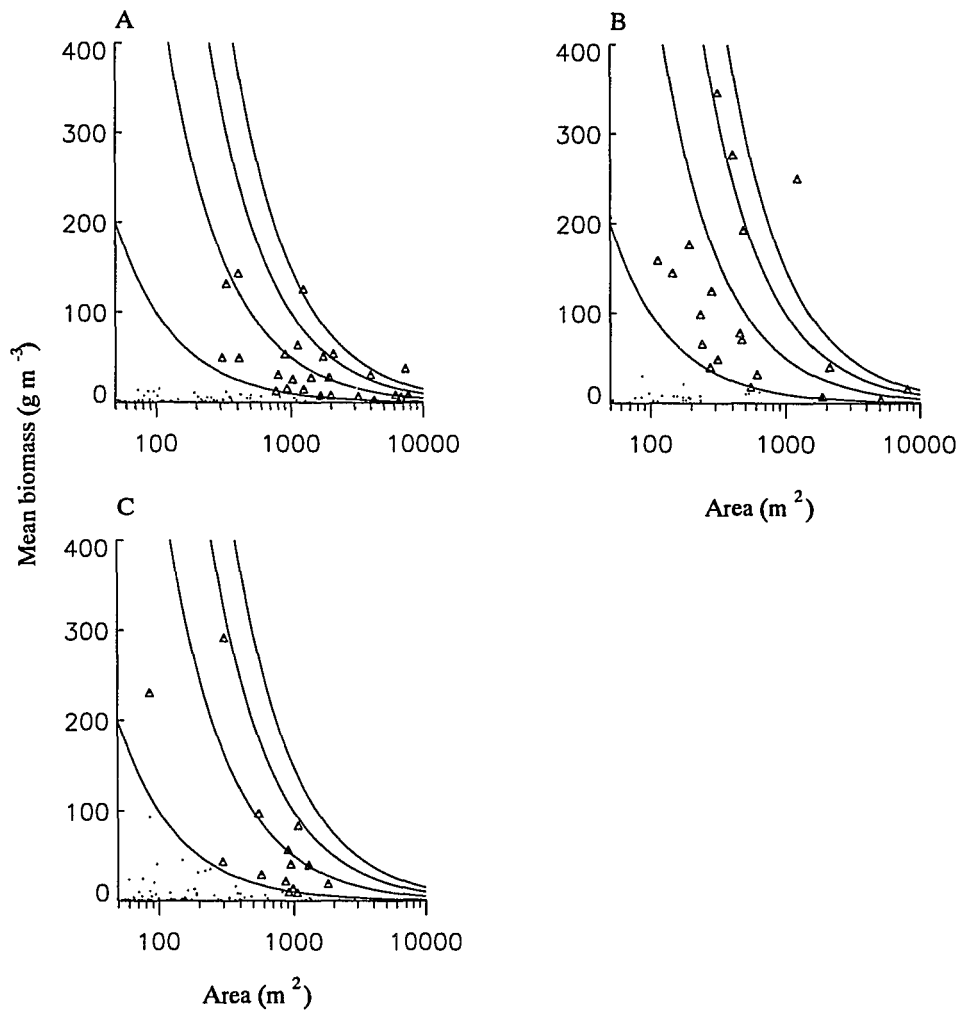


Figure 49: Relationship between cross-sectional area (m^2) and mean biomass (g m^{-3}) for aggregations observed during fall 1993 at locations: A) on the inner shelf, B) near the shelfbreak, and C) all other regions. The Δ and dots, indicate *HB* and all other aggregations, respectively. The solid lines represent the 10, 50, 100, and 150 isolines of total krill biomass (kg m^{-1}), from left to right, respectively. Total krill biomass is computed as aggregation area \times mean biomass.

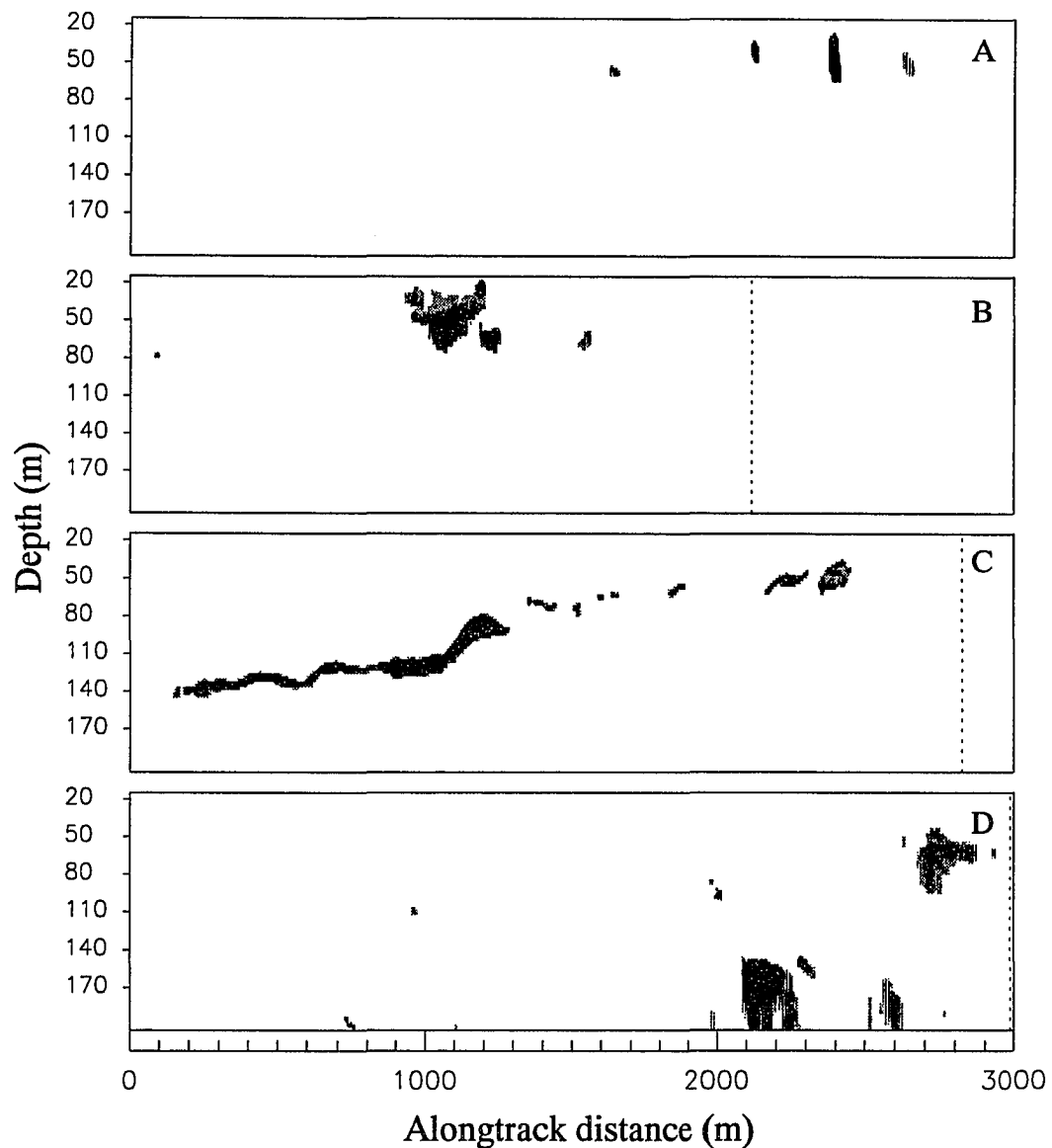


Figure 50: Echograms illustrating different aggregation patterns observed during fall 1993: A) typical pattern of solitary or small groups of aggregations (station 300.140); B) example of large aggregations found on the inner shelf (station 200.000); C) unique, horizontally extensive, layer-like aggregation observed at station 500.020; D) deep, large aggregations observed at shelfbreak station 250.160. The dotted line denotes the end of the acoustic transect. Differences in the graylevel tones reflect the relative strength of the acoustic scattering.

deeper krill depth distribution. One of these stations was located on the inner shelf (500.020, Figure 50c) and one near the shelfbreak (250.160, Figure 50d) and both were characterized by the presence of large *HB* aggregations. No consistent relationships were observed between the vertical profile of krill biomass and any of the pigment profiles (not shown).

4.5.4 Winter (August-September 1993)

4.5.4.1 Environmental conditions

The structure of the upper ocean observed during the winter (August-September 1993) cruise (Figure 51) was obviously quite different from that observed three months earlier (Figure 45). Hydrographic properties and pigment concentrations (Figure 51 and 52) exhibited little geographic variability during winter 1993. Moreover, the upper water column was nearly isothermal and isohaline throughout the region down to the permanent pycnocline (e.g. Figure 13). Sea ice covered the entire study region (Figure 9b) as described previously (section 4.1).

Surface salinities were much higher than observed during the summer and fall 1993, and spanned the narrow range from 33.84 to 34.03, with lowest values observed on the inner shelf (Figure 51a). Chlorophyll concentrations were typically low ($8\text{-}13\text{ mg m}^{-2}$), with slightly elevated levels ($15\text{-}17\text{ mg m}^{-2}$) observed at a few locations along the 600 and 500 lines (Figure 51c). In contrast to the other seasons, the entire study region during winter 1993 was treated as a single habitat group due to the relative uniformity of environmental parameters (Figure 52).

4.5.4.2 Krill population structure

Krill were captured by net in sufficient numbers to determine a length frequency distribution (LFD) at only six locations during winter 1993. One location (500.060) on the inner shelf was sampled over a two-day period and the LFD of krill varied over time at this station. On 6 September, the LFD at station 500.060 was bimodal with one peak including

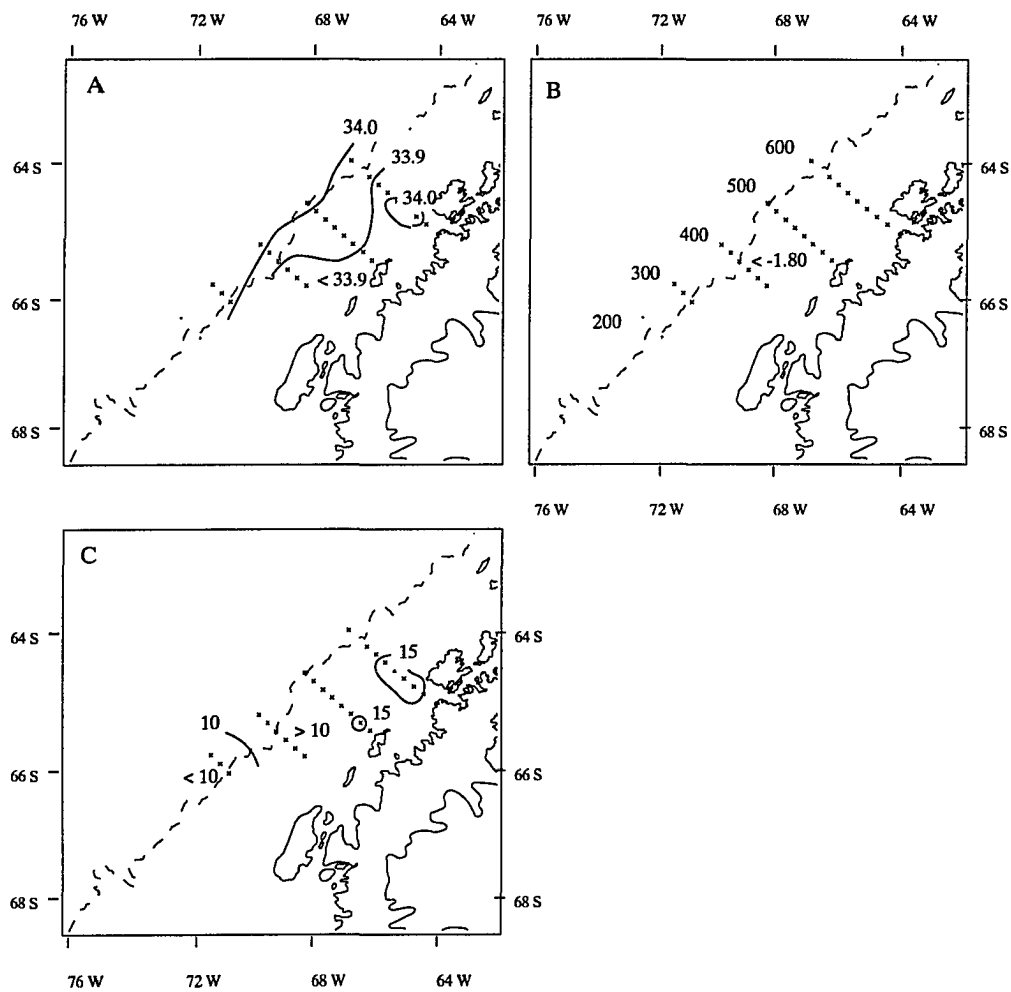


Figure 51: Distribution of A) salinity, B) temperature ($^{\circ}\text{C}$), and C) chlorophyll-a concentration (mg m^{-2}) observed in winter 1993. Hydrographic measurements were averaged over the upper 40 m and pigment concentrations integrated over the upper 80 m of the water column. Station locations are denoted by an X. Dashed line is the 1000-m isobath. Data sources: hydrographic observations (Klinck and Smith, 1994) and pigment concentrations (B. Prézélin, unpublished data).

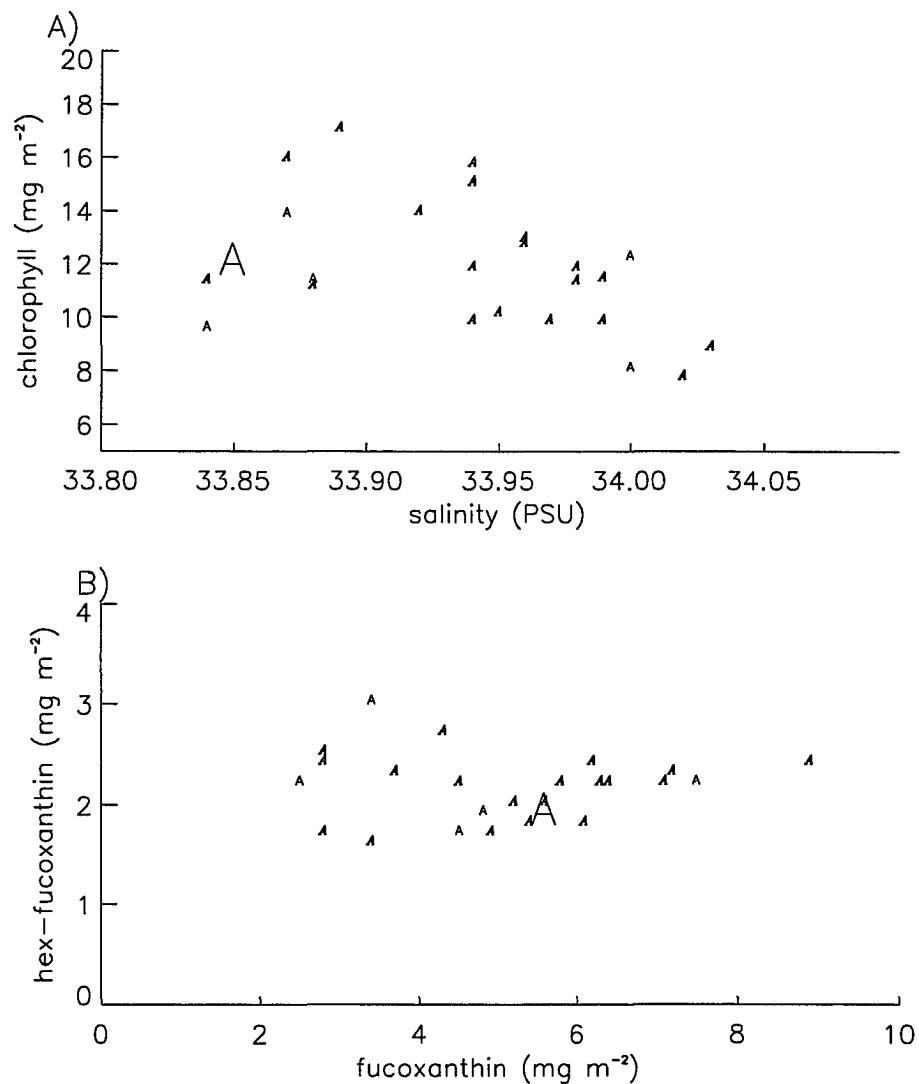


Figure 52: Correlations between selected environmental variables observed at locations sampled during winter 1993: A) salinity and total chlorophyll, and B) fucoxanthin and hex-fucoanthin. Pigment concentrations (mg m^{-2}) were integrated over the upper 80 m and salinity was averaged over the upper 40 m. The size of the letter designating each station is scaled by the magnitude of the mean krill biomass observed at that location, with the minimum and maximum letter size corresponding to 1 and 128 g m^{-2} , respectively. Italics indicate locations where krill were not detected acoustically. Data sources: hydrographic observations (Klinck and Smith, 1994) and pigment concentrations (B. Prézelin, unpublished data).

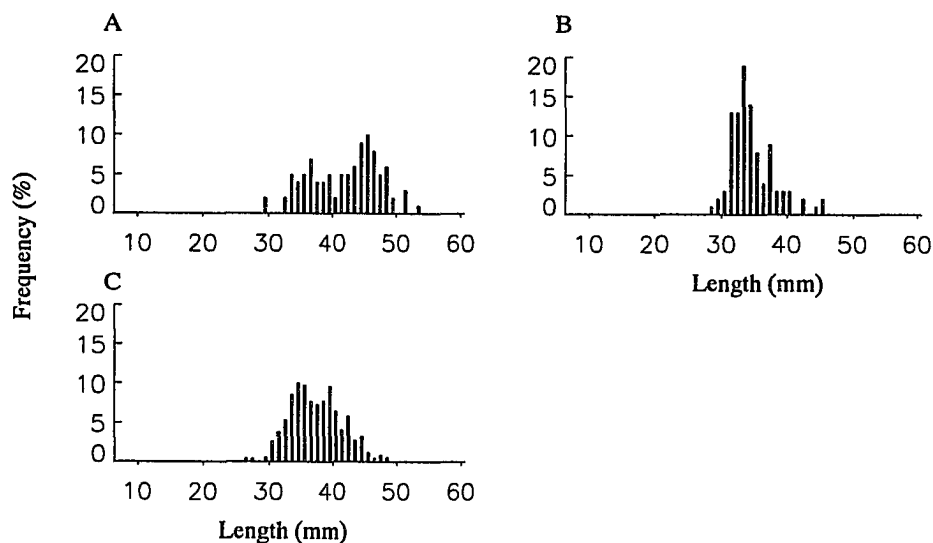


Figure 53: Length frequency distribution (LFD) of krill individuals (1 mm resolution) collected in net samples during winter 1993: A) station 500.060 (6 September), B) station 500.060 (8 September), and C) five stations on outer and middle shelf. Data from net collections provided by R. Ross and L. Quetin (unpublished data).

individuals 32-35 mm in length and the second peak encompassing larger animals (44-47 mm) (Figure 53a). In contrast, the LFD observed two days later (9 September) at this location was dominated by individuals ranging from 33-36 mm (Figure 53b). For the combined net samples collected at five locations on the middle and outer shelf, over 75% of the animals were larger than 34 mm (Figure 53c).

4.5.4.3 Krill biomass distribution

No krill were detected acoustically at 19 of the 25 stations (76%) sampled during winter 1993. Biomass values $<1.0 \text{ g m}^{-2}$ were observed at five stations (Table 12) all of which were located on the outer shelf or beyond the shelfbreak (Figure 54). In contrast, at a single inner shelf station (500.060) (Figure 54), the vertically-integrated krill biomass value was 128 g m^{-2} (Table 12). Acoustic measurements were made at this location (500.060) over a two day period and high krill biomass was observed on both days. The environmental conditions observed at station 500.060 were similar to those of nearby

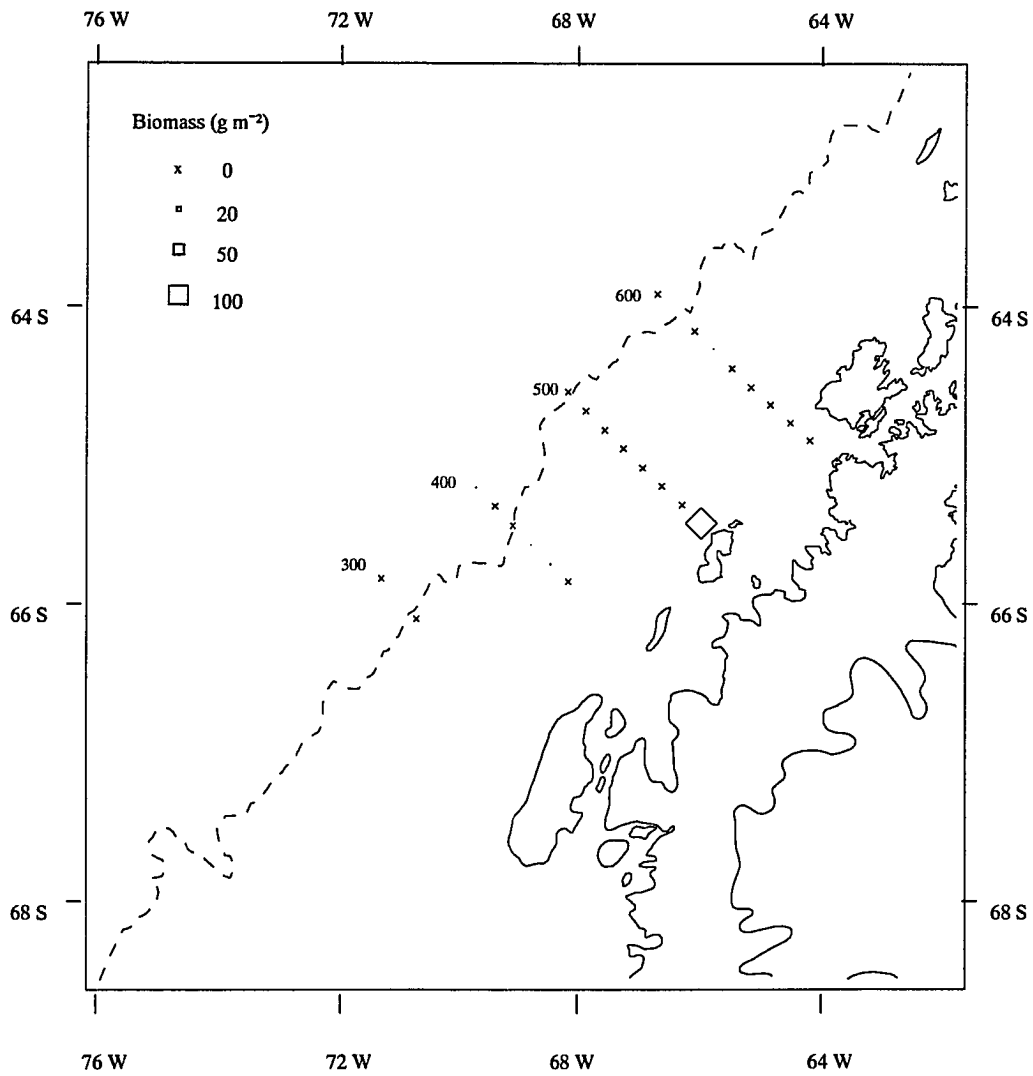


Figure 54: Distribution of vertically-integrated krill biomass (g m^{-2}) observed at locations sampled during winter 1993. The 1000-m isobath is indicated by the dashed line.

Table 12: Acoustically-derived values of krill abundance observed in winter 1993. The mean (g m^{-2}) and coefficient of variability (CV, %) of krill biomass were computed using the number (n_E) of EDSU-based estimates of krill biomass obtained for each station. The transect parameters, number (km^{-1}) and total area ($\text{m}^2 \text{km}^{-1}$), of all and *HB* aggregations are also given. The 19 stations characterized by zero krill biomass were excluded.

Station	Estimates of krill biomass			Transect Parameters			
	Mean	CV	n_E	All Aggregations		<i>HB</i> Aggregations	
				Number	Area	Number	Area
300.180	<1	370	10	0.01	10	0	0.0
400.120	<1	300	9	0.01	10	0	0.0
400.140	<1	270	10	0.3	47	0.0	0
400.200	<1	120	10	0.01	10	0	0.0
500.060	128	170	9	4.8	29373	0.7	28923
600.140	<1	180	3	3.7	553	0.0	0

locations (Figure 52).

4.5.4.4 Aggregation characteristics

The four largest aggregations, in terms of areal coverage, observed on any of the cruises during this study were detected at station 500.060 during winter 1993. These aggregations ranged in length from 630 to 1270 m and in height from 66 to 158 m covering between 20,000 and 100,000 m^2 (e.g. Figure 55). The dimensional characteristics of winter aggregations observed at all other locations were similar to those observed during other seasons.

4.5.4.5 Krill depth distribution

Although the large aggregations observed at station 500.060 were vertically extensive, the biomass was not distributed uniformly within these aggregations with a large percentage of the total biomass generally located within a small region (e.g. Figure 55b,c). The depth distribution observed on the first day this station was sampled indicated that most of the krill were concentrated between 90 and 110 m depth (Figure 55a,b). This vertical placement coincided with well-mixed AASW characterized by near freezing wa-

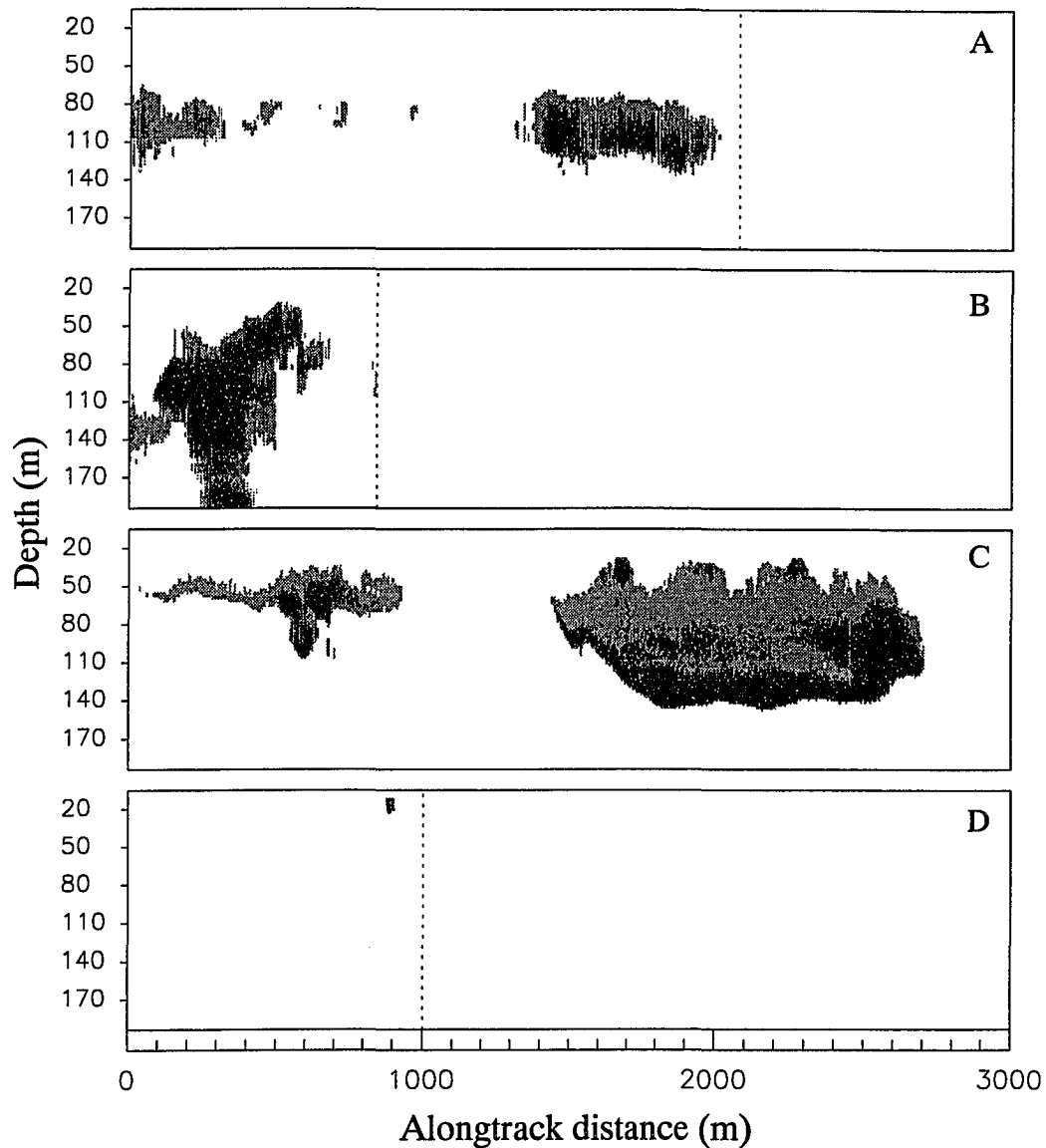


Figure 55: Echograms illustrating different aggregation patterns observed during winter 1993: A) large aggregations observed at station 500.060 on 6 September; B) same as A) for different acoustic transect sampled 30 minutes later; C) same as A) on 8 September; D) typical pattern observed for other stations (400.140). The dotted line denotes the end of the acoustic transect. Differences in the graylevel tones reflect the relative strength of the acoustic scattering.

ter temperatures. On the second day of sampling, the peak in krill biomass was observed somewhat deeper, between 130 and 140 m depth (Figure 55c), and coincided with the upper edge of the permanent pycnocline separating AASW from MCDW. The depth distribution profiles observed at the other locations during winter 1993 were characterized by a unimodal peak in krill biomass in the upper 80 m of the water column (e.g. Figure 55d).

DISCUSSION

The analyses, presented in the Results section, provided descriptions of multidisciplinary observations from four surveys conducted within the waters of the west Antarctic Peninsula continental shelf system (Figure 3). These observations represent an unique Antarctic data set in that full seasonal coverage was provided over a defined region, with three seasons sampled consecutively in a single year. Consequently, seasonal changes in the mesoscale distribution of krill and selected environmental parameters along the west coast of the Antarctic Peninsula can be characterized. In this chapter, variability and factors affecting the variability of the observed physical and biological distributions are discussed. Comparisons are made with results from other Southern Ocean programs that have focused on krill distributions.

5.1 Characterization of physical environment

The hydrographic structure of the study region was characterized by the presence of Antarctic Surface Water (AASW) overlying Circumpolar Deep Water (CDW) as depicted in Figure 56. An important feature of the study region was the across-shelf variation in the maximum temperature observed below the permanent pycnocline, and the term MCDW was used to differentiate cooler CDW over the shelf from warmer CDW beyond the shelfbreak (Figure 18). The ubiquitous occurrence of CDW/MCDW differentiates this region from many other shelf regions around the Antarctic continent, where the water mass, Antarctic Shelf Water, with near freezing temperatures and high salinity (>34.3), resides at depth on the shelf (Mosby, 1934; Deacon, 1937; Hofmann and Klinck, in review). The presence of CDW west of the Antarctic Peninsula provides an important source of heat, salt, and nutrients to the continental shelf (Hofmann *et al.*, in press). Additionally, it has been suggested that CDW is important to the reproductive cycle of Antarctic krill, as the warm temperatures of this water mass accelerate the growth and

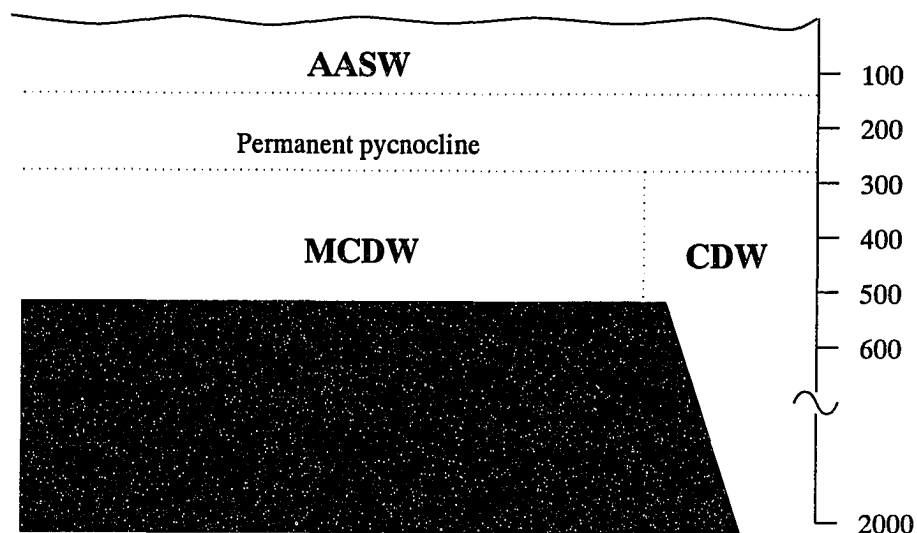


Figure 56: Idealized schematic of the distribution of water masses observed within the region west of the Antarctic Peninsula: Antarctic Surface Water (AASW), Circumpolar Deep Water (CDW), and Modified-CDW (MCDW).

development of krill embryos and larvae (Hofmann *et al.*, 1992).

Analysis of the hydrographic observations collected during this study indicated distinct seasonal changes in the thermohaline character within the upper ocean (AASW) which in turn resulted in an alternation between well-mixed conditions during the winter and spring and vertically stratified conditions during the summer and fall (e.g., Figure 13, 15, and 17). Moreover, these hydrographic observations varied in a manner which was consistent with temporal changes in surface fluxes of heat, salt, and momentum inferred from climatological descriptions of atmospheric forcing, solar irradiance levels, and sea ice coverage for this region (Hofmann *et al.*, in press; Smith *et al.*, in press b; Stammerjohn and Smith, in press).

Across-shelf gradients in the salinity distribution of the upper ocean (AASW) were also observed during all seasons and differences between offshore and inshore salinities were largest during summer and fall (e.g., Figure 38a, 45a). The across-shelf salinity gradient was used to partition the region sampled during summer 1993 into two hydrographic

regimes: an inner shelf and outer shelf regime (Figure 38a). The inner shelf hydrographic regime extended roughly 100 km offshore from the Peninsula during the summer and was observed further offshore during the fall, reaching beyond the shelfbreak (Figure 45a). The across-shelf structure of the surface salinity field suggests that freshwater was being introduced to the study region from coastal regions near the Antarctic Peninsula.

Although the source of the freshwater can not be determined from the existing data sets, potential sources include melting ice (sea ice and glaciers) within the coastal region or alternately the advection of freshwater along the coast from ice melting within regions to the north or south. The annual heat flux from CDW to the upper mixed layer was estimated for this study region by Hofmann *et al.* (in press) based on historical data sets. Sufficient heat is provided by CDW to melt on the order of 0.63 m of ice each year, suggesting that the west Antarctic Peninsula shelf may be a region of ice melt as opposed to a region of ice formation (Hofmann *et al.*, in press) which is consistent with interpretations of sea ice distributions provided by satellite observations (Stammerjohn and Smith, in press a).

5.2 Distribution and abundance of krill

5.2.1 Seasonal variability

Distinct differences were observed between seasons in the spatially-averaged estimates of vertically-integrated krill biomass (Figure 23), the abundance of aggregations, as determined by the transect parameters (Table 6), the dimensional parameters used to characterize individual aggregations (Table 7, Figure 25, 26), the geographic area over which krill were acoustically-detected (Figure 34, 41, 48, 54), and the depth distribution of krill (Figure 27).

Acoustically-derived estimates of krill biomass were highest during the summer and were associated with maximum values in the number and total area of all and *HB* aggregations (Table 9). The summer aggregations were the densest, in terms of mean volumetric biomass (Figure 26), and predominantly occupied the upper 50 m of the water

column (Figure 27). Despite hydrographic conditions similar to those observed during the summer, the fall acoustic observations indicated that spatially-averaged estimates of krill biomass and the abundance of aggregations (no. km^{-1}) had decreased by an order of magnitude (Table 11) and also krill were not detected over a large portion of the region. Dense aggregations ($>100 \text{ g m}^{-3}$) were observed less frequently during the fall, and the frequency distribution of aggregation cross-sectional area had shifted towards larger size classes (Figure 26).

The winter acoustic observations were characterized by the absence of krill throughout most of the region sampled (Figure 54) resulting in low spatially-averaged estimates of krill biomass (Figure 23) and aggregation transect parameters (Table 6). Krill were positioned deeper in the water column (50% of total biomass below 100 m) than all other seasons (Figure 27). The largest aggregations, in terms of cross-sectional area, observed in this study, were detected during the winter. Spring hydrographic conditions were similar to winter observations (Figure 12); however, acoustic observations documented the presence of numerous aggregations in the upper 70 m of the water column throughout the region sampled. Aggregation transect parameters and integrated krill biomass values were an order of magnitude higher than those observed in winter and were similar to the values observed during the summer for the outer shelf hydrographic regime (Table 6, Figure 23).

Quantitative acoustic observations that can be used for direct comparison with the spatially-averaged, vertically-integrated estimates of krill biomass obtained during this study are available for only a few surveys conducted primarily in the region encompassing the Bransfield Strait, South Shetland Islands, and Elephant Island (Figure 57). The magnitude of krill biomass observed in spring 1991 and summer 1993 are consistent with the limited measurements available for direct comparison (Figure 57). Interannual variability is apparent in the combined summer observations and the summer 1993 krill biomass value (110 g m^{-2}) was higher than all other summer estimates ($17\text{-}90 \text{ g m}^{-2}$) with the exception of the 1993 estimate obtained by the U.S. AMLR program (135 g m^{-2} ,

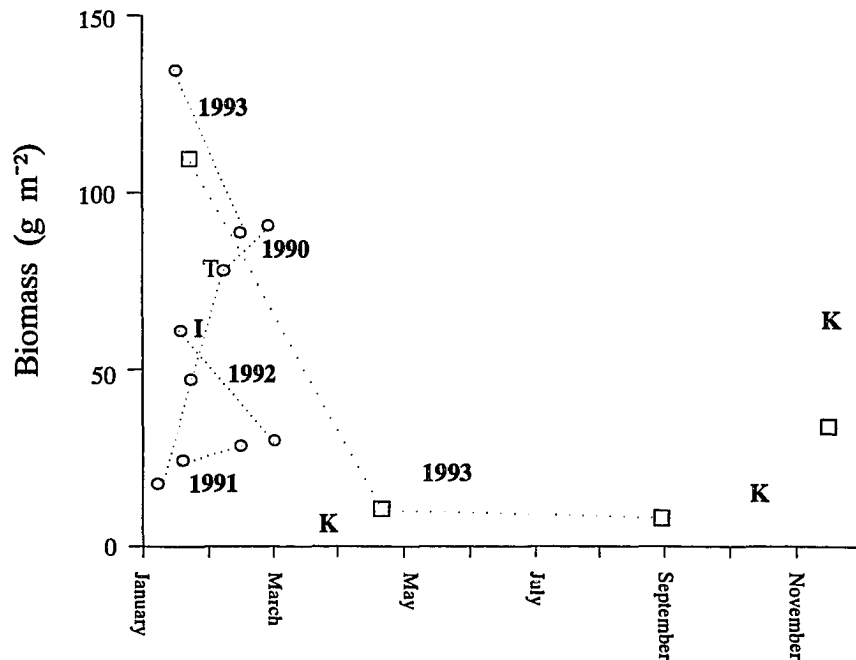


Figure 57: Comparison of acoustically-derived, spatially-averaged estimates of krill biomass (g m^{-2}) by month. Datasets are denoted as: \square - this study; \circ - AMLR study region near Elephant Island (Hewitt and Demer, 1993a; 1993b); I - north of South Shetland Islands (Ichii *et al.*, 1993); K - Elephant Island (Klindt, 1986 as adjusted by Hewitt and Demer, 1993a); and T - southwest Atlantic survey region during FIBEX (Trathan *et al.*, 1995). Estimates collected within the same year by the same program are connected by dotted lines and labelled accordingly.

Hewitt and Demer, 1993b).

The observations used in this analysis represent the only quantitative acoustic estimates of krill abundance available for the west Antarctic Peninsula shelf region from the fall through late winter. The reduction in acoustically-derived estimates of krill biomass by an order of magnitude during the fall and winter compared to summer 1993 in this study, however, is consistent with the seasonal pattern described from analysis of net-derived krill density estimates from Bransfield Strait and around the South Shetland Islands (e.g., Figure 7) (Stepnik, 1982; Godlewska and Rakusa-Suszczewski, 1988; McClatchie, 1988; Siegel, 1988; Siegel, 1992).

These combined data sets suggest that the seasonal changes observed in this study is a recurrent annual pattern at least for the broad region from Adelaide Island to Elephant Island. In addition the variation in spatially-integrated krill biomass is much higher between seasons than between years for waters west of the Antarctic Peninsula. Long term programs, such as the Palmer LTER, which are focused on the characterization of interannual ecosystem variability in this region, should interpret their observations with an understanding of the magnitude of seasonally-induced variability in krill biomass.

5.2.2 Mesoscale variability in krill biomass

The distribution and abundance of krill also varied spatially in this study and a feature common to all seasons was the observation that krill were more abundant at selected locations on the inner shelf, within coastal waters near the Antarctic Peninsula (Figure 34, 41, 48, 54). The geographic area over which krill were acoustically-detected was smallest during winter 1993 and elevated krill biomass ($>100 \text{ g m}^{-2}$) was restricted to a single location which was positioned on the inner shelf near Renaud Island (Figure 54). High biomass levels were observed at this location over a two-day period suggesting that concentrations of krill were remaining in the local area at least over this time scale. The hydrographic parameters and pigment concentrations measured at this location were not

notably different from other locations sampled on the inner shelf (Figure 52).

During fall 1993, the highest krill biomass levels ($10\text{-}90\text{ g m}^{-2}$) were restricted to a few locations on the inner shelf within 60 km of the Peninsula and to a few locations within 20 km of the shelfbreak (Figure 48). These locations were positioned throughout the study region and exhibited a wide range in environmental conditions (Figure 46). The presence of thick pack ice prevented extensive sampling of the inner shelf during spring 1991 and acoustic measurements were made at only two locations within this region. However, the highest krill biomass (96 g m^{-2}) observed during this cruise was found at the inner-most location sampled (Figure 34), in Dallman Bay, which was characterized by a shallow mixed layer depth ($<40\text{ m}$) and elevated chlorophyll (35 mg m^{-2}) and fucoxanthin (12 mg m^{-2}) concentrations.

Observations collected during summer 1993, indicated that the vertically-integrated krill biomass was roughly 5-fold higher for the inner shelf hydrographic regime compared to the outer shelf (227 versus 41 g m^{-2} , Table 10). The geographic area defined by the inner shelf regime encompassed all of the inner shelf as well as portions of the middle shelf and thus instances of elevated krill abundance were observed furthest offshore during summer compared to the other seasons. The difference in krill biomass observed in summer 1993 between the two regimes represents a conservative difference as krill biomass may have been overestimated within the outer shelf hydrographic regime due to the presence of several alternate acoustic scatterers (e.g., salps, pteropods, amphipods) found in net samples throughout much of this region.

An across-shelf gradient in krill biomass was also described by Ichii *et al.* (1993) based on acoustic measurements made during summer 1991, north of the South Shetland Islands. Specifically, krill were an order of magnitude more abundant in inshore waters (138 g m^{-2}), defined as the region within the 150-m isobath, compared to oceanic waters (8 g m^{-2}), defined as the region beyond the shelfbreak (Ichii *et al.*, 1993). Intermediate

levels (24 g m^{-2}) were observed in the frontal region near the insular shelfbreak (Ichii *et al.*, 1993). The acoustically-derived estimate of krill biomass for the inshore waters (138 g m^{-2}) of the South Shetland Islands was similar to the estimate (183 g m^{-2}) obtained for the inner shelf hydrographic regime (surface salinity <33.8) in the LTER study region during summer 1993. Likewise, the outer shelf hydrographic regime in summer 1993 exhibited krill biomass levels (38 g m^{-2}) which were consistent with those observed in the frontal region (24 g m^{-2}) by Ichii *et al.* (1993).

In a more qualitative examination, Witek *et al.* (1981; 1988) described higher concentrations of acoustically-detected krill over the shelf with notably lower biomass values located on the outer-shelf and beyond the shelfbreak (Figure 4), in the large region between Adelaide Island and Elephant Island during summer 1977 and 1979. Mesoscale variability in the abundance of krill has also been described from net-based estimates of krill density (Siegel, 1989; 1992; Brinton, 1991) obtained during several spring and summer surveys within Bransfield Strait and the Scotia Sea. Analysis of krill fishing activity for the broad region from the Antarctic Peninsula to South Georgia (Everson and Goss, 1991) demonstrated that trawling efforts are concentrated in the shelf zone during the summer.

Few observations are available for the fall and winter seasons that can be used to describe mesoscale variations in the distribution of krill. During a RACER cruise conducted in winter 1992, net estimates of krill density were relatively higher ($100\text{-}1000 \text{ ind. per } 1000 \text{ m}^3$) on the inner shelf along a transect from Anvers Island to Crystal Sound (Nordhausen, 1994). Qualitative ADCP measurements obtained on the same cruise, indicated the frequent presence of krill aggregations within Gerlache Strait (Zhou *et al.*, 1994). During a net survey of krill in winter 1986 (Siegel, 1989), krill were found to be most abundant ($>200 \text{ ind. per } 1000 \text{ m}^3$) at a location on the inner shelf, which was positioned in the same general area near Renaud Island where large krill aggregations were acoustically observed during the winter of 1993 in this study (Figure 54).

The results of this study and those described above, clearly establish the inner shelf as a region of relatively higher krill abundance in all seasons. The multidisciplinary observations collected concurrently with the acoustic observations in this study also indicated that the environmental conditions observed on the inner shelf were different from those observed on the outer shelf and beyond the shelfbreak. Consistent across-shelf gradients were observed in hydrographic parameters with surface salinities generally lower and mixed layer depths shallower on the inner shelf. The inner shelf area is typically covered by ice from early winter to mid spring; whereas, ice coverage of the outer shelf exhibits higher interannual variability (Stammerjohn and Smith, in press).

Although the pigment concentrations were variable on the inner shelf, they were typically higher than those observed beyond the shelfbreak. Furthermore, chlorophyll concentrations that are an order of magnitude higher than those observed in this study, were measured during several spring and summer seasons at a series of locations positioned near the 600 line but inshore of the inner-most station sampled in this study (Prézelin, 1992; Moline *et al.*, in review). Periodic polyna formation has been observed in this region during the winter (Stammerjohn and Smith, in press a) and, although undocumented, these events may result in higher winter pelagic phytoplankton levels over short periods. Given that sea ice covers the inner shelf for a longer period of time than the outer shelf (Stammerjohn and Smith, in press a), higher food concentrations in the form of sea ice biota may be available in this region. Thus, the potential exists in all seasons for the inner shelf to represent a region of higher food availability to krill, relative to regions further offshore.

During average winters, the inner shelf within the study region is spatially removed (by at least 100 km) from the ice edge (Stammerjohn and Smith, in press a), where elevated concentrations of krill predators have been shown to overwinter (Ainley *et al.*, 1988; Fraser and Trivelpiece, in press a). Thus krill located on the inner shelf may experience reduced predation pressure during the winter. However, during the summer,

the pattern in predation pressure is reversed and krill located in waters of the inner shelf would be subject to higher predation pressure particularly in areas near seabird rookeries and mammal breeding grounds. The geographic area over which elevated concentrations of krill were observed in this study did extend furthest offshore in summer, which may have located a portion of the krill population away from selected areas of intense predation pressure.

5.2.3 Mesoscale variability in krill size structure

A consistent feature observed during the spring, summer and fall was an across-shelf pattern in the length frequency distribution of krill collected by nets (Figure 33, 40, 47). Analysis of the combined acoustic and net observations indicated that large, mature individuals were more abundant in areas positioned further offshore in comparison to coastal regions characterized by high abundance of small adults. Moreover, this pattern resulted in a general correlation between different size animals and different environmental conditions. For example, the net collections from summer 1993 indicated that small adults (32-38 mm) were associated with the inner shelf hydrographic regime, characterized by low surface salinity, which was located over the inner and middle shelf. Large, reproductively mature, adults (45-60 mm) predominated offshore, beyond the shelfbreak. This region was characterized by higher surface salinity (>33.8) associated with the outer shelf hydrographic regime and by the presence of warm CDW at depth.

During the fall, the geographic extent of the region occupied by small adults (<40 mm) was reduced and confined to the inner shelf and as such was associated with the lowest surface salinities observed at any time during this study. Large adults were found over the broad region extending from slope waters onto the middle shelf and included several locations on the inner shelf. Although large animals were generally located offshore of smaller individuals, their distribution was no longer correlated with the outer shelf hydrographic regime or with CDW. During the spring cruise, large (>40 mm) individuals

were collected only at two locations on the outer shelf, one of which was located over CDW.

In contrast to the other seasons, a distinct pattern in the spatial distribution of different size classes was not observed during the winter; however, krill were collected by nets at only a few locations during this cruise. Net collections from the location on the inner shelf, where large aggregations were acoustically-detected, indicated that large and small adults were utilizing the inner shelf region during the winter.

The spatial pattern in size separation observed in this analysis was consistent with previous observations reported for the Antarctic Peninsula and Bransfield Strait (Quetin and Ross, 1984; Siegel, 1988; 1992; Brinton, 1991; Trathan *et al.*, 1993a; Ichii *et al.*, 1993). Horizontal migration has been suggested to play a role in establishing the spatial variations in krill size class and maturity stages (Siegel, 1988). This hypothesis implies that mature adults move offshore in the early spring, at the onset of the spawning season, and return inshore during the fall, after spawning (Figure 6).

The correlation between the distribution of krill aggregations containing large, mature animals and the presence of CDW observed in summer 1993 is consistent with similar observations from the Bransfield Strait and South Shetland Islands (Hofmann *et al.*, 1992). In a modeling study by Hofmann *et al.* (1992), numerical simulations were used to show that krill eggs spawned in regions with CDW, hatched at depths near 700 m and reached the surface in less than 3 weeks; whereas, eggs spawned where CDW was absent (i.e., cold Antarctic Shelf Water was present), hatched at greater depths and took over 30 days to reach the surface. Hence, krill larvae spawned in regions of CDW, have greater carbon reserves which will allow a longer time period for the location of suitable food conditions (Hofmann *et al.*, 1992).

In the region west of the Antarctic Peninsula, CDW ($>1.5^{\circ}\text{C}$) was generally restricted to waters beyond the shelfbreak; however, the entire shelf region was flooded with

MCDW which was only slightly cooler (1.0 - 1.3°C) (Figure 18). The implication of this water mass distribution is that eggs spawned over the shelf or advected into this region would still encounter warm temperatures at depth that would accelerate larval growth and development. Although a portion of the egg development may occur on the bottom due to shallower depths over the shelf, the presence of MCDW would result in larvae reaching the surface with energy reserves similar to larvae located offshore. However, larvae present over the shelf may encounter higher food concentrations throughout the summer and fall compared to offshore locations, as suggested by the pigment distributions observed as part of this study (B. Prézelin, unpublished data). The nearshore coastal waters west of the Antarctic Peninsula have been characterized as important nursery grounds for Antarctic krill based on the spatial distribution of larvae observed during the RACER program (Huntley and Brinton, 1991; Brinton, 1991).

5.2.4 Implications for interannual and interregional comparisons

The general features of the distribution and abundance of krill described above suggest that comparisons made between years and between regions will be affected by two major factors. First, spatially-averaged estimates of krill biomass are sensitive to the relative proportions of inner shelf, outer shelf, and slope contained within the survey domain. Surveys which focus on shelf waters will result in higher krill biomass estimates than those which split sampling effort between inshore and offshore areas. For example, estimates of krill abundance were five-fold higher for the inner shelf hydrographic regime compared to the outer shelf (227 versus 41 g m⁻²) during summer 1993. Regional comparisons between spring 1991 and summer 1993 indicated that the abundance of krill increased three-fold from spring to summer; however, if comparisons were restricted to locations on the outer shelf, very similar levels of krill biomass were observed in spring and summer (34 versus 38 g m⁻²).

Secondly, interannual variability in recruitment processes will be reflected in krill

abundance as well as the demographic structure of the krill population. Priddle *et al.* (1988) suggested that after years of poor recruitment, krill length frequency distributions will be skewed towards larger size classes; whereas, juvenile krill will dominate after years of good recruitment. Interannual variations in krill cohort strength have been linked to variations in sea ice coverage which directly affects the survival rate of krill larvae during their first winter (Siegel and Loeb, 1995). Multi-year cycles in sea ice parameters have been observed for the region west of the Antarctic Peninsula and a maxima in sea ice coverage occurs every 5-7 years (Fraser *et al.*, 1992; Stammerjohn and Smith, in press a). Based on the combined analysis of almost two decades of krill size class data derived from penguin diet samples and net-based estimates of krill abundance, Fraser and Trivelpiece (in press b) suggested that interannual variations in total krill abundance and the relative abundance of various size classes reflected variations observed in sea ice coverage west of the Peninsula.

There is evidence that the abundance of krill during 1993 was unusually high, both along the west coast of the Antarctic Peninsula and around Elephant Island (Figure 57). The highest concentrations of krill observed on the inner shelf in 1993 were comprised of primarily small adults (30-40 mm, age group 2) and furthermore age group 1 (20-28 mm) was virtually absent. This observation is consistent with the characterization by Siegel and Loeb (1995) of strong recruitment for the 1990/1991 year class and poor recruitment for the 1991/1992 class. The absence of age group 1 during 1993 would lead to the prediction of reduced krill biomass levels on the inner shelf during 1994, as the abundant 1990/1991 year class (30-40 mm individuals observed during 1993 summer cruise) became reproductively mature and moved offshore during the spring of 1994.

5.2.5 Krill aggregations

The analysis approach (Nero and Magnuson, 1989) used to quantify the two-dimensional structure of the acoustic observations, was originally developed to examine

various scales of zooplankton patches observed in the Gulf Stream (Nero *et al.*, 1990). This approach proved to be a powerful tool for rapidly and objectively quantifying the transect and dimensional parameters of krill aggregations. Estimates of aggregation parameters were sensitive to the biomass threshold value and to the discretization scheme used to generate the two-dimensional matrix of acoustic data (see Methods 3.2.5).

A wide variety of sizes, shapes, and volumetric densities were noted; however, over 80% of the aggregations were <50 m in horizontal length, <10 m in vertical height, covered <500 m², with mean biomass values <25 g m⁻³ (e.g., Figure 25, 26). A second characteristic feature observed, in all seasons, was that most of the krill biomass (>80%) was associated with a small subset of larger or denser aggregations (*HB* aggregations in Table 6).

Published descriptions of the dimensional character of aggregations observed during the summer are available for the region along the Antarctic Peninsula between Anvers and Adelaide Islands (Witek *et al.*, 1981), a larger region including Bransfield Strait and the Scotia confluence (Miller and Hampton, 1989a), the south-west Indian Ocean (Miller, 1994; Miller and Hampton, 1989b). Statistics on the size (length, height, cross-sectional area) and volumetric density of aggregations detected during summer 1993 (Table 7) are consistent with those obtained for the historical data sets listed above and confirm earlier characterizations of krill aggregations as small, compact structures.

Quantitative measurements of the dimensions of aggregations during seasons other than summer are limited. Acoustic observations collected from late November through early January in the northern Weddell Sea (Sprong and Schalk, 1992) indicated that smaller aggregations (1000-5000 m²) contributed most to the cumulative backscattering during the spring, whereas larger aggregations (10⁴ m²) dominated during the summer, an observation not consistent with the results presented here. During spring 1991, most of the krill biomass was attributed to aggregations with areas between 300-2000 m²; whereas,

the summer 1993 observations indicated a shift in the biomass distribution to smaller (<500 m²) aggregations (Figure 26).

Acoustics data collected during a series of twelve cruises in the late 1980s, between Anvers Island and the South Shetland Islands, were recently used to describe seasonal differences in the distribution and character of krill aggregations (Ross *et al.*, in press). Although the analysis (Ross *et al.*, in press) was based solely on visual examination of echograms, it represents the only published description of krill aggregations that includes observations from all seasons. Consistent with the current study, a seasonal pattern of maximum aggregation size in winter and smaller sizes in spring and summer was described by Ross *et al.* (in press) based on temporal changes in the horizontal and vertical dimension of individual aggregations. Furthermore, Ross *et al.* (in press) described a seasonal change in aggregation abundance with high values during the summer (0.15-0.23 km⁻¹) and low values (0.04-0.07 km⁻¹) during the winter, which is similar in pattern, although the values were much lower, to observations collected the current study (e.g., Table 6).

5.3 Factors affecting seasonal variations in krill distributions

The distribution and abundance of krill is assumed to be controlled primarily by three factors, circulation, population dynamics, and krill behavior, all of which are affected by environmental variability as depicted in Figure 58. This conceptual model of krill interactions will be used as a framework to discuss which factors are potentially responsible for the observed seasonal variation in krill abundance. Order of magnitude changes in the seasonal abundance of krill are not consistent with the time scales of recruitment and growth exhibited by krill, an animal which can take 2-3 years to become reproductively mature and lives for 5-7 years. For this reason, population dynamics are not considered the driving force behind seasonal changes in krill abundance.

The temporal change in the mesoscale distribution and abundance of krill over an annual cycle is consistent with a shift in the primary habitat of krill between seasons.

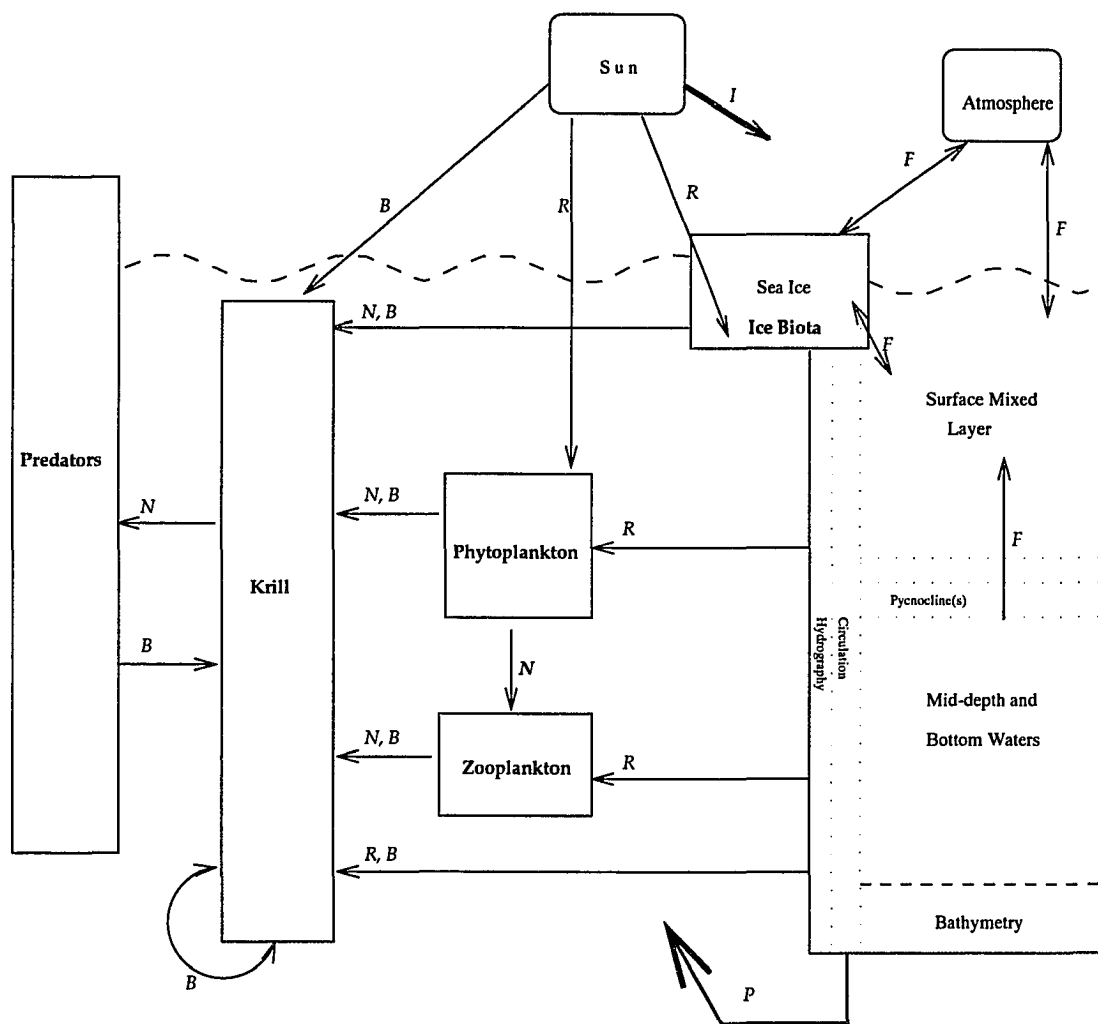


Figure 58: Conceptual model of krill interactions within the Antarctic ecosystem. The arrows are labeled as: **F** fluxes of heat, salt, momentum; **I** solar irradiance; **P** physical advection and diffusion; **N** energy pathway between trophic levels; **R** environmental influence on biological rates; and **B** environmental influence on krill behavior.

Identification of the habitat(s) occupied by krill in the fall and winter can not be addressed directly with the data sets available in this study. However, synthesis of these multidisciplinary observations in combination with historical observations can be used to indirectly examine the potential role of several factors including advection from the study region, a shift to the sea ice habitat, aggregation dispersal, vertical movement out of the depth range sampled, and horizontal migration from the study region. Each of these factors will now be discussed.

5.3.1 Advection

Large-scale advective flow patterns have been described for the Bransfield Strait-South Shetland Islands region (Clowes, 1934; Capella, 1989; Niiler *et al.*, 1991) and the west Antarctic Peninsula shelf (Stein, 1988; Stein and Heywood, 1994, Hofmann *et al.*, in press). These circulation fields (Figure 59) are characterized by two coherent features. The Bransfield Current transports water from west of the Peninsula to the northeast along the axis of the Bransfield Strait (Niiler *et al.*, 1991). The second feature is the presence of clockwise circulation over the shelf which results from northward flow of the Antarctic Circumpolar Current (ACC) at the outer shelf and southward flow (induced by north-northeast winds) along the coast (Hofmann *et al.*, in press). In addition, dynamic height fields indicate complicated flow patterns on the inner and middle shelf throughout the Peninsula region and around the South Shetland Islands, which are assumed to result from complex bottom topographies (Ichii *et al.*, 1993; Hofmann *et al.*, in press).

The passive transport and redistribution of krill by large scale circulation patterns and mesoscale oceanographic features, e.g., frontal zones and eddies, is considered an important factor directly affecting the spatial observations of krill (Amos, 1984; Everson and Murphy, 1987; Maslennikov and Solyankin, 1988; Makarov *et al.*, 1988; Witek *et al.*, 1988; Nast *et al.*, 1988; Sahrhage, 1988). The important role of advection on determining spatial patterns is not addressed here, but rather the focus is on the potential

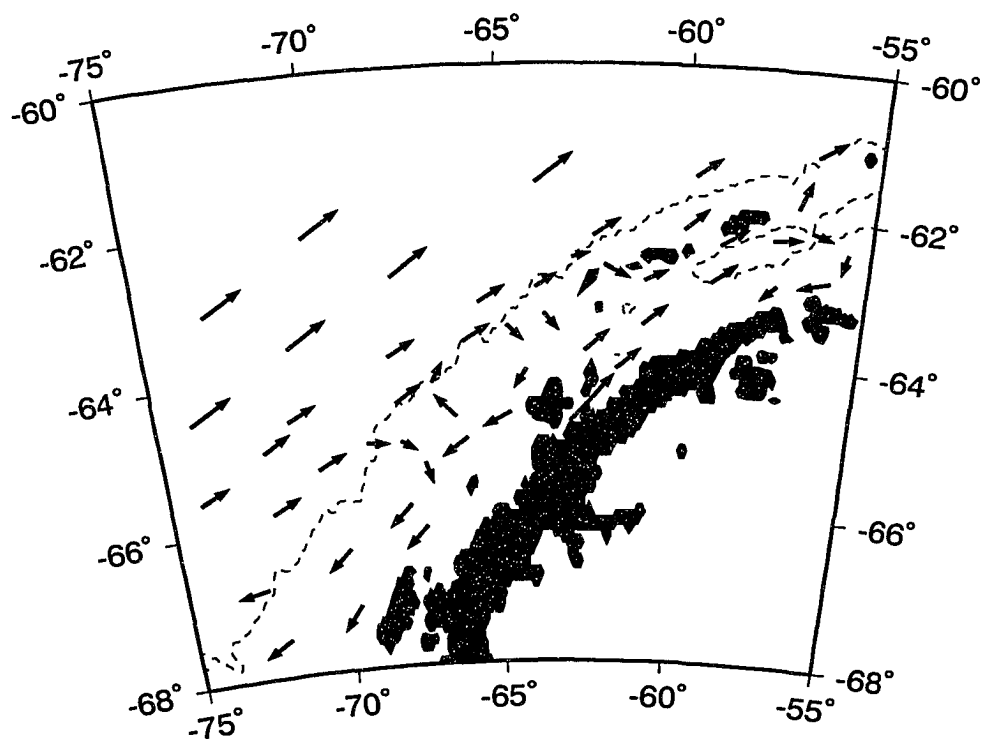


Figure 59: Schematic of the upper ocean circulation west of the Antarctic Peninsula, including Bransfield Strait, constructed from historical data sources. Solid arrows indicate the general flow direction of the upper ocean. The dashed lines represent the 1000-m isobath. Figure adapted from Hofmann *et al.*, (1992).

effect of seasonal variations in the pattern of circulation on seasonal variations in the krill distribution.

To date, changes in the flow field, within the study region, resulting from seasonal fluctuations in atmospheric wind patterns have not been quantified. The monthly-averaged wind stress fields, which were derived from the global atmospheric forecast model of Trenberth *et al.* (1989), show a semi-annual variation in wind stress for this region, with the weakest stress occurring during summer and the strongest stress occurring during winter. However the maximum stress in the winter will be mediated by the presence of sea ice cover during this time period. In addition little variation was observed between months in the direction of the wind (Trenberth *et al.*, 1989).

The hydrographic observations analyzed in this study did not indicate differences between seasons in the hydrographic properties characterizing CDW or in the position of the permanent pycnocline separating the two major water masses in the area. Strong seasonal variations in hydrographic properties were restricted to the upper portion of AASW (0-50 m). These changes were accounted for by surface fluxes of heat due to seasonal changes in solar irradiance and fluxes of salt due to the advance and retreat of annual sea ice. The timing of the change from vertically-stratified to well-mixed conditions within AASW is not consistent with the timing of the order of magnitude change in krill biomass.

Given the large geographic scale of the 1993 fall reduction in krill biomass, the short time period (two months) associated with these changes, and the absence of evidence in the hydrographic observations or wind climatology that support a large-scale change in the idealized circulation, it appears unlikely that advection is solely responsible for the observed seasonal pattern in krill biomass.

5.3.2 Sea ice

Sea ice is a prominent physical feature that modifies the structure and function of

the marine ecosystem of the Antarctic. The seasonal change in the areal extent of sea ice affects more than 20 million km² of the sea surface (Zwally *et al.*, 1983). Sea ice coverage is circumpolar but with marked regional variability and high interannual variability (Parkinson, 1992; Stammerjohn and Smith, in press a). Krill has been characterized as leading a double life, alternating between two different habitats, the pelagic upper ocean and the undersurface of sea ice (Laws, 1985; Siegel *et al.*, 1990; Marschall, 1988). This characterization, however, was based primarily on qualitative observations collected in a few selected regions exhibiting perennial ice cover.

Over the last decade, several studies have employed direct observation of the under-ice habitat by either divers or cameras mounted on remotely operated vehicles (Kottmeier and Sullivan, 1987; O'Brien, 1987; Marschall, 1988; Stretch *et al.*, 1988; Hamner *et al.*, 1989; Daly, 1990; Daly and Macaulay, 1991; Frazer *et al.*, in press). Synthesis of the results of these studies by Quetin *et al.* (1994) indicated that, larvae and adult krill have been observed in close association with sea ice for a variety of geographic regions; however, the coupling was strongest for larval and juvenile life history stages and was most consistently observed during the late winter and early spring for adults.

Under-ice observations obtained during several winters (including 1993 of this study) from west of the Antarctic Peninsula (Quetin *et al.*, in press; L. Quetin and T. Frazer, personal communication), indicate that the abundance of adult krill observed directly beneath sea ice does not account for the abundance levels observed in the upper ocean during the ice-free summer season. The abrupt decrease in acoustically-detectable krill biomass observed over the two-month period between the summer and fall 1993 cruises preceded ice formation in this region, i.e., most of the region was ice-free during both cruises. The fall acoustic observations combined with the diver-provided, under-ice winter observations of Quetin *et al.* (in press) suggest that a simple characterization of krill alternating between pelagic and under-ice habitats is inappropriate for the waters west of the Antarctic Peninsula. Thus a shift to sea ice as the primary fall-winter habitat

of adult krill is not supported by the 1993 observations; however, this does not imply that under-ice habitats are unimportant to the overwintering success of larval krill or to variations in the condition factor of adult krill.

5.3.3 Swarming behavior

Foraging behavior and predator avoidance are often cited as biological factors that influence the formation and maintenance of krill aggregations (see review by Miller and Hampton, 1989a). The tendency to form aggregations is expected to be highest under conditions of high food availability and high predation pressure. Consequently, spatial and temporal changes in the relative abundance of food and predators would affect the swarming behavior of krill.

Analysis of aggregation transect parameters (Table 6) included during this study indicated that aggregations were most abundant in the summer. This season was also characterized by the highest pigment concentrations (Figure 19) and based on historical observations for this region represented the time period of highest predation pressure (Fraser and Trivelpiece, in press a; Costa and Crocker, in press). The lowest abundance of aggregations was detected during the winter (Table 6) coincident with low pigment concentrations (Figure 19) and low predation pressure (Fraser and Trivelpiece, in press a; Costa and Crocker, in press). Thus, the difference in the abundance of krill aggregations between summer and winter is consistent with the expected change in swarming behavior relative to differences in food availability and predation pressure. Moreover, most of the krill biomass observed during the summer 1993 was attributed to aggregations that were smaller ($<500 \text{ m}^2$) and denser ($>100 \text{ g m}^{-3}$) compared to the other seasons analyzed in this study (Figure 26). This change in the character of the aggregation dimensional parameters could be interpreted as a behavioral response to the high predation pressure during the summer, e.g., whales feeding on entire aggregations, as well as other carnivores feeding on individuals within aggregations.

Seasonal changes in krill swarming behavior will directly affect small-scale distributions which in turn alter the ability to accurately estimate the local abundance of krill according to the capabilities of the sampling strategy and equipment employed. A change in behavior which favors dispersal rather than swarming would lead to a more uniform spatial distribution in which krill densities may become too low to be detected acoustically. However, the maximum potential acoustically-undetectable krill biomass was assumed in this study to be approximately 10 g m^{-2} (see section 3.2.3), which is an order of magnitude lower than the spatially-averaged krill biomass value observed in summer 1993. The effect of dispersal on net sampling would be to increase the probability of capturing some krill each net tow, which in turn would decrease the variance observed between samples. The net-derived estimates of krill density obtained during the fall and winter cruises are not consistent with this expectation, e.g., krill were absent from net collections at most of the stations (R. Ross and L. Quetin, personal communication). Thus the tendency to disperse within the upper 200 m of the water column over the study region during the fall and winter is not supported by the 1993 observations as the sole explanation of seasonal variation in vertically-integrated krill biomass.

The presence of large aggregations observed during the fall and winter by this study and others (Zhou *et al.*, 1994; Ross *et al.*, in press) indicate that some portion of the population is remaining in aggregations year-round. The disadvantages to living within large aggregations are numerous including: competition for limited food and oxygen resources and the potential for accumulation of toxic waste products such as ammonia. This leads to the question of what is the advantage of remaining in large aggregations during the winter? One potential answer is that the time scale of swarm formation may be too long to facilitate annual re-swarming in the spring, hence some individuals remain in aggregations year-round. Unfortunately, little is known concerning the temporal integrity of individual aggregations or how much of an individual krill's life is spent in swarms versus how much is spent in a dispersed state. Given the importance of swarming behavior

to the distribution of krill, this information is critical to an improved understanding of krill ecology.

5.3.4 Vertical movements

Movement into the upper 10 m of the water column during the fall would position krill in proximity to newly forming sea ice, although at the cost of increased predation risk, and would effectively remove krill from acoustic detection. Analysis of net-derived krill density estimates obtained during the fall 1993 cruise (R. Ross and L. Quetin, unpublished data), however, does not support relocation of the summer abundance levels of krill into the near surface waters by fall. In addition, extensive swarming by krill at the surface has never been reported during the fall or winter by any program in the Southern Ocean to date.

The downward migration of krill, either as individuals or aggregations, to depths typically not sampled by nets and acoustics could explain the reduced abundance estimates of krill during the fall and winter and this type of movement is supported by several historical observations. A shift from the pelagic to the benthopelagic habitat was observed by Kawaguchi *et al.* (1985) for krill (20 - 45 mm) overwintering under fast ice in a shallow coastal region (Lutzow-Holm Bay, near 40°E latitude). Off South Georgia during the winter of 1983, a combination of acoustic measurements and net collections revealed that krill were present in layers up to 20 m thick near the bottom over parts of the shelf area (Heywood *et al.*, 1985). However, the localized nature of these aggregations, led Heywood *et al.* (1985) to conclude that they could not account for the discrepancy in krill biomass observed between summer and winter in this region. In the southwest Weddell Sea, Gutt and Siegel (1994) used a video camera attached to a benthic remotely-operated vehicle, to document the existence of scattered krill and krill aggregations positioned within 200 cm of the bottom near the shelfbreak in water depths of 400-500 m. Depth-stratified net samples have also shown the occurrence of krill down to 400 m in continental shelf waters

along the Antarctic Peninsula (Siegel, 1985).

In the current study, krill were distributed deepest during the winter (Figure 27) and a few of the largest aggregations observed during the fall and winter extended below the limit of acoustic detection (Figure 55b). However the acoustic measurements were restricted to the depth range from 10 to 200 m and net collections were derived from tows over the upper 120 m. Consequently, the abundance of krill in deeper waters can not be described with these data sets and the movement of krill below 200 m during the fall and winter remains an unquantifiable possibility.

5.3.5 Horizontal migration

Krill have been characterized as highly mobile animals and, based on experimental and field observations, adults appear capable of sustained swimming at speeds between 10-15 cm s⁻¹ over time scales of hours to days (Marr, 1962; Kils, 1981; Kanda *et al.*, 1982). This section will consider across-shelf movements as a potential explanation for seasonal variations in krill abundance. Siegel (1988) was the first to suggest that active migration played a role in establishing the spatial segregation in krill size class. Specifically, he hypothesized that large, reproductive adults migrate offshore in spring and return to coastal waters in the fall (Figure 6). Similarly, Sprong and Schalk (1992) described the migration of aggregations northwards away from the ice edge in the Weddell Sea from late November to early January based on repeated acoustic surveys within this area.

To date, horizontal migration has been described only in terms of the mesoscale movements (100-200 km) of large, reproductively-active adults, which represented only a small percentage of the total krill biomass observed during this study in 1993. The combined acoustic-net observations in this study indicated seasonal changes in the geographic area over which krill were detected and a summer to fall shift in the spatial placement of specific size classes. These observations are consistent with an inshore movement of not

only large (>40 mm) but also small (30-40 mm) adult krill with the scale of movement varying from roughly 100 km for large adults to less than 50 km for small adults.

Traveling at speeds between 10 and 15 cm s⁻¹, it would take 8 to 12 days for krill to move a distance of 100 km if the movement was directed. This time scale would increase as a function of the random component of movement. Evidence of directed swimming has been observed for krill aggregations by divers (Hamner *et al.*, 1983; Hamner, 1984) over small spatial scales. Movement over larger scales is supported by the description provided by a Japanese fishing trawler (Kanda *et al.*, 1982) which tracked two large krill aggregations over a horizontal distance of 116 and 46 miles in time periods of 18 and 8 days, respectively (10-12 km da⁻¹). The time and space scales of observed krill movement by these combined studies are consistent with those required to support seasonal across-shelf migrations.

The acoustic measurements used in this study were not designed to provide direct observations of horizontal movements, therefore, across-shelf migrations remain an unquantifiable possibility. The integrated krill biomass observed on the inner shelf in fall and winter 1993 does not account for the total biomass observed during the summer. One explanation is that adult krill moved further inshore than the region occupied by most sampling programs, including this one. Alternately it may suggest that only a portion of the krill population resides on the inner shelf in the fall and winter.

5.3.6 Interaction of environmental variability and krill behavior

The discussion provided in the previous section indicates that the fall and winter reduction in krill biomass is not explained solely by population dynamics, large-scale changes in circulation patterns, or a simple shift to the sea ice habitat. This suggests that aspects of krill behavior may be important particularly seasonal changes in aggregation dispersal, vertical movements, and horizontal migration. A description is provided next of variations in the environment which are temporally and spatially consistent with the

hypothesis that seasonal changes in the behavior of krill are in part caused by environmental cues.

Seasonal variations in the abundance of krill were not well correlated with the progression of annual changes in the thermohaline character of the upper ocean (AASW). Winter and spring were characterized by a well-mixed upper ocean; whereas, summer and fall were characterized by a vertically-stratified upper ocean (Figure 12). However, high krill biomass was observed during spring and summer compared to the low values observed during the winter and fall (Figure 23). Sea ice coverage was greatest (Figure 8b, Figure 9b) and phytoplankton concentrations were lowest (Figure 19) during the winter and spring and so changes in these parameters were also not synchronous with the observed seasonal change in krill abundance.

The seasonal cycle of increasing and decreasing solar irradiance is consistent with the timing of behavioral changes necessary to produce the observed seasonal changes in krill biomass. Light is thus a strong candidate for triggering seasonal changes in krill behavior; however, it alone can not explain the spatial aspects of the resultant krill distributions. A plausible explanation is that seasonal variations in krill behavior occur in response to seasonal light changes as mediated by mesoscale environmental variability. For example, krill positioned on the inner shelf, which is characterized by a different set of environmental conditions compared to the outer shelf, may disperse or move deep later in the year than those positioned over the outer shelf, thus resulting in relatively higher abundances on the inner shelf.

In the case of horizontal migration, the systematic fall decrease and spring increase in light may induce krill to abandon habitats with hydrographic and food conditions that were considered favorable during the preceding season and to search for habitats of a different and defined character which may be favorable during the subsequent season. This type of movement implies that krill have the capability to detect and respond to

environmental variability. The multidisciplinary data sets analyzed in this study indicate that the environment varies in a somewhat consistent and predictable manner over selected spatial and temporal scales. For example, across-shelf variability in AASW hydrographic parameters, particularly surface salinity, was present during all seasons. The nature of the behavioral response may change ontogenetically, so that habitat conditions considered favorable for sub-adults may be different from those favoring reproductively-active adults. Quantifying what portion of the population overwinters where and identifying the environmental and intrinsic factors responsibility for invoking different strategies represent an important future research area in krill ecology.

5.4 Variability in krill abundance on smaller space and time scales

One of the objectives of this research effort was to identify the environmental factors which play a role in structuring spatial and temporal patterns in the distribution and abundance of krill. In addition to the seasonal and mesoscale processes described previously, processes operating on scales of individual acoustic transects (i.e., stations) potentially affect krill distribution and abundance. The multidisciplinary set of measurements analyzed in this study represent a comprehensive and concurrent collection of variables and thus it was anticipated that environment-krill relationships would be identifiable from the coordinated analysis of these data sets on a location-by-location basis. However, clear relationships did not emerge from analyses done at this scale. Other research programs have also documented poor relationships between krill and hydrographic parameters and pigment concentrations on the scale of tens of km (Witek *et al.*, 1981; Weber and El Sayed, 1985; Daly and Macaulay, 1991; Murray *et al.*, 1995). The ability to discern possible krill-environment correlations may be affected by several factors which include the use of a survey-mode sampling design, diel migration by krill, and uncertainties associated with the acoustic estimation of krill biomass. Each of these factors is discussed below so that future sampling programs can be designed to mitigate these potential sources of error.

5.4.1 Survey-mode sampling design

Survey-mode sampling programs provide only quasi-synoptic snapshot realizations of complex ecosystems. This approach was effective in providing seasonal and mesoscale characterizations of physical and biological distributions in this study and in providing interannual comparisons between studies (e.g., Siegel, 1992; Hewitt and Demer, 1993a). However, it provides no mechanism for incorporating the history of physical and biological processes and their interactions which are responsible for variability on smaller space and time scales. For example, high krill biomass levels were observed coincident with high and low integrated pigment concentrations within the same regional area in this study and others (Witek *et al.*, 1981; Daly and Macaulay, 1991; Murray *et al.*, 1994). This variability may result from a combination of factors which define the scales of interaction between krill and food resources, including: the spatial extent of phytoplankton patches, the time required for krill to locate and graze phytoplankton patches, and environmentally controlled phytoplankton growth rates. In addition, active movements of krill swimming over scales of tens of kilometers within a day or two may also severely limit the ability to address local environmental interactions based on survey-mode sample design alone.

5.4.2 Diel migration

Diel migration is another potential factor affecting the identification of correlations between krill distributions and environmental conditions. Typically, zooplankton respond to light cycles in a deterministic fashion, which results in a distinct pattern of diel depth distribution (see review by Foward, 1988). Although vertical migration is generally considered a behavioral component of krill ecology (Marr, 1962; Mauchline and Fisher, 1969; Everson, 1983), a consistent pattern describing the relationship between the depth distribution of krill and the time of day or diel light cycle is lacking (e.g., Marr, 1962; Witek *et al.*, 1981; Everson, 1983; Godlewska and Klusek, 1987).

In this study, diel migration was observed during spring, summer, and fall but

only when comparisons were made between acoustic estimates derived from locations with similar environmental conditions (Figure 29). Moreover, analysis of krill biomass estimates obtained within the inner shelf hydrographic regime during summer 1993, suggests that the movement of krill aggregations into near surface waters, and above the vertical range of acoustic detection, resulted in lower integrated krill biomass estimates at locations sampled during hours of darkness (e.g., Figure 9). Clearly, changes in krill depth distribution due to diel migration will affect interpretations of geographic spatial distributions obtained from continuous survey-mode sampling.

5.4.3 Uncertainties associated with acoustic techniques

Although many technological advances in the acoustic method have been made over the last decade, the conversion of integrated echo energy into estimates of krill biomass is still affected by uncertainties surrounding the identification of species responsible for acoustic scattering and the determination of related target strength characteristics. The general practice adopted by most Southern Ocean acoustic programs, including this study, is to assume that all scattering returns are due to krill and that target strength is a function solely of the length (or weight) of the individuals (e.g., Hampton, 1985; Witek *et al.*, 1988; Miller and Hampton, 1989a; Hewitt and Demer, 1993a). Clearly the first assumption is not always valid and the potential bias introduced by the inclusion of alternate scatterers is itself a function of the relative target strengths of the scatterering types.

Current target strength estimates for krill and other zooplankton are based on linear regression analysis of empirical data (Weibe *et al.*, 1990; Green *et al.*, 1991). Recent evidence suggest that scattering from individual zooplankters is non-linear (Demer and Martin, in press) and that changes in the orientation or tilt angle of the individuals may have a profound effect on target strength (McGehee and Martin, 1996). Furthermore, the diversity of anatomical features within zooplankton taxa dramatically affects reflective properties as shown by the wide range (19,000 to 1) in the relative average echo energy

per unit biomass observed for elastic shelled gastropods compared to fluid-like salps (Stanton *et al.*, 1994).

The use of multiple acoustic frequencies has recently shown promise in distinguishing between different acoustic size classes of biological scatterers in the Southern Ocean (Madureira *et al.*, 1993a; Demer and Hewitt, in press). However, a quantitative evaluation of the magnitude of overestimates, associated with including small zooplankton or large nekton, for surveys in which multiple frequency data were collected, is still lacking.

The acoustic measurements used in this study were obtained with a single frequency, single beam acoustic system and as such the potential uncertainty introduced by the echo integration assumptions is unquantifiable. However, all of the published descriptions of krill biomass, with which the results of this study were compared, were obtained with similar acoustic systems and thus were subject to the same biases and uncertainties. One strength of this study, however, was the simultaneous collection of net and acoustics measurements at all locations. These combined data sets indicated that krill was the dominant scatterer at most of the locations characterized by large acoustic signals and provided further validation of the acoustic trace signature typified by historical descriptions of krill aggregations. More importantly the concurrent net and acoustic measurements facilitated the identification of locations where alternate scatterers were a problem.

The disproportionate contribution in terms of total krill biomass by a small number of aggregations is a striking feature of this study that was consistently observed during all seasons (Table 6). Characterization of the distribution and abundance of these infrequently observed *HB* aggregations is clearly affected by the the acoustic representation of aggregations as two-dimensional structures and the low sampling effort (several km of acoustic measurements) made at discrete locations (see section 2.2.2 for details). The presence of the *HB* aggregations is also reflected in the skewed nature of the frequency distributions of integrated krill biomass estimates (Figure 22) and the severity of the skewness was

dependent upon the EDSU length scale (Figure 21).

Similar krill biomass frequency distributions have been described by other acoustic survey programs (Miller and Hampton, 1989a; Trathan *et al.*, 1993b; Murray *et al.*, 1995) and these observations have been shown to greatly affect the determination of sampling variance. Estimates of variance not only quantify the reliability of the mean estimate, they also provide valuable information concerning the small scale structure of the distributions. Identifying the most statistically-defensible method for quantifying the uncertainty in survey-based krill biomass estimates was the subject of a recent CCAMLR-sponsored workshop (CCAMLR, 1995). Comparisons were made between design-based estimators using random sampling theory and model-based estimators using geostatistical techniques, however, no consensus was reached concerning the merits of one over the other (CCAMLR, 1995). The adoption of a standard variance estimator by programs conducting acoustic surveys would aid in the interpretation of inter-regional and inter-annual variabilities in the distribution and abundance of krill.

CONCLUSIONS

This study synthesized analyses of multidisciplinary data sets to characterize seasonal and mesoscale variations in the distribution and abundance of Antarctic krill in continental shelf waters west of the Antarctic Peninsula. The analysis of concurrent measurements of krill biomass, aggregation characteristics, and selected environmental parameters resulted in the identification of several features describing krill distributional patterns which are summarized below.

Spatially-averaged estimates of krill biomass increased three-fold from spring to summer (34 to 110 g m⁻²) and then decreased by an order of magnitude to the low values (<10 g m⁻²) observed in fall and winter. The number of aggregations detected per unit sampling effort followed a similar seasonal pattern with maximum and minimum values observed in summer (12.1 aggregations km⁻¹) and winter (0.4 aggregations km⁻¹), respectively. The geographic area over which krill were acoustically detected followed a similar seasonal trend with krill found at 95% and 24% of the locations sampled in summer and winter, respectively. The depth distribution of krill varied between seasons, with most of the krill biomass positioned within the upper 50 m during the summer in contrast to winter when krill were primarily distributed deeper than 100 m.

Krill aggregations occurred in a variety of sizes, shapes, and densities. The frequency distributions of dimensional parameters, which were used to characterize the structure of aggregations, were skewed towards small values, i.e., most aggregations were <50 m in horizontal length, <10 m in vertical height, and had mean biomass values <25 g m⁻³. However, a small number of aggregations, in all seasons, represented a large percentage (>80%) of the total krill biomass and these aggregations were notably larger (>1000 m²) or denser (>50 g m⁻³) than the typical aggregation. A seasonal shift was apparent with small, dense aggregations dominant during the summer and large, less dense aggregations prominent during the winter.

The inner shelf, within 100 km of the Antarctic Peninsula, was characterized as a region of relatively higher krill abundance in all seasons. Across-shelf gradients were observed in the environmental conditions measured concurrently with acoustic observations and differences between the inner and outer shelf were greatest during the summer and fall. Specifically, surface salinities were lower, mixed layer depths were shallower, and pigment concentrations higher on the inner shelf. The geographic extent of elevated krill biomass observed during the summer was spatially correlated with the mesoscale distribution of low salinity surface waters (< 33.8) which characterized the inner shelf hydrographic regime.

An across-shelf gradient in krill size classes was apparent during all seasons except winter. Small adults (< 40 mm) were typically restricted to inshore regions with large (> 40 mm) adults positioned further offshore. During the summer, the distribution of large (> 45 mm), reproducing adults was spatially correlated with surface salinities exceeding 33.8 and the presence of Circumpolar Deep Water at depth.

Diel changes in the vertical distribution of krill were noted when comparisons were made using measurements from environmentally-similar areas. Low krill biomass was observed in summer during the night at several locations on the inner shelf which were adjacent to other locations with higher krill abundance, and this variability may have resulted from the night-time movement of krill into near surface waters and out of the acoustic detection range.

The degree of variability in krill biomass levels and aggregation characteristics exhibited during this study and in those used for comparison, has direct implications for large-scale, multi-year survey programs, such as the Palmer LTER and CCAMLR, and for process-oriented programs, such as JGOFS and GLOBEC. The ability to detect inter-annual and inter-regional differences in krill distribution, abundance, and productivity in part depends upon an understanding of processes affecting krill distributions on smaller

time and space scales. For example, the seasonal variation in krill abundance observed in this study was much greater than inter-annual differences observed for comparisons made between this study and the AMLR program. Based on the mesoscale variations observed in this study, spatially-averaged estimates of krill biomass will also be sensitive to the relative proportions of inner shelf, outer shelf, and slope contained within the region and to the hydrographic conditions of the upper ocean. Clearly, an understanding of spatial and temporal variability in environmental conditions is required so that appropriate data sets can be selected for meaningful comparisons.

Although the existing data sets provide no direct evidence, the results from this analysis are consistent with the hypothesis that the seasonal changes in krill abundance reflect a shift in habitat between seasons. The absence of acoustically-detected krill from the depth range 10-200 m over the study region during the fall and winter, further suggests that seasonal changes in krill behavior, most notably aggregation dispersal, vertical movements, and horizontal migration, may be responsible for a large part of the seasonal variations observed in the distribution of krill. These results point to a critical need for additional studies which characterize the role of behavior in establishing krill distributional patterns and moreover, the need to identify the fall-winter habitat(s) of krill.

Advances in describing and understanding the distribution of Antarctic krill have paralleled advances in sampling methodology. Acoustics technology has been shown to be a significant advancement over net sampling and this approach is widely recognized as the most powerful and available tool for the quantitative assessment of krill abundance. Currently, research and engineering efforts are being directed to provide *in-situ* acoustically-derived estimates of target strength which, in combination with better resolved theoretical models of scattering by differently shaped organisms, would eliminate the dependency on net samples to identify the taxa and size of individual scatterers.

Towed, downward-looking transducers provide continuous measurements of the

two-dimensional structure (vertical, alongtrack) of krill aggregations. There is a clear need, however, to augment this representation with measurements of the across-transect shape of aggregations. Several sonar instruments, e.g., searchlight, side-scan, and sector-scan, have transducers which are moveable such that the beam can be manually or automatically directed (MacLennan and Simmonds, 1992) to insonify sectors of water over a variety of plane angles. By changing the tilt or rotation of the transducer, these instruments have proven useful in determining the horizontal distribution and structure of fish schools, however, they give no information on the school height or density of fish within the school. Collections made simultaneously using two instruments: a standard towed echosounder and an active, high-resolution sector-scanning sonar (Misund *et al.*, 1995) were used recently to map the shape, size, and density of herring schools in the North Sea. The success of this study suggests that the use of a combination of acoustic technologies should be explored for krill assessment. In addition, the development of an autonomous- or remotely-operated-vehicle which supports multiple acoustic systems should be investigated.

There is a general lack of observations that describe the temporal integrity of krill aggregations or the spatial scales of movement, whether active or passive, of individual aggregations. Given the limitations of survey-mode designs, these problems would be best addressed using process-oriented field studies, that apply acoustics techniques to monitor the trajectory path of individual aggregations over short time periods (hours to days). These efforts would provide insight as to the relative importance of advection versus swimming movements in regulating the location of krill individuals. Additionally, changes in the swimming speed and frequency of turning, which determine the scale of movement through space over a given time period, could be evaluated relative to changes in prevailing environmental conditions thereby providing direct evidence of ecosystem linkages. The tracking of aggregations during the late summer may be an effective approach to determining the overwintering strategies employed by various portions of the

krill population.

There is also a need for the development of krill models which complement existing and future field observational programs. The formation, maintenance, and dispersal of krill aggregations may be best examined using a Lagrangian approach in which the movement of individuals is described as a balance between several forces acting upon the individual. Passive transport of individuals due to the direct effects of ocean circulation must be included and since krill are highly mobile organisms, active changes in swimming behavior must be supported. Consistent with the current concept of biodiffusion, this active movement should extend beyond the conventional approach which focuses on random movements to include interactions between individuals, response to external directional stimuli, and response to spatial environmental heterogeneity. The observations of integrated krill biomass and aggregation characteristics provided by the analyses of this study should provide a sufficient basis to begin development and parameterization of a krill swarming model. However, the information obtained from aggregation tracking studies as described above would be essential to the successful implementation of these models.

REFERENCES

- Ainley, D. G. and S. S. Jacobs (1981) Sea-bird affinities for ocean and ice boundaries in the Antarctic marginal ice zone. *Deep-Sea Research*, **28**, 1173-1185.
- Ainley, D. G., W. R. Fraser and K. L. Daly (1988) Effects of pack ice on the composition of micronektonic communities in the Weddell Sea. In: *Antarctic Ocean and Resources Variability*, Sahrhage, D., editor, Springer-Verlag, Berlin, pp. 140-146.
- Amos, A. F. (1984) Distribution of krill and hydrography of the Southern Ocean: large-scale processes. *Journal of Crustacean Biology*, **4**, 306-329.
- Anderson, R. F. (1993) Southern Ocean Science Plan. U. S. JGOFS Planning Report Number 17, Woods Hole Oceanographic Institution, Woods Hole, MA, 67 pp.
- Anon (1981) Convention on the Conservation of Antarctic Marine Living Resources. *Polar Record*, **20**, 383-404.
- Anon (1986) Post-FIBEX acoustic workshop. BIOMASS Report Series, No. 40, Scientific Committee Antarctic Research, Cambridge, England, 106 pp.
- Bargmann, H. E. (1945) The development and life-history of adolescent and adult krill *Euphausia superba*. *Discovery Report*, **23**, 103-176.
- Bergstrom, B., G. Hempel, H. P. Marschall, A. W. North, V. Siegel and J. O. Stromberg (1990) Spring distribution, size composition and behavior of krill *Euphausia superba* in the western Weddell Sea. *Polar record*, **26**, 85-89.
- Bidigare, R. R., J. L. Iriarte, S.-H. Kang, D. Karentz M. E. Ondrusek, and G. A. Fryxell (in press) Phytoplankton: Quantitative and Qualitative Assessments. In: *Foundations for ecological research west of the Antarctic Peninsula*, AGU Antarctic Research Series, Ross, R. M., E. E. Hofmann and L. B. Quetin, editors, American Geophysical Union, in press.
- BioSonics (1990) BioSonics Echo Signal Processor Operators Manual. BioSonics, Inc., Seattle, WA, 373 pp.
- Brinton, E. (1991) Distribution and population structures of immature and adult *Euphausia superba* in the western Bransfield Strait region during the 1986-1987 summer. *Deep-Sea Research*, **38**, 1169-1193.
- Capella, J. E. (1989) Circulation and temperature effects on the development and distribution of eggs and larvae of the Antarctic krill, *Euphausia superba*: A modeling study. Ph.D. Dissertation, Texas A&M University, College Station, TX, 162 pp.
- CCAMLR (1995) Workshop on estimation of variance in marine acoustic surveys, Report of the working group on ecosystem monitoring and management, EMM-95/38. Scientific Committee for the Conservation of Antarctic Marine Living Resources, CCAMLR, Hobart, Australia.

- Chu, D., K. G. Foote and T. K. Stanton (1993) Further analysis of target strength measurements of Antarctic krill at 38 and 120 kHz: Comparison with deformed cylinder model and inference of orientation distribution. *Journal of Acoustical Society of America*, **93**, 2985-2988.
- Clay, C. S. and H. Medwin (1977) *Acoustical Oceanography: Principles and Applications*, Wiley, New York, 544 pp.
- Clowes, A. I. J. (1934) Hydrography of Bransfield Strait. *Discovery Reports*, **9**, 1-64.
- Costa, D. P. and D. E. Crocker (in press) Marine Mammals of the Southern Ocean. In: *Foundations for ecological research west of the Antarctic Peninsula*, AGU Antarctic Research Series, Ross, R. M., E. E. Hofmann and L. B. Quetin, editors, American Geophysical Union, in press.
- Cram, D. L., J. J. Agenbag, I. Hampton and A. A. Robertson (1979) SAS Protea cruise, 1978: The general results of the acoustics and remote sensing study, with recommendations for estimating the abundance of krill (*Euphausia superba* Dana). *South African Journal of Antarctic Science*, **9**, 3-14.
- Daly, K. L. (1990) Overwintering development, growth, and feeding of larval *Euphausia superba* in the Antarctic marginal ice zone. *Limnology and Oceanography*, **35**, 1564-1576.
- Daly, K. L. and M. C. Macaulay (1988) Abundance and distribution of krill in the ice edge zone of the Weddell Sea, austral spring 1983. *Deep-Sea Research*, **35**, 21-41.
- Daly, K. L. and M. C. Macaulay (1991) Influence of physical and biological mesoscale dynamics on the seasonal distribution and behavior of *Euphausia superba* in the Antarctic marginal ice zone. *Marine Ecology Progress Series*, **79**, 37-66.
- Deacon, G. E. R. (1937) The hydrology of the Southern Ocean. *Discovery Report*, **15**, 1-124.
- Demer, D. A. and R. P. Hewitt (in press) *In-situ* target strength measurements of Antarctic zooplankton (*Euphausia superba* and *Salpa thompsoni*) at 120 and 200 kHz, corroboration of scattering models, and a statistical technique for delineating species. *Journal of Acoustical Society of America*, in press.
- Demer, D. A. and L. V. Martin (in press) Zooplankton target strength: volumetric or areal dependence? *Journal of Acoustical Society of America*, in press.
- Eicken, H. (1992) The role of sea ice in structuring Antarctic ecosystems. *Polar biology*, **12**, 3-13.
- El-Sayed, S.Z. (1977) *Biological Investigations of Marine Antarctic Systems and Stocks*. Volume 1, Scott Polar Research Institute, Cambridge, England, 79 pp.
- El-Sayed, S. Z. (1994) History, organization and accomplishments of the BIOMASS Programme. In: *Southern Ocean Ecology: the BIOMASS perspective*, El-Sayed, S. Z., editor, Cambridge University Press, Cambridge, pp. 1-8.

- Endo, Y., T. Imaseki and Y. Komaki (1985) Biomass and population structure of Antarctic krill (*Euphausia superba* Dana) collected during SIBEX II Cruise R.V. *Kaiyo Maru*. *Memoirs of National Institute of Polar Research Special Issue*, **44**, 107-117.
- Ettershank, G. (1984) A new approach to the assessment of longevity in Antarctic krill *Euphausia superba*. *Journal of Crustacean Biology*, **4**, 295-305.
- Everson, I. (1983) Variations in vertical distribution and density of krill swarms in the vicinity of South Georgia. *Memoirs of National Institute of Polar Research Special Issue*, **27**, 84-92
- Everson, I. (1988) Can we satisfactorily estimate variation in krill abundance? In: *Antarctic Ocean and Resources Variability*, Sahrhage, D., editor, Springer-Verlag, Berlin, pp. 199-208.
- Everson, I. and C. Goss (1991) Krill fishing activity in the southwest Atlantic. *Antarctic Science*, **3**, 351-358.
- Everson, I. and D. G. M. Miller (1994) Krill mesoscale distribution and abundance: results and implications of research during the BIOMASS Programme. In: *Southern Ocean Ecology: the BIOMASS perspective*, El-Sayed, S. Z., editor, Cambridge University Press, Cambridge, pp. 129-144.
- Everson, I. and E. Murphy (1987) Mesoscale variability in the distribution of krill *Euphausia superba*. *Marine Ecology Progress Series*, **40**, 53-60.
- Everson, I. and P. Ward (1980) Aspects of Scotia Sea zooplankton. *Biological Journal of Linnean Society*, **14**, 93-101.
- Everson, I., J. L. Watkins, D. G. Bone and K. G. Foote (1990) Implications of a new acoustic target strength for abundance estimates of Antarctic krill. *Nature*, **345**, 338-340.
- Fofonoff, N. P. and N. A. Bray (1981) Available potential energy for MODE eddies. *Journal of Physical Oceanography*, **11**, 30-46.
- Foote, K. G., I. Everson, J. L. Watkins and D. G. Bone (1990) Target strengths of Antarctic krill (*Euphausia superba*). *Journal of Acoustical Society of America*, **87**, 16-24.
- Foward, R. B. (1988) Diel vertical migration: zooplankton photobiology and behaviour. *Oceanography and Marine Biology Annual Review*, **26**, 363-393.
- Fraser, F. C. (1936) On the development and distribution of the young stages of krill, (*Euphausia superba*). *Discovery Report*, **14**, 1-192.
- Fraser, W. R. and W. Z. Trivelpiece (in press a) Factors controlling the distribution of seabirds: winter-summer heterogeneity in the distribution of Adelie penguin populations In: *Foundations for ecological research west of the Antarctic Peninsula*, AGU Antarctic Research Series, Ross, R. M. , E. E. Hofmann and L. B. Quetin, editors, American Geophysical Union, in press.

- Fraser, W. R. and W. Z. Trivelpiece (in press b) Palmer LTER: Relationships between variability in sea ice coverage, krill recruitment and the foraging ecology of Adelie penguins. *Antarctic Journal of the United States*, in press.
- Fraser, W. R., R. L. Pitman and D. G. Ainley (1989) Seabird and fur seal responses to vertically migrating winter krill swarms in Antarctica. *Polar biology*, **10**, 37-41.
- Fraser, W. R., W. Z. Trivelpiece, D. G. Ainley, and S. G. Trivelpiece (1992) Increases in Antarctic penguin populations: reduced competition with whales or a loss of sea ice due to global warming? *Polar biology*, **11**, 525-531.
- Fratt, D. B. and J. H. Dearborn (1984) Feeding biology of the Antarctic brittle star *Ophionotus victoriae* (Echinodermata: Ophiuroidea). *Polar biology*, **3**, 127-139.
- Frazer, T. K., L. B. Quetin and R. M. Ross. (in press) Abundance and distribution of larval krill, *Euphausia superba*, associated with annual sea ice in winter. In: *Antarctic Communities: Species, Structure and Survival*, Battaglia, B., J. Valencia and D. Walton, editors, University Press, Cambridge, in press.
- Garrison, D. L. and K. R. Buck (1989) The biota of Antarctic pack ice in the Weddell Sea and Antarctic Peninsula regions. *Polar biology*, **10**, 211-219.
- Garrison, D. L., K. R. Buck and M. M. Gowing (1993) Winter plankton assemblage in the ice edge zone of the Weddell and Scotia Seas: composition, biomass and spatial distributions. *Deep-Sea Research*, **40**, 311-338.
- GLOBEC, 1993. Towards the Development of an international GLOBEC Southern Ocean Program. GLOBEC Report No. 5, GLOBEC-International Executive Secretary, Chesapeake Biological Laboratory, Solomons, MD, 37 pp.
- Godlewski, M. (1993) Acoustic observations of krill (*Euphausia superba*) at the ice edge (between Elephant I. and South Orkney I., Dec. 1988/Jan. 1989). *Polar biology*, **13**, 507-514.
- Godlewski, M. and Z. Klusek (1987) Vertical distribution and diurnal migrations of krill *Euphausia superba* Dana from hydroacoustical observations, SIBEX, December 1983/January 1984. *Polar biology*, **8**, 17-22.
- Godlewski, M. and S. Rakusa-Suszczewski (1988) Variability of krill, *Euphausia superba*, Dan 1852 (Crustacea, Euphausiacea), distribution and biomass in the Western Antarctic (Bransfield Strait, Drake Passage, Elephant Island) during 1976-1987. *Investigacion Pesquera*, **52**, 575-586.
- Greene, C. H., T. K. Stanton, P. H. Wiebe and S. McClatchie (1991) Acoustic estimates of Antarctic krill. *Nature*, **349**, 110.
- Greenlaw, C. F. (1979) Acoustical estimation of zooplankton populations. *Limnology and Oceanography*, **24**, 226-242.
- Gulland, J. A. (1970) The development of the resources of the Antarctic Seas. In: *Antarctic Ecology, Volume 1*, Holdgate, M., editor, Academic Press, London, pp. 217-223.

- Gutt, J. and V. Siegel (1994) Benthopelagic aggregations of krill (*Euphausia superba*) on the deeper shelf of the Weddell Sea (Antarctic). *Deep-Sea Research*, **41**, 169-178.
- Hamner, W. M. (1984) Aspects of schooling in *Euphausia superba*. *Journal of Crustacean Biology*, **4**, 67-74.
- Hamner, W. M., P. P. Hamner and B. S. Obst (1989) Field observations on the ontogeny of schooling of *Euphausia superba* furciliae and its relationship to ice in Antarctic waters. *Limnology and Oceanography*, **34**, 451-456.
- Hamner, W. M., P. P. Hamner, S. W. Strand and R. W. Gilmer (1983) Behavior of Antarctic krill, *Euphausia superba*: Chemoreception, feeding, schooling, and molting. *Science*, **220**, 433-435.
- Hampton, I (1985) Abundance, distribution and behavior of *Euphausia superba* in the Southern Ocean between 15° and 30° during FIBEX. In: *Antarctic Nutrient Cycles and Food Webs*, Siegfried, W. R. , P. R. Condy and R. M. Laws, editors, Springer-Verlag, Berlin, pp. 294-304.
- Hardy, A. C. and E. R. Gunther (1935) The plankton of the South Georgia whaling grounds and adjacent waters, 1926-1927. *Discovery Report*, **11**, 1-456.
- Hewitt, R. P. and D. A. Demer (1991) Krill abundance. *Nature*, **353**, 310.
- Hewitt, R. P. and D. A. Demer (1993a) Dispersion and abundance of Antarctic krill in the vicinity of Elephant Island in the 1992 austral summer. *Marine Ecology Progress Series*, **99**, 29-39.
- Hewitt, R. P. and D. A. Demer (1993b) AMLR program: Distribution and abundance of krill around Elephant Island, Antarctica, in the 1993 austral summer. *Antarctic Journal of the United States*, **28**, 183-185.
- Heywood, R. B., I. Everson and J. Priddle (1985) The absence of krill from the South Georgia zone, winter 1983. *Deep-Sea Research*, **32**, 369-378.
- Higgenbottom, I. R. and G. W. Hosie (1989) Biomass and population structure of a large aggregation of krill near Prydz Bay, Antarctica. *Marine Ecology Progress Series*, **58**, 197-203.
- Hofmann, E. E. and J. M. Klinck (in review) Hydrography and circulation of Antarctic continental shelves: 150°E to the Greenwich Meridian. Submitted to: *The Sea*, Robinson, A. and K. Brink, editors.
- Hofmann, E. E., C. M. Lascara and J. M. Klinck (1992) Palmer LTER: Upper-ocean circulation in the LTER region from historical sources. *Antarctic Journal of the United States*, **27**, 239-241.
- Hofmann, E. E., J. E. Capella, R. M. Ross and L. B. Quetin (1992) Models of the early life history of *Euphausia superba* –Part I. Time and temperature dependence during the ascent-descent cycle. *Deep-Sea Research*, **39**, 1177-1200.

- Hofmann, E. E., J. M. Klinck, C. M. Lascara and D. A. Smith (in press) Water mass distribution and circulation west of the Antarctic Peninsula and including Bransfield Strait. In: *Foundations for ecological research west of the Antarctic Peninsula*, AGU Antarctic Research Series, Ross, R. M. , E. E. Hofmann and L. B. Quetin, editors, American Geophysical Union, in press.
- Hofmann, E. E., B. L. Lipphardt, R. A. Locarnini and D. A. Smith (1993) Palmer LTER: Hydrography in the LTER region. *Antarctic Journal of the United States*, **28**, 209-211.
- Holliday, D. V. and R. E. Pieper (1980) Volume scattering strengths and zooplankton distributions at acoustic frequencies between 0.5 and 3.0 MHz. *Journal of Acoustical Society of America*, **67**, 135-146.
- Holt, R. S., R. P. Hewitt and J. E. Rosenberg (1991) The U. S. AMLR Program: 1990-1991 field season activities. *Antarctic Journal of the United States*, **26**, 187-188.
- Huntley, M. and E. Brinton (1991) Mesoscale variation in growth and early development of *Euphausia superba* Dana in the western Bransfield Strait region. *Deep-Sea Research*, **38**, 1213-1240.
- Huntley, M., D. M. Karl, P. Niiler and O. Holm-Hansen (1991) Research on Antarctic Coastal Ecosystem Rates (RACER): an interdisciplinary field experiment. *Deep-Sea Research*, **38**, 911-941.
- Ichii, T., H. Ishii and M. Naganobu (1993) Factors influencing Antarctic krill distribution in the South Shetlands. Working group report on krill-93/38, Scientific Committee for the Conservation of Antarctic Marine Living Resources. CCAMLR, Hobart, Australia.
- Kalinowski, J. and Z. Witek (1985) Scheme for classifying aggregations of Antarctic krill. BIOMASS Handbook No. 27, Scientific Committee Antarctic Research, Cambridge, England, 12 pp.
- Kanda, K., K. Takagi, and Y. Seki (1982) Movement of larger swarms of Antarctic krill *Euphausia superba* off Enderby Land during 1976-1977 season. *Journal of Tokyo University Fisheries*, **68**, 24-42.
- Kawaguchi, K., S. Ishikawa and O. Matsuda (1986) The overwintering of Antarctic krill (*Euphausia superba* Dana) under the coastal fast ice off the Ongul Islands in Lutzow-Holm Bay, Antarctica. *Memoirs of National Institute of Polar Research Special Issue*, **44**, 67-85.
- Kellerman, A. K. (in press) Midwater Fish Ecology. In: *Foundations for ecological research west of the Antarctic Peninsula*, AGU Antarctic Research Series, Ross, R. M. , E. E. Hofmann and L. B. Quetin, editors, American Geophysical Union, in press.
- Kils, U. (1981) Swimming behavior, swimming performance and energy balance of Antarctic krill *Euphausia superba*. BIOMASS Scientific Series No. 3, Scientific Committee Antarctic Research, Cambridge, England, 122 pp.

- Klinck, J. M. and R. C. Smith (1994) Oceanographic Data Collected Aboard RV *Polar Duke* August-September 1993. Technical Report No. 94-01, Center for Coastal Physical Oceanography, Old Dominion University, Norfolk, VA, 158 pp.
- Klindt, H. (1986) Acoustic estimates of the distribution and stock size of krill around Elephant Island during SIBEX I and II in 1983, 1984, and 1985. *Archiv für Fischereiwissenschaft*, **37**, 107-127.
- Knox, G. A. (1970) Antarctic marine ecosystems. In: *Antarctic Ecology, Volume 1*, Holdgate, M., editor, Academic Press, London, pp. 69-109.
- Kottmeier, S. T. and C. W. Sullivan (1987) Late winter primary productivity and bacterial production in sea ice and seawater west of the Antarctic Peninsula. *Marine Ecology Progress Series*, **36**, 287-298.
- Lascara, C. M., R. C. Smith, D. Menzies and K. Baker (1993a) Oceanographic Data Collected Aboard RV *Polar Duke* November 1991. Technical Report No. 93-01, Center for Coastal Physical Oceanography, Old Dominion University, Norfolk, VA, 95 pp.
- Lascara, C. M., R. C. Smith, D. Menzies and K. Baker (1993b) Oceanographic Data Collected Aboard RV *Polar Duke* January-February 1993. Technical Report No. 93-02, Center for Coastal Physical Oceanography, Old Dominion University, Norfolk, VA, 307 pp.
- Laws, R. M. (1985) The ecology of the Southern Ocean. *American Scientist*, **73**, 26-40.
- Macaulay, M. C., T. S. English and O. A. Mathisen (1984) Acoustic characterization of swarms of Antarctic krill (*Euphausia superba*) from Elephant Island and Bransfield Strait. *Journal of Crustacean Biology*, **4**, 16-44.
- Mackintosh, N. A. (1972) Life cycle of Antarctic krill in relation to ice and water conditions. *Discovery Report*, **36**, 1-94.
- Mackintosh, N. A. (1973) Distribution of postlarval krill in the Antarctic. *Discovery Report*, **36**, 95-156.
- MacLennan, D. N. and E. J. Simmonds (1992) *Fisheries Acoustics*, Chapman and Hall, London, 325 pp.
- Madureira, L. S. P., P. Ward and A. Atkinson (1993) Differences in backscattering strength determined at 120 and 38 kHz for three species of Antarctic macroplankton. *Marine Ecology Progress Series*, **93**, 17-24.
- Makarov, R. R., V. V. Maslennikov, E. V. Solyankin, V. A. Spiridonov and V. N. Yakovlev (1988) Variability in population density of Antarctic krill in the Western Scotia Sea in relation to hydrological conditions. In: *Antarctic Ocean and Resources Variability*, Sahrhage, D., editor, Springer-Verlag, Berlin, pp. 231-236.
- Marr, J. W. S. (1962) The natural history and geography of the Antarctic krill (*Euphausia superba* Dana). *Discovery Report*, **32**, 33-464.

- Marschall, H. P. (1988) The overwintering strategy of Antarctic krill under the pack-ice of the Weddell Sea. *Polar biology*, **9**, 129-135.
- Maslennikov, V. V. and E. V. Solyankin (1980) Role of water dynamics in the maintenance of *Euphausia superba* population in the Weddell Sea. *Oceanology*, **20**, 192-195.
- Mauchline, J. and L. R. Fisher (1969) The biology of euphausiids. *Advances in Marine Biology*, **7**, 1-454.
- McClatchie, S. (1988) Food-limited growth of *Euphausia superba* in Admiralty Bay, South Shetlands Islands, Antarctica. *Continental Shelf Research*, **8**, 329-345.
- McGehee, D. E. and L. V. Martin (1996) Acoustic target strengths of Antarctic krill at 120 and 200 kHz. *Eos Transactions, American Geophysical Union*, **76**(3), Ocean Sciences Meeting Supplement, OS144.
- Miller, D. G. M. (1994) The spatial distribution of Antarctic krill (*Euphausia superba* Dana) aggregations. Ph.D. Dissertation, University of Cape Town, Cape Town, South Africa, 319 pp.
- Miller, D. G. M. and I. Hampton (1989a) Biology and Ecology of the Antarctic krill (*Euphausia superba* Dana): A Review. BIOMASS Scientific Series No. 9, Scientific Committee Antarctic Research, Cambridge, England, 166 pp.
- Miller, D. G. M. and I. Hampton (1989b) Krill aggregation characteristics: spatial distribution patterns from hydroacoustic observations. *Polar biology*, **10**, 125-134.
- Moline, M. A. and B. Prézelin (in review) High-resolution time-series data for primary production and related parameters at a Palmer LTER coastal site: Implications for modeling carbon fixation in the Southern Ocean. Submitted to *Marine Ecology Progress Series*, in review.
- Morris, D. J. (1985) Integrated model of moulting and feeding of Antarctic krill *Euphausia superba* off South Georgia. *Marine Ecology Progress Series*, **22**, 207-217.
- Morris, D. J. and C. Ricketts (1984) Feeding of krill around South Georgia. I: A model of feeding activity in relation to depth and time of day. *Marine Ecology Progress Series*, **16**, 1-7.
- Mosby, H. (1934) The waters of the Atlantic Antarctic Ocean. *Scientific Research Norwegian Antarctic Expeditions 1927-1928*, **11**, 1-131.
- Murphy, E. J., D. J. Morris, J. L. Watkins and J. Priddle (1988) Scales of interaction between Antarctic krill and the environment. In: *Antarctic Ocean and Resources Variability*, Sahrhage, D., editor, Springer-Verlag, Berlin, pp. 120-130.
- Murray, A. W. A., J. L. Watkins and D. G. Bone (1995) A biological acoustic survey in the marginal ice-edge zone of the Bellingshausen Sea. *Deep-Sea Research*, **42**, 1159-1175.

- Nast, F. (1979) The vertical distribution of larval and adult krill (*Euphausia superba*) on a time station south of Elephant Island, South Shetlands. *Meeresforschung*, **27**, 103-118.
- Nast, F., K. H. Kock, D. Sahrhage, M. Stein and J. E. Tiedtke (1988) Hydrography, krill and fish and their possible relationships around Elephant Island. In: *Antarctic Ocean and Resources Variability*, Sahrhage, D., editor, Springer-Verlag, Berlin, pp. 183-198.
- Nero, R. W. and J. J. Magnuson (1989) Characterization of patches along transects using high resolution 70 kHz integrated acoustic data. *Canadian Journal of Fisheries and Aquatic Sciences*, **46**, 2056-2064.
- Nero, R. W., J. J. Magnuson, S. B. Brandt, T. K. Stanton and J. M. Jech (1990) Finescale biological patchiness of 70 kHz acoustic scattering at the edge of the GulfStream – EchoFront 85. *Deep-Sea Research*, **37**, 999-1016.
- Niiler, P. P., A. Amos and J. -H Hu (1991) Water masses and 200 m relative geostrophic circulation in the western Bransfield Strait region. *Deep-Sea Research*, **38**, 943-959.
- Nordhausen, W. (1994) Winter abundance and distribution of *Euphausia superba*, *E. crystallorophias*, and *Thysanoessa macrura* in Gerlache Strait and Crystal Sound, Antarctica. *Marine Ecology Progress Series*, **109**, 131-142.
- O'Brien, D. P. (1987) Direct observations of the behavior of *Euphausia superba* and *Euphausia crystallorophias* (Crustacea: Euphausiacea) under pack ice during the Antarctic spring of 1985. *Journal of Crustacean Biology*, **7**, 437-448.
- Parkinson, C. L. (1992) Interannual variability of monthly southern ocean sea ice distributions. *Journal of Geophysical Research*, **97**, 5349-5363.
- Prézelin, B., N. P. Boucher, M. Moline, E. Stephens, K. Seydel and K. Scheppe (1992) Palmer LTER program: Spatial variability in phytoplankton distribution and surface photosynthetic potential within the peninsula grid, November 1991. *Antarctic Journal of the United States*, **27**, 242-244.
- Priddle, J., J. P. Croxall, I. Everson, E. J. Murphy, P. A. Prince and C. B. Sear (1988) Large-scale fluctuations in distribution and abundance of krill - A discussion of possible causes. In: *Antarctic Ocean and Resources Variability*, Sahrhage, D., editor, Springer-Verlag, Berlin, pp. 169-181.
- Quetin, L. B. and R. M. Ross (1984) School composition of the Antarctic krill *Euphausia superba* in the waters west of the Antarctic peninsula in the austral summer of 1982. *Journal of Crustacean Biology*, **4**, 96-106.
- Quetin, L. B., R. M. Ross and A. Clarke (1994) Krill energetics: seasonal and environmental aspects of the physiology of *Euphausia superba*. In: *Southern Ocean Ecology: the BIOMASS perspective*, El-Sayed, S. Z., editor, Cambridge University Press, Cambridge, pp. 165-184.

- Quetin, L. B., R. M. Ross, T. K. Frazer and K. L. Haberman (in press) Factors affecting distribution and abundance of zooplankton with an emphasis on Antarctic krill, *Euphausia superba*. In: *Foundations for ecological research west of the Antarctic Peninsula*, AGU Antarctic Research Series, Ross, R. M. , E. E. Hofmann and L. B. Quetin, editors, American Geophysical Union, in press.
- Quetin, L. B., R. M. Ross, K. L. Haberman, K. L. Hackey and T. Newberger (1992) Palmer LTER program: Biomass and community composition of euphausiids within the peninsula grid, November 1991 cruise. *Antarctic Journal of the United States*, **27**, 244-245.
- Rosenberg, J. (1991) United States Antarctic marine living resources 1990/1991 field season report. National Marine Fisheries Service, La Jolla, California, 97 pp.
- Ross, R. M. and L. B. Quetin (1988) *Euphausia superba*: A critical review of estimates of annual production. *Comparative Biochemistry and Physiology*, **90B**, 499-505.
- Ross, R. M., L. B. Quetin and C. M. Lascara (in press) Distribution of Antarctic krill and dominant zooplankton west of the Antarctic Peninsula. In: *Foundations for ecological research west of the Antarctic Peninsula*, AGU Antarctic Research Series, Ross, R. M. , E. E. Hofmann and L. B. Quetin, editors, American Geophysical Union, in press.
- Sahrhage, D. (1988) Some indications for environmental and krill resources variability in the Southern Ocean. In: *Antarctic Ocean and Resources Variability*, Sahrhage, D., editor, Springer-Verlag, Berlin, pp. 33-40.
- Siegel, V. (1985) The distribution pattern of krill, *Euphausia superba*, west of the Antarctic Peninsula in February 1982. *Meeresforschung*, **30**, 292-305.
- Siegel, V. (1986) Structure and composition of the Antarctic krill stock in the Bransfield Strait (Antarctic Peninsula) during the Second International BIOMASS Experiment (SIBEX). *Archiv für Fischereiwissenschaft*, **37**, 51-72.
- Siegel, V. (1988) A concept of seasonal variation of krill (*Euphausia superba*) distribution and abundance west of the Antarctic Peninsula. In: *Antarctic Ocean and Resources Variability*, Sahrhage, D., editor, Springer-Verlag, Berlin, pp. 219-230.
- Siegel, V. (1989) Winter and spring distribution and status of the krill stock in Antarctic Peninsula waters. *Archiv für Fischereiwissenschaft*, **39**, 45-72.
- Siegel, V. (1992) Assessment of the krill (*Euphausia superba*) spawning stock off the Antarctic Peninsula. *Archiv für Fischereiwissenschaft*, **41**, 101-130.
- Siegel, V. and V. Loeb (1995) Recruitment of Antarctic krill (*Euphausia superba*) and possible causes for its variability. *Marine Ecology Progress Series*, **123**, 45-56.
- Siegel, V., B. Bergstrom, J. O. Stromberg and P. H. Schalk (1990) Distribution, size frequencies and maturity stages of krill, *Euphausia superba*, in relation to sea-ice in the northern Weddell Sea. *Polar biology*, **10**, 549-557.

- Shulenberg, E., J. H. Wormuth and V. J. Loeb (1984) A large swarm of *Euphausia superba*: overview of patch structure and composition. *Journal of Crustacean Biology*, 4, 75-95.
- Smith, D. A., R. C. Smith and D. Menzies (1993a) Oceanographic Data Collected Aboard RV Nathaniel B. Palmer March-May 1993. Technical Report No. 93-05, Center for Coastal Physical Oceanography, Old Dominion University, Norfolk, VA, 152 pp.
- Smith, D. A., R. A. Locarnini, B. L. Lipphardt, Jr and E. E. Hofmann (1993b) Hydrographic Data Collected Aboard RV Nathaniel B. Palmer March-May 1993. Technical Report No. 93-04, Center for Coastal Physical Oceanography, Old Dominion University, Norfolk, VA, 215 pp.
- Smith, D. A., C. M. Lascara, J. M. Klinck, E. E. Hofmann and R. C. Smith (in press) Palmer LTER: Hydrography in the inner shelf region. *Antarctic Journal of the United States*, in press.
- Smith, R. C., H. Dierssen and M. Vernet (in press a) Phytoplankton biomass and productivity in the Western Antarctic Peninsula Region. In: *Foundations for ecological research west of the Antarctic Peninsula*, AGU Antarctic Research Series, Ross, R. M., E. E. Hofmann and L. B. Quetin, editors, American Geophysical Union, in press.
- Smith, R. C., S. Stammerjohn and K. S. Baker (in press b) Surface air temperature variations of the Western Antarctic Peninsula region. In: *Foundations for ecological research west of the Antarctic Peninsula*, AGU Antarctic Research Series, Ross, R. M., E. E. Hofmann and L. B. Quetin, editors, American Geophysical Union, in press.
- Smith, R. C., K. Baker, W. Fraser, E. Hofmann, D. Karl, J. Klinck, L. Quetin, B. Prézélin, R. Ross, W. Trivelpiece and M. Vernet (1995) The Palmer LTER: A Long-Term Ecological Research Program at Palmer Station, Antarctica. *Oceanography*, 8, 77-86.
- Snedecor, G. W. and W. G. Cochran (1978) *Statistical Methods*, Iowa State University Press, Ames, 593 pp.
- Sprong, I. and P. H. Schalk (1992) Acoustic observations on krill spring-summer migration and patchiness in the northern Weddell Sea. *Polar biology*, 12, 261-268.
- Stammerjohn, S. E. and R. C. Smith (in press a) Spatial and temporal variability in western Antarctic Peninsula sea ice coverage. In: *Foundations for ecological research west of the Antarctic Peninsula*, AGU Antarctic Research Series, Ross, R. M., E. E. Hofmann and L. B. Quetin, editors, American Geophysical Union, in press.
- Stammerjohn, S. E. and R. C. Smith (in press b) Palmer LTER: Sea ice coverage in the LTER region. *Antarctic Journal of the United States*, in press.
- Stein, M. (1988) Variation of geostrophic circulation off the Antarctic Peninsula and in the

- southwest Scotia Sea. In: *Antarctic Ocean and Resources Variability*, Sahrhage, D., editor, Springer-Verlag, Berlin, pp. 81-91.
- Stein, M. and R. B. Heywood (1994) Antarctic environment – physical oceanography: the Antarctic Peninsula and southwest Atlantic region of the Southern Ocean. In: *Southern Ocean Ecology: the BIOMASS perspective*, El-Sayed, S. Z., editor, Cambridge University Press, Cambridge, pp. 11-24.
- Stein, M. and S. Rakusa-Suszczewski (1984) Mesoscale structure of water masses and bottom topography as the basis for krill distribution in the SE Bransfield Strait, February-March 1981. *Meeresforschung*, **30**, 73-81.
- Stepnik, R. (1982) All year populational studies of Euphausiacea (Crustacea) in the Admiralty Bay (King George Island, South Shetland Islands, Antarctica). *Polish Polar Research*, **3**, 49-68.
- Stanton, T. K. (1989) Simple approximate formulas for backscattering of sound by spherical and elongated objects. *Journal of Acoustical Society of America*, **86**, 1499-1510.
- Stanton, T. K., D. Chu, P. H. Wiebe and C. S. Clay (1993) Average echos from randomly oriented random-length finite cylinders: Zooplankton models. *Journal of Acoustical Society of America*, **94**, 3463-3472.
- Stanton, T. K., P. H. Wiebe, D. Chu, M. C. Benfield, L. Scanlon, L. Martin and R. L. Eastwood (1994) On acoustic estimates of zooplankton biomass. *International Council for the Exploration of the Sea*, **51**, 505-512.
- Stretch, J. J., P. P. Hamner, W. H. Hamner, W. C. Michel, J. Cook and C. W. Sullivan (1988) Foraging behavior of Antarctic krill *Euphausia superba* on sea ice microalgae. *Marine Ecology Progress Series*, **44**, 131-139.
- Trathan, P. N., I. Everson, D. G. M. Miller, J. L. Watkins and E. J. Murphy (1995) Krill biomass in the Atlantic. *Science*, **373**, 201-202.
- Trathan, P. N., J. Priddle, J. L. Watkins, D. G. M. Miller and A. W. A. Murray (1993a) Spatial variability of Antarctic krill in relation to mesoscale hydrography. *Marine Ecology Progress Series*, **98**, 61-71.
- Trathan, P. N., D. Agnew, D. G. M. Miller, J. L. Watkins, I. Everson, E. Murphy, A. W. A. Murray and C. Goss (1993b) Krill biomass in Area 48 and Area 58: Recalculations of FIBEX data. Selected Scientific Papers 1992, Committee for the Conservation, Hobart, Australia, 157-182 pp.
- Trenberth, K. E., J. G. Olson and W. G. Large (1989) A global ocean wind stress climatology based on ECMWF analyses, NCAR Technical Note, NCAR/TN-338+STR, Boulder, CO, 93 pp.
- Trivelpiece, W. Z. and W. R. Fraser (in press) The breeding biology and distribution of Adelie penguins: Adaptations to environmental variability In: *Foundations for ecological research west of the Antarctic Peninsula*, AGU Antarctic Research Se-

- ries, Ross, R. M. , E. E. Hofmann and L. B. Quetin, editors, American Geophysical Union, in press.
- UNESCO (1983) Algorithms for computations of fundamental properties of seawater. Technical Papers in Marine Science No. 44, United Nations Educational, Scientific and Cultural Organization, Paris, 53 pp.
- Waters, K. J. and R. C. Smith (1992) Palmer LTER: A sampling grid for the Palmer LTER program. *Antarctic Journal of the United States*, **27**, 236-239.
- Weber, L. H. and S. Z. El-Sayed (1985) Spatial variability of phytoplankton and the distribution and abundance of krill in the Indian sector of the Southern Ocean. In: *Antarctic Nutrient Cycles and Food Webs*, Siegfried, W. R. , P. R. Condy and R. M. Laws, editors, Springer-Verlag, Berlin, pp. 1327-1343.
- Wiebe, P. H., C. H. Greene, T. K. Stanton and J. Burczynski (1990) Sound scattering by live zooplankton and micronekton: empirical studies with a dual-beam acoustical system. *Journal of Acoustical Society of America*, **88**, 2346-2360.
- Witek, Z., J. Kalinowski and A. Grelowski (1988) Formation of Antarctic krill concentrations in relation to hydrodynamic processes and social behavior. In: *Antarctic Ocean and Resources Variability*, Sahrhage, D., editor, Springer-Verlag, Berlin, pp. 237-244.
- Witek, Z., J. Kalinowski, A. Grelowski and N. Wolnomiejski (1981) Studies of aggregations of krill (*Euphausia superba*). *Meeresforschung*, **28**, 228-243.
- Zhou, M., W. Nordhausen and M. Huntley (1994) ADCP measurements of the distribution and abundance of euphausiids near the Antarctic Peninsula in winter. *Deep-Sea Research*, **41**, 1425-1445.
- Zwally, H. J., C. L. Parkinson and J. C. Comiso (1983) Variability of Antarctic sea ice and changes in carbon dioxide. *Science*, **220**, 1005-1012.

VITA

Cathy Meyer Lascara
1120 Trantwood Avenue
Virginia Beach, VA 23454

Education:

- B. S. Marine Biology, Florida Institute of Technology, 1978.
- M. S. Marine Science, College of William and Mary, 1982.
- Ph.D. Oceanography, Old Dominion University, 1996.

Professional Experience:

- 1991 - 1996 Graduate Research Assistant, Old Dominion University, Norfolk, Va.
- 1988 - 1991 Software Development Manager, The Jonathan Corporation, Norfolk, Va.
- 1983 - 1987 Computer Systems Developer, The Jonathan Corporation, Norfolk, Va.
- 1981 - 1983 Research Technician, McNeese State University, Lake Charles, La.
- 1978 - 1981 Graduate Research Asst., Va. Inst. of Marine Sci., Gloucester Pt, Va.

Publications:

- Hofmann, E. E. and C. M. Lascara (in review) A Review of Predictive Modeling for Coastal Marine Ecosystems. In: *The Sea*, Robinson, A. and K. Brink, editors.
- Hofmann, E. E., J. M. Klinck, C. M. Lascara and D. A. Smith (in press) Water mass distribution and circulation west of the Antarctic Peninsula. In: *Foundations for ecological research west of the Antarctic Peninsula*, Ross, R. M., E. E. Hofmann and L. B. Quetin, editors, American Geophysical Union, in press.
- Lascara, C. M., E. E. Hofmann, R. M. Ross and L. B. Quetin (1993) Palmer LTER: Overview of krill acoustic studies and results from the Peninsula grid. *Antarctic Journal of the United States*, **28**, 212-214.
- Lascara, C. M., L. B. Quetin and R. M. Ross (1993) Palmer LTER: Krill distribution and biomass within coastal waters near Palmer Station. *Antarctic Journal of the United States*, **28**, 214-217.
- Ross, R. M., L. B. Quetin and C. M. Lascara (in press) Distribution of Antarctic krill and macrozooplankton west of the Antarctic Peninsula. In: *Foundations for ecological research west of the Antarctic Peninsula*, Ross, R. M., E. E. Hofmann and L. B. Quetin, editors, American Geophysical Union, in press.
- Wheless, G. H., C. M. Lascara, A. Valle-Levinson, D. P. Brutzman, W. Sherman, and W. L. Hibbard (in press) The Chesapeake Bay Virtual Ecosystem (CBVE): Initial results from the prototypical system. *International Journal of Supercomputing Applications*, in press.

Published Abstracts:

- Lascara, C. M., E. E. Hofmann, R. M. Ross and L. B. Quetin (1992) Acoustically-derived distribution of krill (*Euphausia superba*) swarms off the Antarctic Peninsula. *Eos*, **73**, 319.
- Lascara, C. M., E. E. Hofmann, R. M. Ross and L. B. Quetin (1994) Seasonal changes in the mesoscale distribution of Antarctic krill in the waters west of the Antarctic Peninsula. *Eos*, **75**, 188.
- Lascara, C. M. and E. E. Hofmann (1996) Modeling the growth dynamics of Antarctic krill. *Eos*, **76**, 188.